

THE USE OF SYNTHETIC PLATELETS TO AUGMENT HEMOSTASIS

By Andrew J. Shoffstall

Submitted in partial fulfillment of the requirements
for the degree of Doctor of Philosophy

Dissertation Advisor: Dr. Erin B. Lavik

Department of Biomedical Engineering

CASE WESTERN RESERVE UNIVERSITY

May 2013

CASE WESTERN RESERVE UNIVERSITY
SCHOOL OF GRADUATE STUDIES

We hereby approve the thesis/dissertation of:

Andrew Shoffstall

candidate for the **Doctor of Philosophy** degree *.

(signed)

(chair of the committee) Erin Lavik, Sc.D., Associate Professor, Biomedical Engineering

Horst von Recum, Ph.D., Associate Professor, Biomedical Engineering

Jeff Ustin, M.D., Assistant Professor, Surgery

Robert Miller, Ph.D., Professor, Neuroscience

(date) 03/14/13

*We also certify that written approval has been obtained for any proprietary material contained therein.

Copyright © 2013

by Andrew Shoffstall

TABLE OF CONTENTS

LIST OF TABLES	8
LIST OF FIGURES	9
ACKNOWLEDGMENTS	15
LIST OF ABBREVIATIONS	17
ABSTRACT	24
CHAPTER 1: INTRODUCTION	26
WORKS CITED IN THIS CHAPTER	29
CHAPTER 2: MANAGING HEMORRHAGE IN TRAUMA	31
TRAUMA, HEMORRHAGE AND HEMOSTASIS	31
<i>Prevalence, impact and etiology</i>	31
<i>Hemostasis</i>	34
<i>Pathologies of hemostasis</i>	39
TREATMENT OF HEMORRHAGE	42
<i>Fluid resuscitation paradigms</i>	42
<i>Topical hemostats</i>	44
<i>Intravenous synthetic hemostats</i>	46
POLYMER NANOPARTICLE SYNTHESIS METHODS.....	50
<i>Overview</i>	50
<i>Emulsion and nanoprecipitation</i>	53
<i>Collection, storage and resuspension</i>	54
<i>Targeting</i>	56
IN VITRO MODELS OF COAGULATION	58
<i>Platelet aggregation</i>	58
<i>Platelet adhesion/aggregation</i>	60
<i>Whole blood coagulation</i>	61
IN VIVO MODELS OF HEMOSTASIS.....	64
<i>Mouse</i>	64
<i>Rat</i>	65
<i>Rabbit</i>	66
<i>Pig</i>	67
<i>Primate</i>	68
WORKS CITED IN THIS CHAPTER	68
CHAPTER 3: SYNTHETIC PLATELETS IN LETHAL LIVER TRAUMA*	79
INTRODUCTION	79
MATERIALS AND METHODS.....	82
<i>Materials</i>	82

<i>Particle synthesis</i>	82
<i>Coacervate precipitation and resuspension</i>	84
<i>Characterization</i>	84
<i>In vitro coagulation assay (ROTEM)</i>	85
<i>In vivo liver injury model</i>	86
<i>Surgical procedure</i>	86
<i>Procedure and statistics</i>	87
<i>Biodistribution</i>	88
<i>Imaging injury surface and adherent clots</i>	88
RESULTS	89
<i>Particle synthesis and characterization</i>	89
<i>In vivo injury model development</i>	92
<i>1-Hour survival</i>	93
<i>Blood loss</i>	94
<i>Imaging injury surface</i>	95
<i>Biodistribution</i>	96
<i>In vitro coagulation model</i>	98
DISCUSSION.....	100
<i>Administration of hemostatic nanoparticles increased 1-hour survival</i>	100
CONCLUSION	102
WORKS CITED IN THIS CHAPTER	103
CHAPTER 4: VARYING PEPTIDE CONCENTRATION: EFFECTS ON HEMOSTASIS* .106	
INTRODUCTION	106
MATERIALS AND METHODS.....	108
<i>Nanoparticle Synthesis</i>	108
<i>Characterization</i>	109
<i>Liver Trauma Model</i>	110
<i>Biodistribution</i>	110
<i>Histology</i>	111
<i>In vitro Assay</i>	111
<i>Statistics</i>	111
RESULTS	112
<i>GRGDS conjugation density</i>	112
<i>In vitro test of GRGDS NP100</i>	114
<i>NP100 particles in liver injury model</i>	115
<i>Biodistribution</i>	119
<i>In vitro test of GRGDS-NP blends</i>	124
DISCUSSION.....	128

CONCLUSION	131
WORKS CITED IN THIS CHAPTER.....	132
CHAPTER 5: PORCINE LIVER TRAUMA MODEL	135
INTRODUCTION	135
METHODS.....	136
<i>Liver resection model</i>	136
<i>Naïve administration/response model</i>	139
RESULTS	140
<i>Making a reproducible injury</i>	140
<i>Nanoparticle administration exacerbates bleeding during liver injury</i>	142
<i>Nanoparticle administration in naïve pig induces CARPA</i>	147
<i>Varying nanoparticle charge (zeta potential) mitigates CARPA</i>	151
DISCUSSION.....	155
<i>Possible causes of CARPA in this model</i>	155
<i>Potential causes for apparent coagulopathy during liver injury model</i>	157
<i>Mitigation of response</i>	161
CONCLUSION	163
WORKS CITED IN THIS CHAPTER.....	164
CHAPTER 6: CONCLUSIONS	167
WORKS CITED IN THIS CHAPTER	170
CHAPTER 7: RECOMMENDATIONS FOR FUTURE WORK.....	171
RESUSPENSION WITHOUT SONICATION	171
PULMONARY SAFETY	171
PEPTIDE CONJUGATION DENSITY	172
ELUCIDATING CARPA MECHANISMS AND ITS MITIGATION.....	172
OTHER POTENTIAL APPLICATIONS OF THIS TECHNOLOGY	174
<i>Gastrointestinal bleeding</i>	174
<i>Spinal cord injury</i>	175
<i>Other traumas</i>	176
WORKS CITED IN THIS CHAPTER	177
APPENDIX	179
LIVER INJURY MODEL DEVELOPMENT	179
<i>Regression model showing significance of body mass and liver resection mass on blood loss outcomes (Minitab Output)</i>	179
<i>Power analysis of survival (SAS Code)</i>	183
<i>Binomial logistic regression analysis for lethality data (SAS Code)</i>	183
<i>Analysis for nanoparticle biodistribution via histology (Matlab Code)</i>	184

BIBLIOGRAPHY187

List of Tables

Table 1: Common coagulopathies (bleeding disorders)	39
Table 2: Prevention of the lethal triad of coagulopathy, hypothermia, and acidosis. Reproduced with permission from Seyednejad, H.; Imani, M.; Jamieson, T.; Seifalian, A. M., Topical haemostatic agents. The British journal of surgery 2008, 95 (10), 1197-225. Copyright 2008, British Journal of Surgery Society Ltd.....	41
Table 3: Shear rates and shear stresses in the vasculature. Reproduced with permission from Michelson, A. D., Platelets. 2nd ed.; Academic Press/Elsevier: Amsterdam ; Boston, 2007; p xlii, 1343 p. Copyright 2007 Elsevier.....	60
Table 4: Synthesis scale-up. Reaction times were optimized and batch sizes increased, to produce nearly 8x the polymer mass in one-third the time as previously reported by Bertram et al. ²² Shoffstall method (1) forms nanoparticles with the triblock polymer PLGA-PLL-PEG and then conjugates the RGD peptide to nanoparticles. Shoffstall (2) forms nanoparticles from the previously RGD-conjugated quadblock polymer PLGA-PLL-PEG-GRGDS.....	89
Table 5: Particle characterization: size, polymer composition, and amino acid content.	90
Table 6: SURVIVAL TIME AND BLOOD LOSS grouped by dose (mg/kg). All 4/4 lactated ringers control pigs survived the entire 240 minutes, with a mean blood loss of 775 ml +/- 225 S.D. The optimal dosing appears to be between 0.1-0.2 mg/kg, where the adverse impact appears to be minimized. Interestingly, dosing down to 0.03 mg/kg, appears to also exacerbate the injury model, however, not as drastically as was observed with doses >2.0 mg/kg. Rather, animals are susceptible to prolonged bleeding times instead of induction of rapid hemorrhage.....	143

List of Figures

- Figure 1: Synthetic platelet design, consisting of a poly(lactic co glycolic)-poly-lysine (PLGA-PLL) core, with poly(ethylene glycol) (PEG) arms decorated with RGD targeting moieties. Reproduced with permission from Bertram, J. P.; Williams, C. A.; Robinson, R.; Segal, S. S.; Flynn, N. T.; Lavik, E. B., Intravenous hemostat: nanotechnology to halt bleeding. *Science translational medicine* 2009, 1 (11), 11ra22. Copyright 2009, Science Translational Medicine..... 28
- Figure 2: Injury mechanism in 289 traumatic deaths in Denver, 1992. MCA=motorcycle accident; PED=pedestrian; MVA = motor vehicle accident; SW=stab wound; GSW = gunshot wound. Reproduced with permission from Sauaia, A.; Moore, F. A.; Moore, E. E.; Moser, K. S.; Brennan, R.; Read, R. A.; Pons, P. T., Epidemiology of trauma deaths: a reassessment. *J Trauma* 1995, 38 (2), 185-93. Copyright 1995, Williams & Wilkins. 33
- Figure 3: Distribution by time, demographics, injury mechanism, and ISS of 289 traumatic deaths occurring in Denver 1992. Reproduced with permission from Sauaia, A.; Moore, F. A.; Moore, E. E.; Moser, K. S.; Brennan, R.; Read, R. A.; Pons, P. T., Epidemiology of trauma deaths: a reassessment. *J Trauma* 1995, 38 (2), 185-93. Copyright 1995, Williams & Wilkins..... 33
- Figure 4: Cell-based clotting cascade model: initiation, amplification, propagation. Reproduced with permission from Vine, A. K., Recent advances in haemostasis and thrombosis. *Retina* 2009, 29 (1), 1-7. Copyright 2009, Ophthalmic Communications Society, Inc..... 38
- Figure 5: Review of topical hemostatic agents and their mechanism of action. Reproduced with permission from Rossaint, R.; Cerny, V.; Coats, T. J.; Duranteau, J.; Fernandez-Mondejar, E.; Gordini, G.; Stahel, P. F.; Hunt, B. J.; Neugebauer, E.; Spahn, D. R., Key issues in advanced bleeding care in trauma. *Shock* 2006, 26 (4), 322-31. Copyright 2006, The Shock Society..... 46
- Figure 6: Depiction of H12-targeted liposomes, Okamura et al. Reproduced with permission from Okamura, Y.; Eto, K.; Maruyama, H.; Handa, M.; Ikeda, Y.; Takeoka, S., Visualization of liposomes carrying fibrinogen gamma-chain dodecapeptide accumulated to sites of vascular injury using computed tomography. *Nanomedicine* 2010, 6 (2), 391-6. Copyright 2010 Elsevier, Inc..... 49
- Figure 7: Nanoparticle systems researched for drug delivery applications. Reproduced with permission from Letchford, K.; Burt, H., A review of the formation and classification of amphiphilic block copolymer nanoparticulate structures: micelles, nanospheres, nanocapsules and polymersomes. *European journal of pharmaceuticals and biopharmaceutics : official journal of Arbeitsgemeinschaft fur Pharmazeutische Verfahrenstechnik e.V* 2007, 65 (3), 259-69. Copyright 2007, Elsevier. 51
- Figure 8: Nanoparticle synthesis methods, by particle type. Adapted with permission from Letchford, K.; Burt, H., A review of the formation and classification of

amphiphilic block copolymer nanoparticulate structures: micelles, nanospheres, nanocapsules and polymersomes. European journal of pharmaceutics and biopharmaceutics: official journal of Arbeitsgemeinschaft fur Pharmazeutische Verfahrenstechnik e.V 2007, 65 (3), 259-69. Copyright 2007, Elsevier..... 52

Figure 9: TEG/TEM parameters, including clotting time (R/CT), clot formation time (CFT/K), clot strength (MCF/MA), and fibrinolysis (CL/Ly). Reproduced from: Johansson, P. I.; Stensballe, J.; Ostrowski, S. R., Current management of massive hemorrhage in trauma. Scandinavian journal of trauma, resuscitation and emergency medicine 2012, 20, 47. Open Access Copyright 2012 Johansson et al.; licensee BioMed Central Ltd..... 63

Figure 10: Particle synthesis, nanoprecipitation and collection methods. 1) PLGA-PLL-cbz conjugation (DCC/DMAP), 2) Carbobenzyloxy (Cbz) group deprotection (HBr/Chloroform), 3) Pegylation (CDI diactivated PEG), 4) Nanoprecipitation, 5) GRGDS conjugation (to CDI-activated PEG), 6) Flocculation (poly(acrylic acid)), 7-9) Rinsing and lyophilization. 83

Figure 11: Varying nanoparticle size by changing polymer:solvent ratios during nanoprecipitation..... 84

Figure 12: Nanoparticle Schematic and Characterization. a) Hemostatic nanoparticles (GRGDS-NPs) consist of PLGA-PLL biodegradable polymer cores, with PEG arms that expose the GRGDS moiety for targeting activated platelets. b) SEM shows nanoparticle size distribution and morphology. c) ¹H-NMR spectral analysis confirms the pegylation of the co-block-polymer and the PEG-coronal structure of the nanoparticles. Deuterated water (top, gray overlay) and deuterated chloroform (bottom, black overlay). d) These are administered intravenously via the tail vein after a partial hepatectomy in the rat. The medial lobe (ML) is transected in this model. Right (RL), left (LL) and caudate lobes (CL) are labeled for reference..... 91

Figure 13: NMR tracing of nanoparticles in deuterated water (blue) and deuterated chloroform (black), showing increased relative PEG content in water, confirming the PEG-coronal structure of nanoparticles. 92

Figure 14: Injury reproducibility. Resected liver mass normalized by total liver mass (left) and body mass (right). The liver mass is tightly controlled in this injury model and is extremely reproducible in size, both in ratio to body mass (1.00% +/- 0.13% S.D.) and in ratio to the remaining liver (22.8 % +/- 2.8% S.D.). The dotted lines on the resected liver graph show the inclusion criteria for this study. Error bars represent SEM. 93

Figure 15: 1-hour survival. Survival is significantly increased by treatment with the hemostatic GRGDS-functionalized nanoparticles. Error bars represent SEM. 94

Figure 16: Blood loss outcomes. There is a trend toward a reduction in blood loss with the GRGDS-NP group, but is not significantly significant. 100% of animals with a blood volume loss less than 32% survive, but rapidly increases above this threshold. Error bars represent SEM..... 95

- Figure 17: Injury Surface Characterization. a) Hemostatic nanoparticles loaded with C6 (green) are found integrated with the adherent clot after it is removed and examined under fluorescent microscopy. b) The majority of bleeding appears to occur from the 2-4 major transected blood vessels in this injury model. c) Scanning electron microscopy is used to verify the presence of the nanoparticles (black arrow) and their integration with the fibrin mesh..... 96
- Figure 18: Biodistribution. a) 31% of hemostatic GRGDS-NPs locate in the clot, versus 7% for the scrambled-NP control group. Total mean nanoparticle recovery is 53.7% of total injected dose for GRGDS and 29.6% for scrambled. b) The “Liver” group is representative of the particle distribution to the uninjured lower left lobe of the liver. Minimal particle distribution is found in the spleen and kidneys. Approx. 20% is found in the lungs for each formulation. This may be indicative of microemboli in the lung or nanoparticles still in pulmonary circulation..... 97
- Figure 19: In vitro Testing. Outcomes include CT+CFT (a) and MCF (b). The GRGDS group had a lower (faster) clotting time and a higher clot firmness compared to saline. Error bars represent SEM. 99
- Figure 20: AMINO ACID ANALYSIS. Peptide conjugation efficiency Arg:Lys ratio. Peptide conjugation levels are approximately 100-fold higher when the conjugation reaction is performed in DMSO instead of aqueous phase. This leads to the nomenclature, NP100 and NP1 for the organic and aqueous phase polymers respectively. Interestingly the scrambled peptide, GRADSP, had a slightly higher conjugation efficiency in aqueous phase relative to GRGDS, while the GRGDS peptide had a slightly higher conjugation efficiency in aqueous relative to the scrambled GRADSP, possibly suggesting an interaction of the hydrophobic proline residue during this reaction in the different phases. Error bars denote SEM.113
- Figure 21: *IN VITRO* DOSE RESPONSE GRGDS-NP100. a-b) Total clotting time (CT+CFT) and maximum clot firmness (MCF) dose-responses, recapitulates the *in vivo* response observed: high doses have adverse impact on clotting parameters. This is observed until dosing down to 0.25 mg/ml. (n=1) C-D) 0.25 mg/ml is then further tested (n=6) to show that CT+CFT is reduced compared to saline (p=0.0346), with no significant impact on MCF. Dotted lines represent the normalization of clotting outcomes to saline-treated baseline sample. Error bars denote SEM..... 115
- Figure 22: *IN VIVO* DOSE RESPONSE GRGDS-NP100. Dose response with GRGDS-NP100 in rat liver injury model (n=3 for pilot study). a) Blood loss is significantly reduced in the 2.5 mg/ml dose, and not significantly changed with either 20 mg/ml or 10 mg/ml doses compared to the saline control. b) Percentage of animals surviving to 1-hour is reduced in the 20 mg/ml and 10 mg/ml groups, but increased in the 2.5 mg/ml dose. c) Survival curves, showing 2.5 mg/ml is significantly improved compared to saline, log-rank (Mantel-Cox) test, p=0.0148. D) Mean survival time is reduced with the 20 mg/ml and 10 mg/ml doses, suggesting an adverse “overdose” effect. Error bars denote SEM. 117
- Figure 23: LIVER INJURY RESULTS NP100. Rat medial liver injury model at 2.5 mg/ml dose. a) 1-hour survival was increased to 92%, compared to a scrambled peptide

control, 45% (OR=14.4, 95% CI=[1.36, 143]), a saline control, 47% (OR=13.5, 95% CI=[1.42, 125]), and GRGDS-NP1, 80% (OR=1.30, n.s.). b) Blood loss was significantly reduced in the GRGDS-NP100 group compared to saline (p=0.0073). c) Survival curves display increased survival with GRGDS-NP100 compared to the scrambled and saline groups, log-rank (Mantel-Cox) test, p=0.0362. Error bars denote SEM. 118

Figure 24: BIODISTRIBUTION (HPLC ASSAY). An assay for fluorescent C6 was performed using HPLC. Data is normalized to dry organ mass to reflect amount of nanoparticles found as a percent of the injected dose. There is a large proportion of the injected dose of nanoparticles accumulating in the lung tissue with the GRGDS group compared to the previous study and to the scrambled peptide group. However, it should be noted that since the total mass of particles injected is 8x less than the previous study.¹ The liver accumulates 7.5-10.5% of the injected dose (GRGDS, scrambled respectively), while ~11% becomes entrapped in the adherent clot found in the abdominal cavity post-mortem, regardless of the peptide group. Less than 1% is found in the kidney and spleen, and the particles are rapidly cleared from the blood plasma, with only 2% remaining in circulation at the end of the 1-hour experiment. Error bars denote SEM. 120

Figure 25: BIODISTRIBUTION (HPLC) COMPARISON BETWEEN NP1 AND NP100. There is a total of 8x fewer particles in the tissues overall, equating to approximately 2 mg in the lungs from the NP1 study versus 0.57 mg for the present study with GRGDS-NP100 particles..... 121

Figure 26: HISTOLOGY AND QUANTIFICATION. Histology was performed on the kidneys, uninjured left lobe of the liver, lungs, and injured medial lobe of the liver with adherent clot intact. Sections are 20um, and were not stained to prevent displacement of the nanoparticles. Quantification of the particles is measured in triplicate for n=3 rats per group, and represented as pixels/mm². a) Kidneys show no significant differences between treatment groups, b) Uninjured liver (left lobe), contains higher density of particles in the scrambled group compared to GRGDS (p=0.0467). c) Lungs show a larger proportion of particles accumulating in the GRGDS group compared to scrambled, but at an average of 37 pixels/mm², this does not reflect the large proportion of particles suggested by the biodistribution determined by HPLC. The portion of the lung sampled for histology consisted of the deep lung (capillary beds), while the HPLC sample, consisted of the whole lung, including higher order vasculature, potentially explaining this discrepancy. d) Clot adherent to remaining liver. Green = coumarin-6 (C6) loaded hemostatic nanoparticles; Red = Tissue background fluorescence (DsRed filter) used as reference channel. While the concentration of particles in the adherent clot is equal between groups, the particles in the GRGDS group appear as clusters, while the scrambled particles appear evenly dispersed. Error bars denote SEM..... 123

Figure 27: BLEND-COATED PLATE; PLATELET AGGREGATION ASSAY. ADP activated platelet aggregation assay, shows that higher GRGDS-loaded blends are associated with a larger amount of platelet aggregation. Error bars denote SEM. 125

Figure 28: *IN VITRO* DOSE RESPONSE GRGDS-NP_x BLENDS. ROTEM was used to titrate the dose responses of GRGDS-NP blends (100%, 10%, 1%) with the high dose of 20 mg/ml was chosen as it produced the largest impact on clotting parameters in the ROTEM assay. However, there is significant interaction of the blend*concentration term which may be further exploited to optimize this treatment in the future. a) CT+CFT, showing no effect of the GRGDS-NP100, a decrease of 15% compared to saline for the GRGDS-NP10, and an adverse increase of 31% (p=0.020) for the GRGDS-NP1 blend compared to saline. b) This is mirrored in the MCF values, showing no effect with the GRGDS-NP100, an increase of 7% with the GRGDS-NP10, and an adverse decrease of 8% with the GRGDS-NP1 particles compared to saline. This data demonstrates the utility of the ROTEM to assay relative efficacy of these blended formulations of intravenous hemostatic nanoparticles. 127

Figure 29: Making a reproducible liver injury. The left lobe (LL) is isolated from the underlying anatomy and medial lobe (left LML; right RML) with a malleable retractor, and measured and marked with cautery 2" from the apex (1). Two additional measurements are made from the apex to the lateral aspects of the resection line to ensure consistent equilateral angles (2 & 3). Ring clamps are used to hold the liver while the injury is made. The liver is resected to the left lobe midline (1), starting from patient-right. This is allowed to bleed for 1 minute with ring clamps still holding proximal to the injury line, and then the remaining liver is cut. After the injury is made, the left lobe is placed back in its natural resting place to prevent alteration of normal hepatic blood flow. VC=hepatic inferior vena cava. 138

Figure 30: CUMULATIVE BLOOD LOSS, LACTATED RINGERS CONTROL. The liver injury is made at time = 0, and allowed to bleed freely. Blood is collected via suction. This curve represents cumulative blood loss averaged from 4 experiments. The majority of blood loss occurs in the first 5 minutes. The dotted lines denote SEM. 141

Figure 31: BLOOD LOSS, divided into 4 time ranges, pre-administration (0-5 min, 380+/-59 ml), post-administration (5-15 min, 174+/-106 ml), post-infusion 1 (15-30 min, 150+/-111 ml), and post-infusion 2 (30-60 min, 70+/-95 ml). +/- represents S.D. 142

Figure 32: NP1 RATE OF BLOOD LOSS (0.1 mg/kg dose at 5 min post-injury). While blood loss in the pre-administration (0-5 min) window was consistent between groups, the post-administration (5-60 min) blood loss was exacerbated greatly in the both the GRGDS (560 +/-118 ml) and scrambled (533 +/- 146 ml) groups compared to the saline control (395 +/-104 ml). Mean survival time was 26 min for scrambled and 144 min for GRGDS, compared to 240 min for the saline control. +/- represents S.D. 145

Figure 33: NP100 RATE OF BLOOD LOSS. (0.1 mg/kg dose at 5 min post-injury). While blood loss in the pre-administration (0-5 min) window was consistent between groups, the post-administration (5-60 min) blood loss was exacerbated greatly in the both the GRGDS (777+/-177 ml) and scrambled (968+/-183 ml) groups compared to the saline control (395+/-104 ml). Mean survival time was 73 min for

scrambled and 172 min for GRGDS, compared to 240 min for the saline control. +/- represents S.D.	146
Figure 34: Pig 1: First administration of 2 mg/kg PLA-PEG-NP's -PAA (zeta=-30mV). CARPA is present immediately after injection at t=1-2 min, 8-12 min, and 61-65 min after initial injection at t=0 min.	148
Figure 35: Pig 1: Second administration of PLA-PEG nP +PAA (zeta=-30 mV) at 85 minutes after initial particle injection.....	150
Figure 36: Clotting times during naive particle administration. Coagulopathy does not appear to be innately present.....	151
Figure 37: First administration 60mg PLGA-PLL-PEG -pAA (zeta=-1.29 mV). No adverse effects were seen, including coagulation profiles measured by ROTEM (NATEM) and Hemochron (APTT).....	152
Figure 38: Second administration 2 mg/kg PLGA-PLL-PEG-NP's +pAA (zeta=+22.97 mV)	153
Figure 39: Blood loss after liver injury induced post-CARPA episode. There is an apparent coagulopathy, compared to the saline-treated pigs. Particles were administered at time=0min. Blood loss in the acute phase (0-5 min) is exacerbated to 519 ml from 380ml +/-59 ml (S.D.) in the saline control group. This coagulopathy continues in the 5-60 min time range, exacerbating bleeding to 814 ml compared to 395 ml in the saline control group. Survival in the CARPA (+injury) experiment was 82 minutes, compared to 240 minutes for (n=4/4) pigs treated with saline.	154

Acknowledgments

I would like to acknowledge the vast amount of support from my advisor Dr. Erin Lavik, under whose direction all this work was made possible. I had the pleasure of joining the lab in 2009, when it was just being established at Case Western, and have enjoyed watching it grow with equipment, projects and people. Her guidance and mentorship, interpreting data (good and bad), patience, critical review of my writing, and pushing our research forward has been invaluable for this project and my personal development as a scientist-in-training. Thank you.

I would also like to thank my committee members: Dr. Jeff Ustin, Dr. Horst von Recum, and Dr. Robert Miller. In addition to their thoughtful input during committee meetings, I would also like to thank them individually: Dr. Ustin for his tremendous support (often at 5am, or after a long stint of being on-call) in teaching me surgical techniques and his help in developing our porcine liver injury model, Dr. von Recum for giving me a temporary home in his lab and my first co-authorship on a paper as a graduate student, and Dr. Miller for his unrivaled acumen and critical advice on my projects when presenting at his lab meetings.

I have to thank my lab mates, including some whom I've never worked with directly, but whose protocols are doctrine in the LavikLab survival guide (James Bertram, in particular). My fellow graduate students in the lab, Donny Campbell, Meg Lashof-Sullivan, and Lydia Everhart have all contributed enormously to this project, and my continued sanity. Thank you. Rebecca Groynom, Kristyn Atkins, Erin Shoffstall, and Blaine Martyn-Dow, I want to thank for their enormous contributions to this project,

their willingness to help out with seemingly anything and everything, and for their terrific senses of humor, which set the tone in the lab. I have also had the opportunity to work with a large number of great undergraduate researchers who have contributed significantly to the multitude of tasks involved in this project. In particular, I want to thank Matt Varley, Larry Wu, Ali Kolberg, Zach Galliger, Adam Shick, and Alex Yau.

My friends from other labs I thank for all of their input, both research-related and not: Manfred Franke, Shannon Moore, and Derek Jones, made the transition as a first-year graduate student, racing to Case, a fun one. I tremendously enjoyed our SFB chapter, and the people in it – Alyssa Master, Luis Solario, Michael Bruckman, and Christa Modery, thank you for being willing to discuss biomaterials over drinks.

Finally, I wish to thank my family, in-laws, extended family and friends for their support while working on my Ph.D.. I spent long hours working (sometimes ignoring you) and thank you all for keeping me sane and well fed. I truly appreciate all the times you have listened to me talk about research, and all the times you have forced me to stop talking about research. I cannot thank my parents and siblings enough for their encouragement and confidence in me.

My wife Kelly, whom received the brunt of the ignoring and incessant talks about research (and who appropriately imposed the no-talking-about-research rule), has entirely made this work possible. If I were allowed, it would entirely be appropriate for me to list her as a co-author. Her support and love are truly what made this possible.

Thank you.

List of Abbreviations

<i>A</i>	
AAA, amino acid analysis.....	108
ADP, adenosine diphosphate, signals platelet activation.....	11, 34, 35, 58, 60, 124
<i>C</i>	
C.I., confidence interval.....	10, 92, 117, 167
C6, coumarin-6, a fluorescent dye.....	9, 11, 81, 87, 89, 94, 95, 109, 118, 119, 122
Ca ⁺⁺ , Calcium ions.....	36
CARPA, Complement activation related pseudoallergy.....	6, 12, 13, 24, 28, 66, 146, 147, 148, 150, 151, 152, 153, 154, 155, 156, 160, 161, 162, 167, 168, 171, 172, 173
CDI, 1,1'-Carbonyldiimidazole.....	9, 81, 82
CFT, see in vitro assays.....	8, 10, 62, 85, 110, 113, 114, 124
cLABL, Cyclo-(1,12)-PenITDGEATDSGC.....	56, 106
Clotting factors	
FIX, factor in intrinsic pathway missing in hemophilia B.....	38
FV, forms prothrombinase complex with FXa.....	36
FVII activates intrinsic pathway and cross-activates instrinsic pathway (amplification).....	36
FVIII, factor in intrinisc pathway missing in hemophilia A.....	38, 39
FX, forms prothrombinase complex with FVa.....	36
FXII, activation initiates the intrinsic pathway.....	36, 44, 156, 171
FXIIIa, crosslinks fibrin.....	35
TF, tissue factor-3, activates the extrinsic pathway with FVII.....	36
CNS, central nervous system.....	31, 63, 166, 174, 177
cRGD	
see GRGDS.....	173
CT, See in vitro assays.....	8, 10, 11, 62, 77, 84, 85, 97, 98, 110, 113, 114, 124, 126, 160, 166, 174

D

DAPI, nuclei staining 87, 110

DDAVP, desamino-8-arginine vasopressin treatment for vWF disease 39

DLS, dynamic light scattering 84, 89

DMSO, dimethyl sulfoxide 10, 107, 112

dodecapeptide

 dodecapeptide, see H12 8, 25, 29, 48, 49, 71, 72, 79, 103, 163

 H12, fibrinogen gamma chain dodecapeptide, platelet targeting agent 34

E

ECM, extracellular matrix 34, 55, 59

EPR, enhanced permeability and retention effect 55

ETCO₂, end-tidal CO₂ 138

F

FDA, food and drug administration 50, 103, 187

FFP, fresh frozen plasma 40

G

GLM, generalized linear model 124

GNP, gold nanoparticle 159

GPIIb/IIIa, glycoprotein IIb/IIIa, integrin $\alpha_{2b}\beta_3$ 34, 47, 57, 58, 71, 105, 106, 128, 132, 161, 173

GRADSP

 See Scrambled 10, 26, 80, 81, 89, 91, 107, 112, 141, 146, 167

GRGDS

 cRGD, cyclic RGD 173

 GRGDS, gly-arg-gly-asp-ser, active targeting oligopeptide 5, 9, 10, 11, 12, 26, 80, 81, 82, 89, 90, 92, 95, 96, 97, 98, 107, 108, 111, 112, 113, 115, 119, 120, 121, 122, 130, 141, 142, 144, 145, 154, 161, 167, 173

GRGDS-NP1, Active nanoparticles, 100-fold lower conjugation than GRGDS-NP100	10, 12, 23, 113, 114, 117, 118, 125, 126, 127, 128, 154, 167
GRGDS-NP10, Active nanoparticles, 10% GRGDS-NP100 and 90% pegylated PLGA	11, 125, 126
GRGDS-NP100, Active nanoparticles, 100-fold higher conjugation than GRGDS-NP110	11, 24, 113, 114, 115, 116, 117, 118, 120, 121, 125, 126, 127, 128, 129, 167
GRGDS-NPs, Active platelet-targeting nanoparticles	9, 10, 26, 27, 79, 80, 84, 86, 90, 92, 93, 94, 95, 96, 99, 110, 166
RGD, arg-gly-asp	7, 25, 27, 34, 48, 55, 57, 68, 72, 79, 88, 105, 106, 111, 143, 161, 173
GSW, gunshot wound	8, 32
<i>H</i>	
H&E, hematoxylin and eosin staining	110
HBOC-201, hemoglobin-based oxygen carriers	42
HBr, hydrogen bromide	9, 81, 82
HemCon, A topical hemostatic powder derived from chitosan	31, 166
HPLC, high performance liquid chromatography	11, 84, 87, 108, 109, 118, 119, 120, 121, 122
HR, heart rate	138, 150, 152
<i>I</i>	
IACUC, Institutional Animal Care and Use Committees	135
ICAM-1, Intercellular Adhesion Molecule 1	56, 74, 106, 132
In vitro assays	
ACT, activated clotting time	61
APTT, activated partial thromboplastin time	13, 61, 150, 151, 156, 160, 172
CFT or K, clot formation time	62
CT or R, clotting time	62
CT+CFT, sum of CT and CFT, combined clotting time	10, 11, 85, 97, 98, 110, 113, 114, 124, 126
Impact Cone, shear-dependent in vitro assay	60

ly or CL, fibrinolysis	62
MCF or MA, maximum clot formation	62
NATEM, nonactivated TEM	13, 84, 110, 150, 151, 160
PFA-100, Platelet function analyzer, measures closure time in capillary	60, 61, 74
Plate(let) Analyzer, Imaging paradigm linked to Impact Cone	60
PT, prothrombin time	61
ROTEM, Rotational thromboelastometry. 5, 11, 13, 24, 74, 80, 84, 97, 101, 106, 110, 111, 113, 123, 124, 126, 127, 130, 131, 138, 150, 151, 160, 166, 167	
Verify Now, method similar to classical aggregometry	58
Integrins	
GPIa/IIa, platelet integrin that binds subendothelial matrix	33
GPIb-V-IX, platelet integrin binds vWF	34
GPVI, platelet integrin binds collagen	34
IVIG, immune globulin	39
 <i>L</i>	
LL, left lobe	9, 12, 90, 137
LML, left medial lobe	12, 137
LR, Lactated Ringers	196
 <i>M</i>	
MAC-1, Macrophage antigen-1	157, 159
MAP, mean arterial pressure	43, 138, 150, 151, 152
MCA, motorcycle accident	8, 32
MCF, See in vitro assays	8, 10, 12, 62, 85, 97, 98, 110, 113, 114, 124, 126, 166
Minitab, statistics software	6, 86, 111, 191
MVA, motor vehicle accident	8, 30, 32
MWCO, molecular weight cutoff	107

N

NMR, nuclear magnetic resonance (1H proton) 9, 84, 89, 90, 108
NP100, See GRGDS-NP100.....5, 10, 11, 12, 112, 113, 114, 117, 119, 120, 141, 142, 143, 145
NPs, See GRGDS-NPs..... 106, 131
NSAID, nonsteroidal anti-inflammatory 58

O

OR, Odds ratio (statistical comparison of two binomial variables)..... 10, 93, 116, 117, 167

P

PAA, poly(acrylic acid) 12, 13, 139, 147, 148, 149, 150, 154, 157, 158, 159, 160
PBS, phosphate buffered saline 81, 83, 84, 86, 97, 107, 109
PED, pedestrian accident.....8, 32
PEG, poly(ethylene glycol)..... 7, 9, 26, 27, 52, 55, 80, 81, 82, 84, 89, 90, 91, 105, 107, 108, 111, 173
PLGA, poly(lactic co glycolic acid)..... 26, 56, 80, 81, 88, 89, 107, 171, 172
PLL, poly(ϵ -l-lysine)26, 80, 81, 84, 88, 89, 108
PLL-cbz, protected PLL 81
PPP, platelet poor plasma 58
PRP, platelet rich plasma..... 58
PVA, poly(vinyl alcohol), surfactant52, 54

Q

Quadblock, PLGA-PLL-PEG-GRGDS..... 7, 88, 107, 130, 171
QuikClot, A topical hemostatic powder (initially Zeolite, now Kaolin)25, 31, 43, 70, 163, 166

R

RFVIIa, Recombinant factor VIIa (NovoSeven ®)78, 79
RGD
See GRGDS..... 7, 25, 27, 34, 48, 55, 57, 68, 72, 79, 88, 105, 106, 111, 143, 161, 173

RML, right medial lobe	12, 137
ROTEM	
See in vitro assays.....	5, 11, 13, 24, 74, 80, 84, 97, 101, 106, 110, 111, 113, 123, 124, 126, 127, 130, 131, 138, 150, 151, 160, 166, 167
<i>S</i>	
SAS, statistics software.....	6, 86, 111, 195
SCI, spinal cord injury.....	174
Scrambled	
GRADSP, gly-arg-ala-asp-ser-pro, scrambled control oligopeptide...	10, 26, 80, 81, 89, 91, 107, 112, 141, 146, 167
Scrambled-NP1, Control nanoparticles, 100-fold lower conjugation than Scrambled-NP100.....	113, 128
Scrambled-NP100, Control nanoparticles, 100-fold higher conjugation than Scrambled-NP1	113, 128
Scrambled-NPs, Control nanoparticles (non-targeted)	26, 80
See RBC	25, 42, 48, 79
SEM, scanning electron microscopy	9, 10, 11, 12, 84, 87, 89, 90, 92, 93, 94, 98, 112, 114, 116, 117, 119, 123, 124, 140
SPO2, oxygen saturation.....	138
SW, stab wound	8, 32
Synthocytes, fibrinogen coated albumin microparticles.....	25, 49, 71, 79, 181
<i>T</i>	
TNF-alpha, tissue necrosis factor	159
Triblock, PLGA-PLL-PEG.....	7, 13, 81, 88, 107, 108, 129, 151, 171
Tween 80, polysorbate 80	54, 170
<i>U</i>	
UV-Vis, ultraviolet-visible spectroscopy.....	81

V

VC, vena cava 12, 137

vWF, von Willebrand factor 34, 35, 38, 47, 58, 61

Abstract

The Use of Synthetic Platelets to Augment Hemostasis

By

ANDREW J. SHOFFSTALL

Uncontrolled hemorrhage comprises 60-70% of trauma-associated mortality in the absence of other lethal conditions (e.g. damage to central nervous or cardiac system). Immediate intervention is critical to improving chances of survival. While there are several products to control bleeding for external wounds including pressure dressings, tourniquets or topical hemostatic agents there are few, if any, effective treatments that can be administered in the field to help staunch internal bleeding.

Intravenous hemostatic nanoparticles that augment blood clotting when administered after trauma have been previously shown to half bleeding times in a femoral artery injury model in rats. The aims of the present study were to: 1) Determine their efficacy in a lethal hemorrhagic liver injury model, 2) determine the impact of targeting ligand concentration on hemostasis, and 3) test them in a clinically relevant porcine model of hemorrhage.

Nanoparticle administration (GRGDS-NP1, 40 mg/kg) after lethal liver resection in the rat increased 1-hour survival to 80% compared to 40-47% in controls. Targeting

ligand conjugation was then increased 100-fold (GRGDS-NP100), and a dosing study performed. GRGDS-NP100 hemostatic nanoparticles (2.5 mg/kg) were efficacious at doses 8-fold lower than GRGDS-NP1, and increased 1-hour survival to 92%. *In vitro* analysis using rotational thromboelastometry (ROTEM) confirmed the increased dose-sensitivity of GRGDS-NP100 and laid the foundation for methods to determine optimal ligand concentration parameters.

Hemostatic nanoparticles were then tested in a clinically relevant porcine liver injury model, which elucidated an unexpected adverse reaction, comprised of a massive hemorrhagic response. A naïve (uninjured) porcine model was then employed. These experiments revealed an adverse reaction consistent with complement activation related pseudoallergy (CARPA), which could be mediated by tuning nanoparticles' zeta potential. Neutralizing the nanoparticle charge mitigated the onset of CARPA, while negative (-30 mV) or positive (+20 mV) zeta potential led to adverse CARPA symptoms (e.g., cardiopulmonary dysfunction with spontaneous recovery within minutes). While the sensitivity to CARPA is exaggerated in the pig model compared to humans, its consequences when triggered during hemorrhagic injury could be catastrophic in a subset of the population. Therefore, minimizing its risk will be paramount to the clinical translation of this technology.

Chapter 1: Introduction

Trauma is the leading cause of death for individuals between ages 1-44.¹ More than one-third of patients die before reaching the hospital.¹ In military trauma, outcomes are even worse.² Injuries are often more severe and can have the additional complication of a prolonged prehospital phase, defined as the time between injury and admission to the hospital.^{2,3} Hemorrhage accounts for 50% of penetrating battlefield trauma mortality, and 80% of these deaths are secondary to injury in the torso, where conventional methods for hemostasis, such as pressure dressing and tourniquets are impossible.^{2,4-6} If the hemorrhage is internal, even novel hemostatic agents such as QuikClot cannot be used, since its use is limited to topical application. For civilian and non-civilian application, there is a tremendous unmet need for a field-administrable hemostatic agent to address internal hemorrhage.³

Intravenous hemostatic nanoparticles that target activated platelets have been investigated by a number of groups with some promise and a range of challenges.⁷⁻¹⁰ RGD conjugated red blood cells (RBCs) called thromboerythrocytes showed promise *in vitro* but did not significantly reduce prolonged bleeding times in thrombocytopenic primates.^{7,11} Fibrinogen-coated albumin microparticles, "Synthocytes"¹² and liposomes carrying the fibrinogen γ chain dodecapeptide (HHLGGAKQAGDV)^{13,14} showed success in bleeding models in thrombocytopenic rabbits. However, Synthocytes were ineffective in treating bleeding in normal rabbits¹², and the liposomes from Okamura et al.^{13,14} do

not appear to have yet been studied for this purpose, although they have recently been shown to improve survival after lethal liver trauma in rabbits.¹⁵

The Lavik lab has developed novel hemostatic nanoparticles (GRGDS-NPs) that can be administered intravenously to reduce bleeding times by ~ 50% in a model of rat femoral artery injury, performing better than saline or recombinant factor VIIa (rFVIIa) controls.¹⁶ These nanoparticles are made of biodegradable polymers, reducing the risk of long-term immunological and inflammatory reactions. The salient features of these nanoparticles include a 400 nm core made of biodegradable block copolymer of poly(lactic-co-glycolic acid) (PLGA) and poly- ϵ -L-lysine (PLL) with poly(ethylene glycol) (PEG) arms terminated with arginine-glycine-aspartic acid (**GRGDS**)-based targeting ligands (Figure 1) GRADSP ligands are used as a scrambled peptide to control for nonspecific actions of the particles (Scrambled-NPs). For research purposes, the nanoparticles have been loaded with coumarin-6, a fluorescent dye that allows us to track their biodistribution.¹⁶

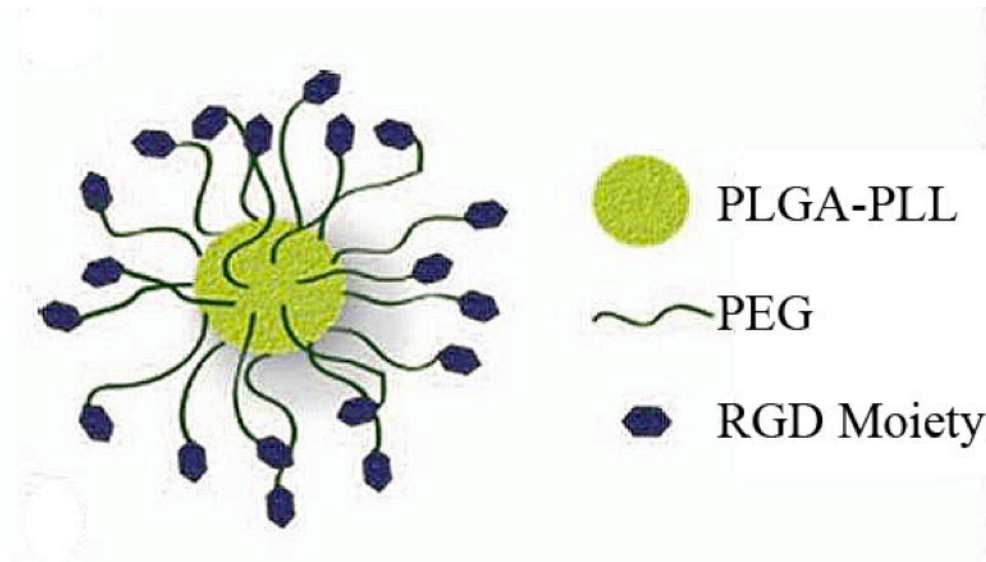


Figure 1: Synthetic platelet design, consisting of a poly(lactic co glycolic)-poly-lysine (PLGA-PLL) core, with poly(ethylene glycol) (PEG) arms decorated with RGD targeting moieties. Reproduced with permission from Bertram, J. P.; Williams, C. A.; Robinson, R.; Segal, S. S.; Flynn, N. T.; Lavik, E. B., Intravenous hemostat: nanotechnology to halt bleeding. *Science translational medicine* 2009, 1 (11), 11ra22. Copyright 2009, Science Translational Medicine.

The purpose of my dissertation work was to investigate whether administration of these hemostatic nanoparticles would augment hemostasis in a lethal trauma, and whether this would correlate to improved survival.

In these studies, we first investigated the impact of intravenous delivery of the GRGDS-NPs on blood loss and survival in a model of blunt lethal liver injury model to determine whether the nanoparticles had an effect in a complex solid organ injury. We looked at blood loss and mortality outcomes, followed by *in vitro* clotting parameters to better understand the mechanism by which the nanoparticles augment hemostasis. A key component of this work involved the scale-up of the nanoparticle synthesis methods to enable their investigation in a multitude of *in vitro* and *in vivo* studies.

An additional challenge was to investigate the sensitivity of surface ligand conjugation on hemostasis. This is a key parameter for nanoparticle targeting. Too many surface ligands can actually limit targeting through self-steric hindrance, while too few, will lead to ineffective targeting. Surface ligand density was increased, characterized, and tested in both an *in vivo* model of lethal liver trauma as well as an *in vitro* thromboelastometry assay.

Finally, in order to address the difference in hemodynamics between small and large animal models, we studied the efficacy of the hemostatic nanoparticles in a clinically relevant porcine model of hemorrhage, and discovered an adverse complication, namely complement activation related pseudoallergy (CARPA). We then tested various factors to determine the cause, and a potential way to mitigate the reaction.

This work demonstrated the ability of these hemostatic nanoparticles to reduce blood loss to a great enough extent to increase survival after trauma. It also identified several key parameters that may be tuned to improve their hemostatic efficacy and reduce the risk for complications, namely targeting ligand density and zeta potential. This work laid the foundation for the optimization of these parameters in both *in vitro* and *in vivo* models, and demonstrated methods for their tuning.

WORKS CITED IN THIS CHAPTER

1. Kauvar, D.S., Lefering, R. & Wade, C.E. Impact of hemorrhage on trauma outcome: an overview of epidemiology, clinical presentations, and therapeutic considerations. *J Trauma* **60**, S3-11 (2006).

2. Champion, H.R., Bellamy, R.F., Roberts, C.P. & Leppaniemi, A. A profile of combat injury. *J Trauma* **54**, S13-19 (2003).
3. Holcomb, J.B., *et al.* Causes of death in U.S. Special Operations Forces in the global war on terrorism: 2001-2004. *Ann Surg* **245**, 986-991 (2007).
4. Kauvar, D.S. & Wade, C.E. The epidemiology and modern management of traumatic hemorrhage: US and international perspectives. *Crit Care* **9 Suppl 5**, S1-9 (2005).
5. Clifford, C.C. Treating traumatic bleeding in a combat setting. *Mil Med* **169**, 8-10, 14 (2004).
6. Morrison, J.J. & Rasmussen, T.E. Noncompressible torso hemorrhage: a review with contemporary definitions and management strategies. *Surg Clin North Am* **92**, 843-858 (2012).
7. Alving, B.M., Reid, T.J., Fratantoni, J.C. & Finlayson, J.S. Frozen platelets and platelet substitutes in transfusion medicine. *Transfusion* **37**, 866-876 (1997).
8. Blajchman, M.A. Platelet substitutes. *Vox Sang* **78 Suppl 2**, 183-186 (2000).
9. Blajchman, M.A. Novel platelet products, substitutes and alternatives. *Transfus Clin Biol* **8**, 267-271 (2001).
10. Modery-Pawlowski, C.L., *et al.* Approaches to synthetic platelet analogs. *Biomaterials* **34**, 526-541 (2013).
11. Coller, B.S., *et al.* Thromboerythrocytes. In vitro studies of a potential autologous, semi-artificial alternative to platelet transfusions. *J Clin Invest* **89**, 546-555 (1992).
12. Levi, M., *et al.* Fibrinogen-coated albumin microcapsules reduce bleeding in severely thrombocytopenic rabbits. *Nat Med* **5**, 107-111 (1999).
13. Okamura, Y., *et al.* Hemostatic effects of phospholipid vesicles carrying fibrinogen gamma chain dodecapeptide in vitro and in vivo. *Bioconjug Chem* **16**, 1589-1596 (2005).
14. Okamura, Y., *et al.* Visualization of liposomes carrying fibrinogen gamma-chain dodecapeptide accumulated to sites of vascular injury using computed tomography. *Nanomedicine* **6**, 391-396 (2010).
15. Nishikawa, K., *et al.* Fibrinogen gamma-chain peptide-coated, ADP-encapsulated liposomes rescue thrombocytopenic rabbits from non-compressible liver hemorrhage. *Journal of thrombosis and haemostasis : JTH* **10**, 2137-2148 (2012).
16. Bertram, J.P., *et al.* Intravenous hemostat: nanotechnology to halt bleeding. *Science translational medicine* **1**, 11ra22 (2009).

Chapter 2: Managing Hemorrhage in Trauma

The scope of this literature review will focus on the role of hemorrhage in trauma, the current practices for its treatment, and the development of novel therapies in regards to their potential advantages and associated challenges. I will also briefly review the current practices and challenges with *in vitro* and *in vivo* models of hemostasis and hemorrhagic trauma.

TRAUMA, HEMORRHAGE AND HEMOSTASIS

Prevalence, impact and etiology

Trauma is the leading cause of death for people ages 5-44; worldwide in 1998, trauma accounted for 5.8 million fatalities.¹ Domestically, these traumas result from a broad range of incidents, such as motor vehicle accidents (MVA), falls, burns, and penetrating injuries such as gun shot or stab wounds (Figure 2).²

More than one-third of patients who die as a result of injury, do so before reaching the hospital³, and in military trauma, outcomes are even worse.⁴ Injuries are often more severe and can have the additional complication of a prolonged prehospital phase, defined as the time between injury and admission to the hospital.^{4,5} New tactics seen in Iraq and Afghanistan, developed to circumvent the advancements in our troops' body armor (e.g. improvised explosive devices) have resulted in different wounding patterns than seen previously.⁶ Dismounted personnel are the target, and often present with severe traumas.⁶ When these traumas are not isolated to the extremities, they become exceedingly difficult to control in the field.⁷

Role of Hemorrhage in Trauma

Hemorrhage accounts for 50% of penetrating battlefield trauma mortality, and 80% of these deaths are secondary to injury in the torso, where conventional methods for hemostasis, such as pressure dressings and tourniquets are impossible (noncompressible injuries).^{4,7-9} Other noncompressible traumas include trauma to the central nervous system (CNS), junctional trauma, and blast trauma, which generally damages the air-filled organs such as the ears, lungs, and abdomen.^{4 5,10} A large focus in the military has been on techniques for stopping noncompressible hemorrhage by using topically applied powders such as QuikClot and HemCon (e.g. for junctional trauma) which rapidly absorb water from the blood and concentrate clotting factors at the site of injury. However, few products have been pursued that can augment hemostasis with internal hemorrhage (e.g. CNS trauma, blast trauma). Rather, these are treated primarily by fluid resuscitation alone, until definitive surgery can be performed.⁶

Time to Intervention

The fallacy of a “golden hour” has led to the coined term “platinum 5 minutes”, referring to the fact that with massively exsanguinating trauma, the initial minutes following injury are crucial for stabilizing the injured patient.^{9,11} This is reflected in the data collected from one trauma center in Denver, showing the disproportionately large number of fatalities “found dead” due to penetrating trauma (which characteristically involves internal hemorrhage in the head, chest or abdomen), despite rapid response times (Figure 3).² Early intervention is critical for saving lives after hemorrhagic trauma.^{12,13}

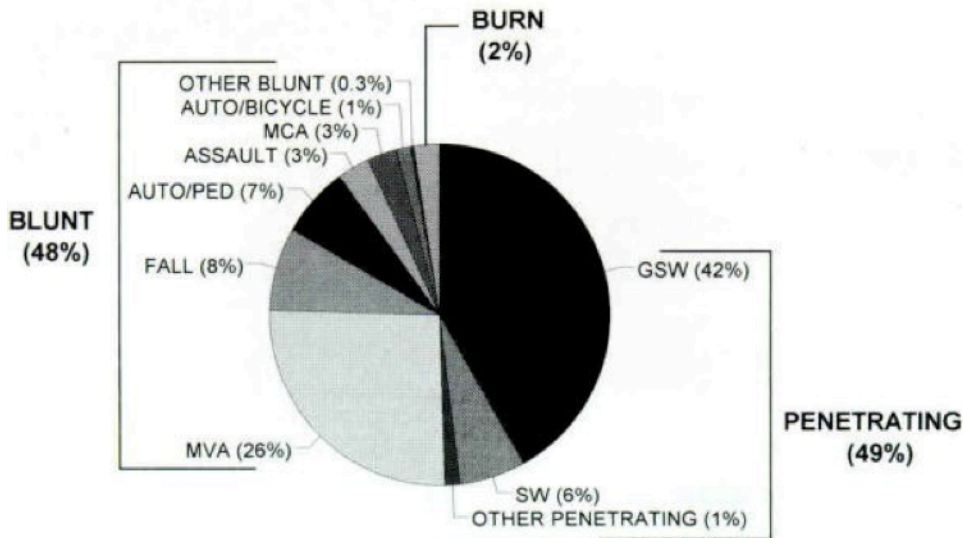


Figure 2: Injury mechanism in 289 traumatic deaths in Denver, 1992. MCA=motorcycle accident; PED=pedestrian; MVA = motor vehicle accident; SW=stab wound; GSW = gunshot wound. Reproduced with permission from Sauaia, A.; Moore, F. A.; Moore, E. E.; Moser, K. S.; Brennan, R.; Read, R. A.; Pons, P. T., Epidemiology of trauma deaths: a reassessment. J Trauma 1995, 38 (2), 185-93. Copyright 1995, Williams & Wilkins.

	Prehospital (n = 98)		In-Hospital (n = 191)		
	Found Dead (n = 52)	Scene (n = 46)	Acute (n = 154)	Early (n = 11)	Late (n = 26)
Age (yr) ^a	37.5 ± 2.5	38.0 ± 3.0	33.2 ± 1.5	40.0 ± 4.8	52.0 ± 4.3
Male	39 (75%)	32 (70%)	122 (79%)	9 (82%)	23 (88%)
Mechanism					
Blunt	5 (10%)	24 (52%)	80 (52%)	11 (100%)	19 (73%)
Penetrating	47 (90%)	19 (41%)	73 (47%)	0	4 (15%)
Burns	0	3 (7%)	1 (1%)	0	3 (12%)
ISS*	34.9 ± 2.9	44.4 ± 3.8	37.6 ± 1.7	29.0 ± 5.8	24.3 ± 3.0

Values are mean ± SE.

^a $p < 0.05$ (ANOVA); comparing scene, acute, early, and late.

Figure 3: Distribution by time, demographics, injury mechanism, and ISS of 289 traumatic deaths occurring in Denver 1992. Reproduced with permission from Sauaia, A.; Moore, F. A.; Moore, E. E.; Moser, K. S.; Brennan, R.; Read, R. A.; Pons, P. T., Epidemiology of trauma deaths: a reassessment. J Trauma 1995, 38 (2), 185-93. Copyright 1995, Williams & Wilkins.

Hemostasis

The stages of hemostasis are generally divided into immediate vasoconstriction, followed by primary and secondary hemostatic mechanisms.¹⁴

Vasoconstriction

The first event following vascular injury is a strong vasoconstriction response, causing a decrease in local blood flow to prevent the loss of blood. This is mediated by the smooth muscle cells in the tunica media, and is pronounced in the smaller arteries and arterioles. This vasospasm can last from minutes to hours depending on injury severity, and allows primary and secondary hemostasis to occur by reducing flow rates through the damaged vessel.¹⁵

Primary Hemostasis

Platelets are anuclear cells, derived from budding off from their precursor megakaryocytes, that circulate in the bloodstream in a quiescent state until injury occurs. They have a life span of around 5-9 days and contain both alpha and dense granules, which contain pro-coagulation signals and clotting factors. The contents of these granules can be quickly secreted through a transport system called the open canalicular system.¹⁶

Primary hemostasis involves the adhesion, activation, and aggregation of platelets to form the platelet plug.¹⁵ Upon injury of a blood vessel, the damaged endothelial lining exposes the underlying layer subendothelium matrix¹⁷, which includes collagen¹⁸, fibronectin¹⁹, and laminin.²⁰ Platelets can bind directly to this matrix through the glycoprotein GPIa/IIa receptor.¹⁶ However, these interactions are

most effective in low shear binding.²¹ Under high shear, platelets bind mostly to von Willibrand Factor (vWF) which is, itself, bound to subendothelial matrix.²² This association is brief however, as platelet GPIb-V-IX/vWF binding has a very high dissociation rate. This leads to the characteristic “rolling” of platelets along a damaged endothelium, slowing its progress enough to allow for additional integrin binding to extracellular matrix proteins (e.g. GPVI-collagen or GPIa/IIa-fibrin) to finally arrest its motion.¹⁶

Platelets can become activated by a number of different mechanisms, including adenosine diphosphate (ADP), thromboxane, thrombin, and cyclooxygenase.¹⁶ Upon activation, they change their conformation from a bi-discoid shape to a stellate morphology. This is characterized by rapid polymerization of actin filament in the cytoskeleton which causes the both the gross shape change as well as specific conformational change of the surface receptor glycoprotein IIb/IIIa (GPIIb/IIIa, integrin $\alpha_{2b}\beta_3$) and release of platelet alpha and dense granules.¹⁶

The change in the GPIIb/IIIa conformation exposes binding domains for both fibrinogen and vWF. Interestingly, fibrinogen has multiple binding domains, including the common RGD (arg-gly-asp) motif at each end, as well as a dodecapeptide-H12, which allows for it to act as a platelet-platelet bridging molecule.²³⁻²⁵ Upon activation, and in concert with fibrinogen, and other extracellular matrix (ECM) proteins, platelets rapidly aggregate, adhere to the injury surface, and begin to spread across the surface, such that they become indistinguishable from one another under scanning electron microscopy.¹⁶

The granules translocate to the center of the platelet, where their contents are emptied into the open-canalicular system, and then diffuse into the extracellular space.¹⁶ Dense granules contain pro-aggregatory factors, such as ADP, serotonin, histamine, and bivalent cations, calcium and magnesium required in hemostasis. Alpha granules secrete adhesion factors such as glycoproteins, vWF, fibrinogen and clotting factors, which are critical for adhesion and clot production.²⁶ The secretion of these granules leads to a positive feedback by further activation and recruitment of platelets. Activated platelets act as a procoagulatory stimulus both through the paracrine signaling mentioned above, and directly, by acting as a substrate for the ten-ase complex which produces prothrombinase (part of the clotting cascade).¹⁶

Secondary Hemostasis

Subsequently, and immediately, secondary hemostasis is initiated, consisting of a tightly regulated clotting cascade. The end-result of the clotting cascade is to regulate clotting factors that enable the enzyme thrombin to convert fibrinogen to its active monomer fibrin.²⁷⁻²⁹ This activated fibrin then polymerizes and is crosslinked by FXIIIa to form a mesh that stabilizes the initial platelet plug at the injury site. The final step in hemostasis, involves the dissolution of this clot by the activation of the fibrin-degrading enzyme plasmin. The equilibrium between pro-coagulation and anticoagulation (fibrinolysis) is one that is tightly regulated by feedback mechanisms in the clotting cascade.³⁰

Classically, the clotting cascade has been split into intrinsic and extrinsic pathways, referring to their respective mechanisms of activation.²⁹ Both pathways

converge to a common pathway which produces fibrin to stabilize the platelet plug. The intrinsic pathway is initiated with the activation of factor FXII, occurring when it comes in contact with negatively charged surfaces such as glass, activated platelet membranes and phospholipids.²⁷ It is called the intrinsic pathway because all the components are intrinsically present in the blood, as opposed to the extrinsic pathway which is initiated by contact with tissue factor (TF) located in the blood vessel walls.²⁹

The intrinsic pathway was largely dismissed as a key player in initiation of hemostasis since a person lacking factor FXII experienced increased *in vitro* clotting times, but no significant *in vivo* clinical clotting dysfunction.³¹⁻³³ It was subsequently shown that TF/FVII cross-activated the intrinsic pathway³⁴, suggesting a slightly new clotting model, in which the extrinsic pathway was responsible for clotting activation, while the intrinsic pathway's major role was of amplification and propagation for thrombin-burst generation (Figure 4).³⁵

The common pathway, or the "propagation" phase below, is comprised of the activation of the FX to FXa and its activation FV and association with FVa, in the presence of Ca⁺⁺ and phospholipids to form the prothrombinase complex. This prothrombinase complex then converts prothrombin to thrombin, the enzyme responsible for fibrin conversion.³⁵

Together primary and secondary hemostasis surmount a rapid response to vascular injury at the cellular and molecular level, resulting in a clot, visible and active

at the macroscopic level. For most mild, moderate and many severe cases, it is sufficient to staunch bleeding.

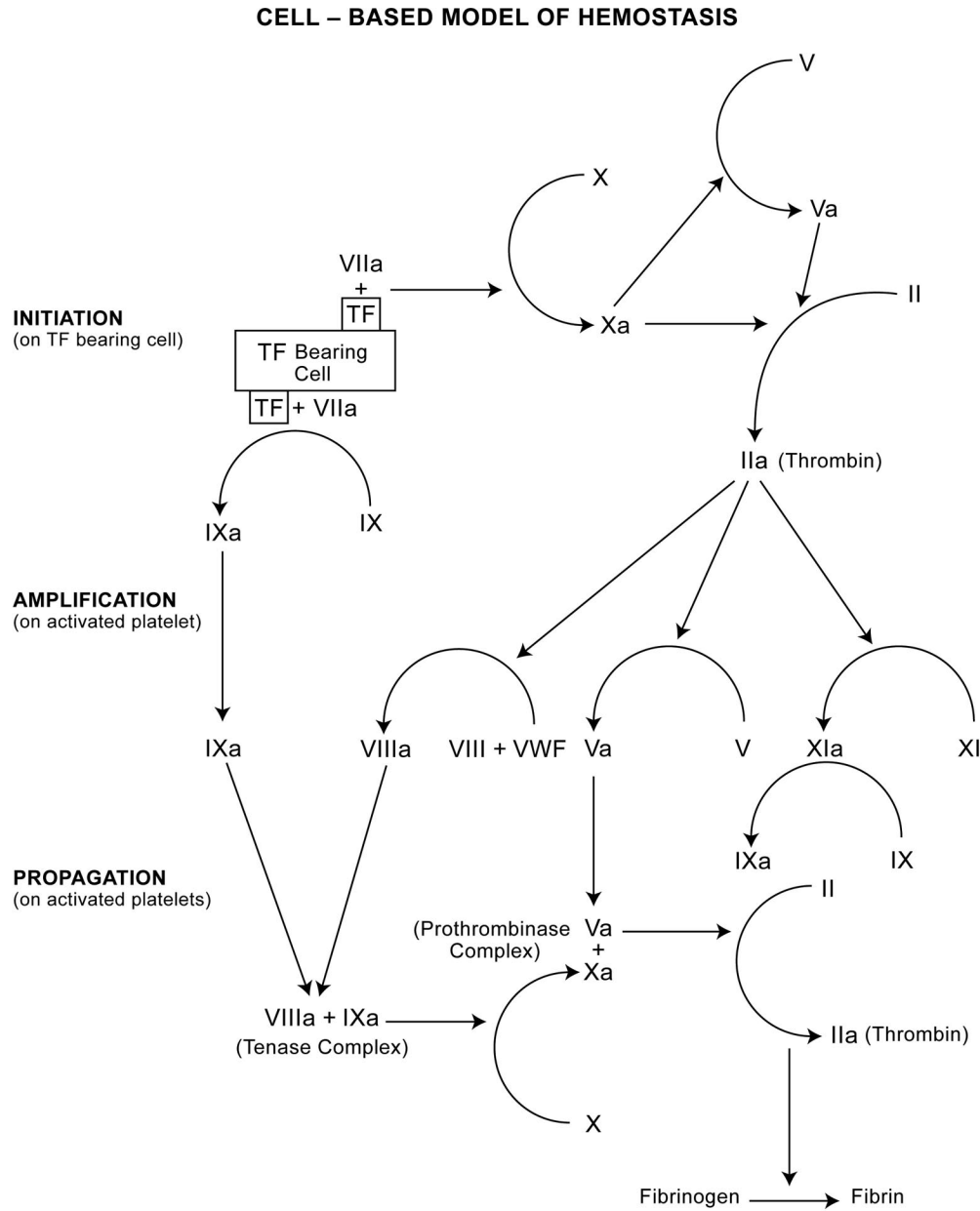


Figure 4: Cell-based clotting cascade model: initiation, amplification, propagation. Reproduced with permission from Vine, A. K., Recent advances in haemostasis and thrombosis. Retina 2009, 29 (1), 1-7. Copyright 2009, Ophthalmic Communications Society, Inc.

Pathologies of hemostasis

Table 1: Common coagulopathies (bleeding disorders)

Inherited Bleeding Disorders	Acquired Bleeding Disorders	Platelet Dysfunction
<ul style="list-style-type: none"> • Hemophilia A and B • von Willebrand disease • Other bleeding disorders <ul style="list-style-type: none"> ○ Factor deficiencies ○ Hypofibrinogenemia ○ Dysfibrinogenemia • Fibrinolytic bleeding disorders 	<ul style="list-style-type: none"> • Acquired factor inhibitors • Vitamin K deficiency • Super-warfarin poisoning • Liver disease • Thrombocytopenia, secondary to chemotherapy or radiation therapy 	<ul style="list-style-type: none"> • Acquired disorders <ul style="list-style-type: none"> ○ Drug effect ○ Myeloproliferative disorders • Congenital disorders <ul style="list-style-type: none"> ○ Glanzmann's thrombasthenia ○ Bernard-Soulier syndrome ○ Platelet storage pool disorders

Hemophilia and Clotting Factor Deficiencies

Hemophilia is an inherited bleeding disorder, with prevalence of 1/5,000 (hemophilia A) and 1/25,000 (hemophilia B).³⁶ Genetic mutations result in clotting factor FVIII and FIX deficiencies, respectively.³⁷ Its diagnosis consists of direct assay for the missing clotting factors and/or genetic screening. The deficiency of these factors results in a debilitated thrombin burst response, resulting in a destabilized clot that often cannot maintain integrity. Treatment of the missing clotting factors successfully treats these conditions. More recently recombinant factor VIIa (NovoSeven ®) has been used as both acute interventions for hemophiliacs during bleeding episodes as well as prophylactically.^{38,39}

von Willebrand Disease

von Willebrand disease is a deficiency of vWF, which is responsible for binding to the subendothelium and forming a strong binding site for activated platelets. A deficiency of this factor, results in the inability to form the initial platelet plug, causing a coagulopathy.³⁷ This is normally a hereditary disease, although there are many different

variations. vWF in addition to its role in mediating platelet binding to the subendothelium, also stabilizes FVIII in blood circulation.⁴⁰ Unsurprisingly von Willebrand disease is therefore also linked to FVIII deficiency. Treatment includes replacement of these missing factors, or induction of increased vWF release from endothelial cells with DDAVP (desamino-8-arginine vasopressin).⁴¹

Thrombocytopenia

Thrombocytopenia, a low platelet count ($<100 \times 10^9$ platelets/L, versus normal: $150-450 \times 10^9$) can arise from multiple disease states, as well as be acquired through drug treatment, especially chemotherapy and heparin. Treatment of thrombocytopenia depends largely on the etiology of its development. For example, in auto-immune cases, treatment usually consists of a combination of immune suppression, with corticosteroids, intravenous (i.v.) immune globulin (IVIG), or splenectomy, with newer treatment consisting of Rituximab, an anti-CD20 monoclonal antibody which prophylactically destroys CD20+ B-lymphocytes.⁴² On the other hand, management of thrombocytopenia during cancer therapy can be difficult as there is the opposite risk of thromboembolic events, as well as bleeding risks due to the conflicting pathophysiology.⁴³ These are approached, on a case-by-case basis depending on the type of cancer and the course of treatment.

Managing Clinical Trauma

Trauma can have very complex presentation, with multiple injuries and pathophysiology. Classically, the management of trauma has followed the ABC approach, defining the priority of systems to stabilize in a trauma victim: airway,

breathing, and circulation.⁴⁴ However it has been proposed that a new approach be considered, which includes the management of catastrophic bleeding as well, the <C> ABC approach.⁴⁴ The first priority is to rapidly control bleeding to prevent additional blood loss, followed by volume replacement therapy (crystalloid or blood product) and control blood pressure (vasopressors, inotropic agents).⁴⁵

The concept of the lethal triad was introduced to depict the need to manage the interplay between coagulopathy, hypothermia and metabolic acidosis. Together, these can lead a rapid decline in patients' status, due to decreased perfusion, shock and coagulopathy.⁴⁵ This may lead to additional bleeding, further antagonizing the situation. These factors and their management are listed in the table below (Table 2).

Table 2: Prevention of the lethal triad of coagulopathy, hypothermia, and acidosis. Reproduced with permission from Seyednejad, H.; Imani, M.; Jamieson, T.; Seifalian, A. M., Topical haemostatic agents. The British journal of surgery 2008, 95 (10), 1197-225. Copyright 2008, British Journal of Surgery Society Ltd.

Goal	Measures
Prevention of further bleeding	Immobilization Careful patient movement Damage control surgery
Maintenance of tissue oxygenation	Increase tissue perfusion (fluids and inotropic agents) Awareness of abdominal compartment syndrome
Coagulation support	FFP Factor concentrates Platelets
Normothermia	External measures to prevent further heat loss Warm fluids Rewarming devices (e.g., convective air warming system)

TREATMENT OF HEMORRHAGE

There is a dearth of tools to address internal bleeding. Methods that have been pursued include blood and blood product transfusions, and treatment with clotting factors such as recombinant factor VIIa (rFVIIa).⁴⁶ Recently, some groups have pursued novel strategies to engineer platelet substitutes to decrease the risk of allogenic transfusions, improve storage requirements, and decrease dependence on donor sources.⁴⁷⁻⁵⁰ The strategies listed below constitute tactics that are in use, or have been investigated for use, in damage control resuscitation.^{51,52}

Fluid resuscitation paradigms

Crystalloid

Crystalloid fluid resuscitation consists of isotonic saline, lactated ringers, or a variety of sugar-based solutions. Especially in the pre-hospital setting, resuscitation can be extremely important to prevent decreased tissue perfusion and hypovolemic shock. During the Vietnam era, lactated ringers solution became the standard crystalloid of choice to prevent hemorrhagic shock. However, this strategy came under scrutiny due to the edemic side effects of large volume resuscitation, leading to acute respiratory distress in some cases.⁵³ One study showed that hypertonic saline performed much better as a volume-expander, requiring less fluid to achieve the same rise in blood pressure.^{53,54} While fluid resuscitation is often indicated after trauma, there are some concerns about high-volume resuscitation leading to increased blood pressure during active hemorrhage as well as producing dilutional coagulopathy, which may further compromise hemostasis.^{52,55}

Colloid

Colloidal resuscitation fluids were introduced to the field as a result of the observation that crystalloid infusions significantly reduced the oncotic pressure (colloid osmotic pressure) of the blood, due to the introduced discrepancy in circulating plasma proteins, compared to colloidal fluids which significantly increased the oncotic pressure. Colloid resuscitation includes starches and hemoglobin-based oxygen carriers (HBOC).⁵⁶ However, several studies have shown that hydroxyethyl starch increased both *in vitro* and *in vivo* clotting times and decreased clot integrity.⁵⁷ HBOC, with its active component hemoglobin, was developed to compensate for the lost oxygen-carrying function of the lost blood. It has great potential, but may have limited clinical acceptance due to its vasoactivity, or propensity to increase blood pressures.⁵⁸

*Whole Blood and Blood Products*⁵⁹

Resuscitative strategies with whole blood or blood components—red blood cells (RBCs), fresh frozen plasma, platelets—are limited by their necessity for donor sources, immunocompatibility, need for refrigeration and risk of loss of activity during storage or preservation methods.⁴⁶ These complications limit their use to hospital settings. In the military, the development of walking blood banks, has provided one solution to sourcing blood donors on an as-needed basis. Essentially, volunteers are pre-screened every 90 days and volunteer to be called upon, and if needed, donate their blood to a specific person in need of transfusion.⁶ Blood and blood component resuscitation is the gold standard for treatment of massive hemorrhagic shock, but is unfortunately limited by supply and storage requirements.⁵³

Permissive Hypotension

Various strategies have been researched to deal with the issues of balancing fluid resuscitation to recover blood pressure, while simultaneously wanting to minimize the risk for rebleeding events and dilutional coagulopathy and edema.^{6,53} These range from resuscitating from a lower-than-normal blood pressure (mean arterial pressure, MAP=40 mmHg, compared to normotensive MAP=60-80), to maintaining a slow, but constant fluid infusion rate, to delaying resuscitation until definitive hemorrhage control is achieved.⁵³

Topical hemostats

Topical hemostats are useful for bleeding that is external in nature and cannot be controlled by tourniquets or pressure dressings and also for intraoperative, surgical bleeding where the bleeding is exposed and visible.^{60,61} The most common examples are made from collagen, gelatin, cellulose, polysaccharides, inorganic minerals, polymers and proteins such as albumin, fibrin and thrombin.⁶¹ Depending on the application, each hemostatic agent can have advantages and disadvantages, and may play a different role in augmenting hemostasis (Figure 5).

Gelatin, cellulose, crosslinked albumin (BioGlue ®) and some hydrogel-based products simply provide a tamponade effect as well as provide an adhesive matrix for protein, platelet and clot attachment.⁶¹ A mineral based topical hemostat, QuikClot ®, was previously comprised of hygroscopic zeolite mineral. This provided a tamponade effect by rapidly absorbing water from the injury site, allowing clotting factors to aggregate and form a clot. However, because this was such a highly exothermic reaction

(1st generation) and caused burns, the Z-Medica then altered its formulation to a mesh version of the zeolite that produced less heat (2nd generation), and now a kaolin-version (3rd generation) which has essentially the same absorbent effect as before, but less exothermic and additionally provides the direct clotting cascade activation of FXII and FXI.⁶²

Collagen, fibrin, thrombin and chitosan-based hemostats play an active role in the clotting cascade. Collagen can activate platelets, as well as provide a matrix for adhesion and recruitment. Fibrin and thrombin both help provide substrate for clot production and play an active role in signaling, and amplifying the coagulation cascade. Chitosan, with its strongly positively charged backbone, aids in cell recruitment, attachment and release of clotting factors.⁶¹

These topical agents have fundamentally changed trauma care, especially on the battlefield, and improved survival. They are light-weight, temperature stable, and extraordinarily effective at staunching bleeding in otherwise difficult-to-control places, such as junctional traumas (groin).⁶³

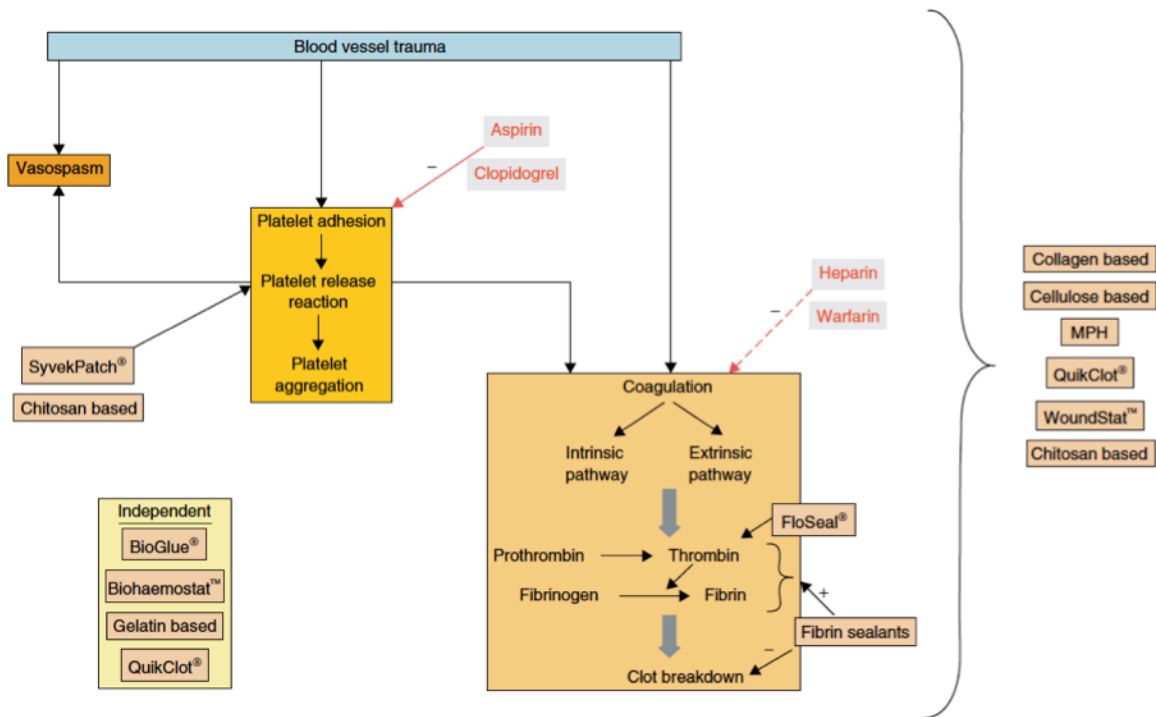


Figure 5: Review of topical hemostatic agents and their mechanism of action. Reproduced with permission from Rossaint, R.; Cerny, V.; Coats, T. J.; Duranteau, J.; Fernandez-Mondejar, E.; Gordini, G.; Stahel, P. F.; Hunt, B. J.; Neugebauer, E.; Spahn, D. R., Key issues in advanced bleeding care in trauma. Shock 2006, 26 (4), 322-31. Copyright 2006, The Shock Society.

Intravenous synthetic hemostats

Intravenous treatment with pharmacological agents that induce, or augment hemostasis is desirable in circumstances where the bleeding cannot be visualized, accessed, or stopped using topical hemostatic agents. Synthetic formulations of these agents, compared to blood component therapy, has been developed to avoid immunogenic response and donor source issues.⁵⁰

Tranexamic Acid

Tranexamic acid is a strong antagonist of plasminogen activation, and therefore acts as an antifibrinolytic. There is convincing evidence that its administration after trauma greatly improves outcomes, reducing (all cause) mortality by 23.9%-17.4%, in one study of 896 wounded soldiers at a military hospital in Afghanistan.^{64,65} However, it has the potential drawbacks of increasing risk of diffuse intravascular coagulation, increased risk when administered 3-8 hours after trauma, and increased risk when co-administered with blood products, and the practice of permissive hypotension due to a decreased glomerular filtration rate.⁶⁴ Nevertheless, it has tremendous potential, and may become incorporated in standard damage control resuscitation.⁷

Recombinant Factor VIIa (rFVIIa)⁶⁶⁻⁷¹

The administration of recombinant factor VIIa intravenously to reduce bleeding after acute trauma has been a topic of debate.^{9,11,69,70} Several studies have shown that perioperative administration of rFVIIa reduces the volume of blood transfusion. However, it is unclear whether the benefit is large enough to have any associated effect on mortality after hemorrhagic trauma.⁶⁶⁻⁶⁸ Its potential use in the prehospital phase is further diminished due to its high cost, potential for adverse effects, and necessity to be stored at 2-8 degrees C.^{11,68}

Synthetic Platelets

Intravenous administration of hemostatic nanoparticles that target activated platelets have been investigated by a number of groups with some promise and a range of challenges.^{47,48,72} These have been dubbed “synthetic platelets” or intravenous

hemostatic nanoparticles. However, it is important to note that these particles do not mimic the vast majority of platelet functions (factor secretion, pro-aggregatory stimulus, substrate). Most of these designs only act by augmenting platelet aggregation through the GPIIb/IIIa receptor, similar to fibrinogen (Figure 6).^{48,49,73-78} However, some groups have demonstrated increased hemostatic efficacy with heteromultivalent ligand approaches such that the particles (in this case liposomes) are both aggregatory through GPIIb/IIIa and adhesive to the activated endothelial cell adhesion molecule, P-selectin, vWF, or collagen.⁷⁹⁻⁸¹

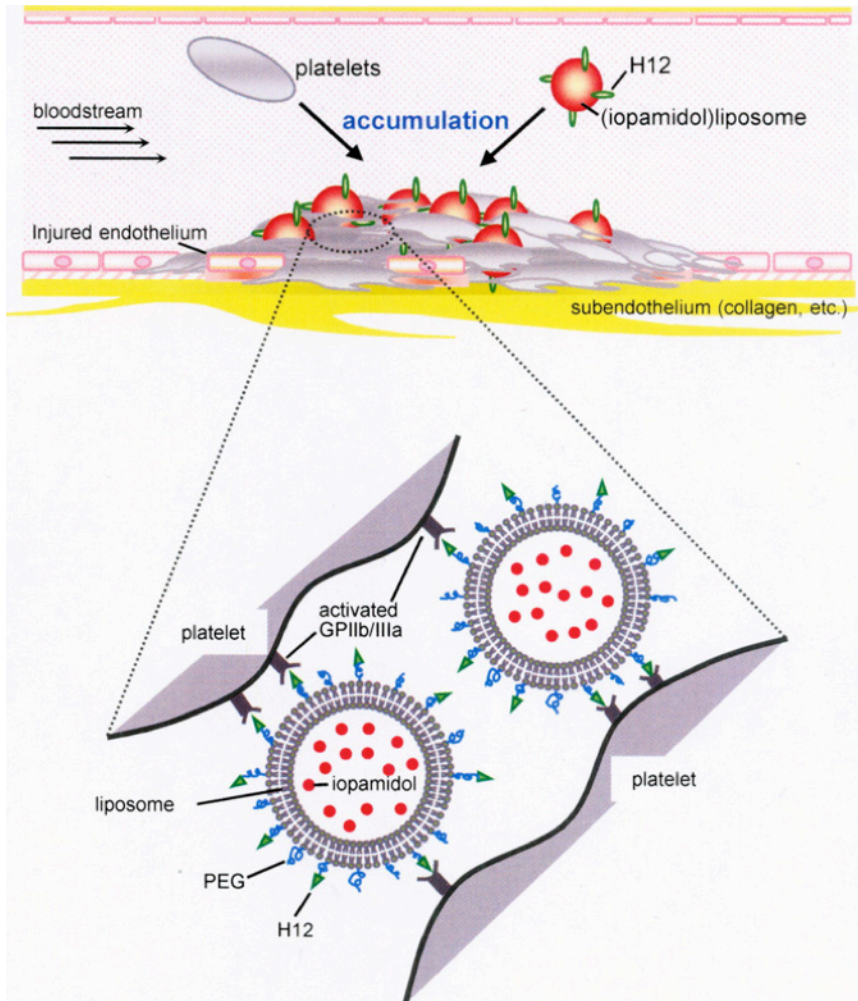


Figure 6: Depiction of H12-targeted liposomes, Okamura et al. Reproduced with permission from Okamura, Y.; Eto, K.; Maruyama, H.; Handa, M.; Ikeda, Y.; Takeoka, S., Visualization of liposomes carrying fibrinogen gamma-chain dodecapeptide accumulated to sites of vascular injury using computed tomography. *Nanomedicine* 2010, 6 (2), 391-6. Copyright 2010 Elsevier, Inc.

One of the first designs of a platelet substitute was introduced in 1992 and included both fibrinogen or RGD conjugated RBCs called thromboerythrocytes.^{49,75,82} These showed promise *in vitro* but did not significantly reduce prolonged bleeding times in thrombocytopenic primates.^{72,75} This work did elucidate the effect of linker length for the RGD-GPIIb/IIIa binding, showing with various n glycine repeats in the

peptide, (G)_nRGD, covalently bound to polyacrylonitrile beads, the optimal number was approximately 9-11 repeats, or 11-32 Å.⁸³

Fibrinogen-coated albumin microparticles, “Synthocytes”⁷⁷ and liposomes carrying the fibrinogen γ chain dodecapeptide H12 (HHLGGAKQAGDV)^{78,84} showed success in bleeding models in thrombocytopenic rabbits. However, Synthocytes were ineffective in treating bleeding in normal rabbits⁷⁷, and the liposomes from Okamura et al.^{78,84} do not appear to have yet been studied for this purpose. However, liposomes decorated with H12 were recently shown to significantly improve survival after a massive liver trauma model in thrombocytopenic rabbits.⁸⁵

POLYMER NANOPARTICLE SYNTHESIS METHODS

Overview

There are many different materials that have been engineered into nanoparticles (loosely defined as 1-1000 nm) for a vast number of applications: gold, iron oxide, diamond, polymers, naturally occurring biomaterials, and lipids to name a few.^{86,87} In the medical field, these applications have (non-inclusively) ranged from targeted drug delivery, gene delivery, photosensitizing agents for photodynamic therapy, imaging contrast agents, and theranostics (therapeutic & diagnostic hybrids).^{87,88}

For the application of synthetic platelets, one would want a nanoparticle that could be safely injected intravenously, augment platelet aggregation, reduce bleeding times, and also be degradable and cleared as the wound heals.^{73,89} This review will focus on the techniques used to create, collect and target nanoparticles made from

amphiphilic copolymers, as these are among the most studied nanoparticle systems that match the above criteria, and some even have clinical US Food and Drug Administration (FDA) track records.^{87,90}

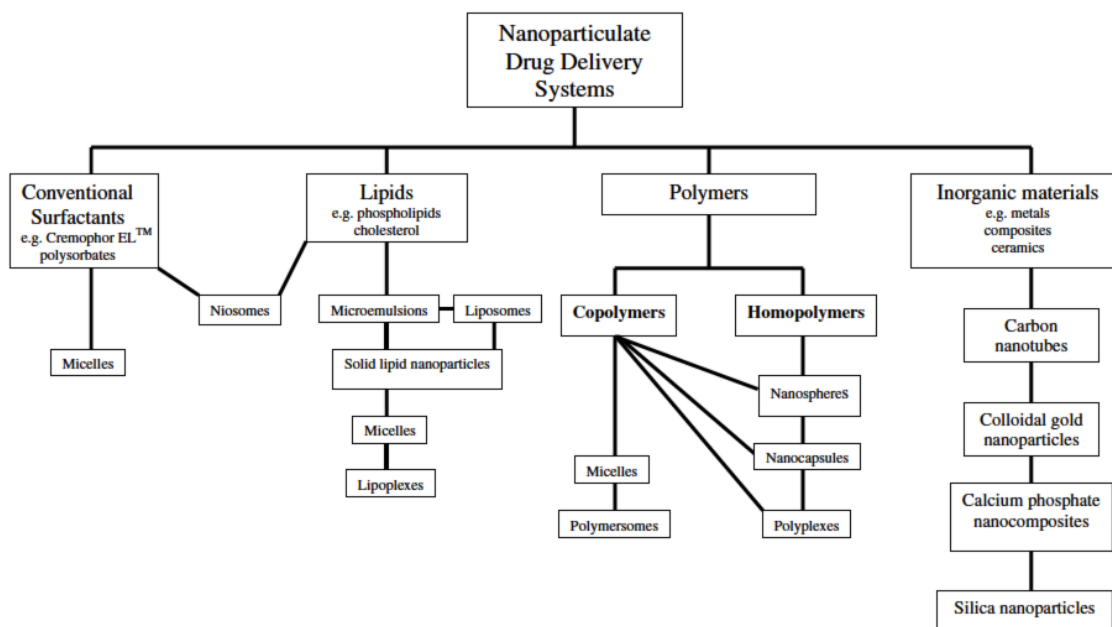


Figure 7: Nanoparticle systems researched for drug delivery applications. Reproduced with permission from Letchford, K.; Burt, H., A review of the formation and classification of amphiphilic block copolymer nanoparticulate structures: micelles, nanospheres, nanocapsules and polymersomes. European journal of pharmaceutics and biopharmaceutics : official journal of Arbeitsgemeinschaft fur Pharmazeutische Verfahrenstechnik e.V 2007, 65 (3), 259-69. Copyright 2007, Elsevier.

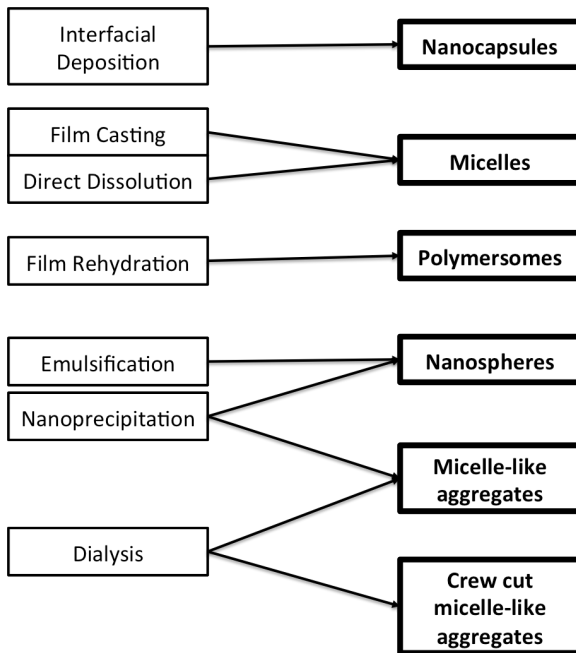


Figure 8: Nanoparticle synthesis methods, by particle type. Adapted with permission from Letchford, K.; Burt, H., A review of the formation and classification of amphiphilic block copolymer nanoparticulate structures: micelles, nanospheres, nanocapsules and polymersomes. European journal of pharmaceutics and biopharmaceutics: official journal of Arbeitsgemeinschaft fur Pharmazeutische Verfahrenstechnik e.V 2007, 65 (3), 259-69. Copyright 2007, Elsevier.

There are several well established methods to make biodegradable nanoparticles from amphiphilic coblock polymers: micelles, nanospheres, nanocapsules and polymersomes, each with a variety of methods to achieve particle formation (Figure 7, Figure 8).⁹⁰ These vary in their size, stability and characteristics of their core (which change their characteristics for drug loading).⁹⁰ For this review, I will focus on the nanospheres, which consist of amalgams of copolymer unimers locked together in a “frozen” state.⁹⁰ The most common synthesis methods for nanospheres are emulsion and nanoprecipitation.

Emulsion and nanoprecipitation

Emulsion

Emulsion is a process of nanosphere formation where the water-immiscible polymer is dissolved in an organic phase, and emulsified with an aqueous phase by mixing, vortexing, or higher energy inputs such as homogenization and sonication.^{91,92} The hydrophobic polymer is thermodynamically driven into the lowest energy state, a sphere, and dispersed with a surfactant—often poly(vinyl alcohol) (PVA), poly(ethylene glycol) (PEG), etc.).^{91,93} This emulsion can then be quenched by addition to a larger volume of aqueous phase (and sometimes further sonication), followed by removal of the organic phase by a combination of stirring, heat, evaporation, and/or vacuum.⁹⁴ Small hydrophobic drugs can be encapsulated in these nanoparticles by dissolving the drug in the organic phase during processing. Water soluble drugs can be loaded through a double emulsion processes, where drug is dissolved in the aqueous phase, emulsified in a an organic/polymer phase and then transferred into a larger volume, forming polymer particles with encapsulated drug in aqueous phase pockets.⁹²

Nanoprecipitation

Solvent displacement, or nanoprecipitation, is performed by dissolving a polymer in a water miscible solvent, and dropping it into a stirred aqueous phase.⁹⁵ Upon interacting with the aqueous phase, the organic phase diffuses away from the polymer, producing interfacial turbulence.⁹⁶ As above, these polymers are thermodynamically driven into spheres to minimize their surface energy and precipitate as the organic phase is diluted.⁹⁶

The pertinent issues to the design and production of synthetic platelets are: size distribution, repeatability, and scalability (heavily linked to cost). Varying size distribution with emulsion processes depends on solvent/polymer ratios, as well as energy imparted during the emulsification process. For nanoparticles this involves sonication, which can vary widely between labs, as well as within a lab person-to-person. Tuning size with nanoprecipitation can be performed just by changing solvent/polymer ratios, which remain consistent between investigators.^{95,97}

As for scalability, various microfluidic techniques have been employed to produce emulsions on a continuous basis. However, these preparations are generally done on a small batch-scale. For nanoprecipitation, because the main requirements are maintaining solvent/polymer/surfactant/aqueous ratios, this lends itself to continuous production methods as has been employed by Flash Nanoprecipitation method.⁹⁸⁻¹⁰³

Collection, storage and resuspension

Collection

Rinsing (solvent and surfactant removal) and nanoparticle collection is performed at laboratory scale by spray drying, freeze drying or most commonly by ultrafiltration (dialysis) or centrifugation.¹⁰⁴ Low yields and temperature stability limit spray drying's potential, and inefficiency and aggregate-formation limits the use of freeze drying.¹⁰⁴ Centrifugation and ultrafiltration (dialysis) are the most commonly performed. However, one of the greatest challenges of dialysis, is the low filtration rate and need to perform this method at low concentrations.¹⁰⁵ This is further limited with biodegradable polymers sensitive to hydrolysis. Centrifugation also presents a

challenge for suspending particles as these high-speed centrifugation steps often have tradeoffs between collection efficiency and aggregate formation. Finally, this collection method generally does not lend itself to scale up.¹⁰⁴

Several alternatives to these collection methods have been proposed by D'Addio et al. and Matteucci et al. involving flocculation of nanoparticles into loose open aggregates which can then be easily filtered or centrifuged at low speeds.^{104,106 107}

Storage and Resuspension

Nanoparticles are stored in suspension, frozen, or as a lyophilized product, depending on their stability in each phase. For biodegradable polymer nanoparticles, they are generally lyophilized for long-term storage. However, due to crystallization during processing, aggregates are formed, which then require sonication in order to recover pre-lyophilization size distributions.¹⁰⁶ This has led to the development and use of cryo- and lyo-protectants. Some of these involve sugars such as trehalose and sucrose, polymers PVA, poly(vinyl pyrrolidone) (PVP), and even matrices, such as gelatin.¹⁰⁸ Some concerns exist as to the concentrations of these excipients required in order to stabilize nanoparticles, for example a 1:1 w/w ratio in the case of trehalose, which could constitute a substantial dose of sugar depending on the application.¹⁰⁸ Since trehalose is normally digested and taken up in the blood stream normally as glucose, i.v. delivery may require further into safety and toxicity.¹⁰⁹ The use of surfactants such as Tween 80 (polysorbate 80), and other excipients are used to minimize the energy required to resuspend nanoparticles after lyophilization, however toxicity is always a potential concern.¹¹⁰

Targeting

Nanoparticles can be targeted, depending on the application, both passively and actively. Passive targeting is commonly found in cancer applications that take advantage of the endothelial permeability retention (EPR) effect.¹¹¹ Active targeting mechanisms include antibody-antigen, ligand-receptor interaction, nucleic acid hybridization, and gene expression among other application specific targeting mechanisms.¹¹¹ For the purposes of producing a temperature stable, cost-effective and fully synthetic targeted nanoparticle, short peptides provide an effective solution.¹¹¹

Peptide/Linker Length

The RGD moiety has been studied as a targeting peptide in a variety of applications as it is a ubiquitous peptide expressed in ECM molecules. It has been attached to a variety of synthetic platelet analogs including erythrocytes, albumin microparticles and polymeric nanoparticles.^{73,75,77} The effect of linker length for the RGD-GPIIb/IIIa binding was studied by Beer et al. using polyglycine as a spacer. They determined that 11-32 Å provided optimal spacing for this interaction.⁸³ Bertram et al. also investigated this interaction by examining platelet aggregation in the presence of plates bound with RGD with PEG spacers of various molecular weight (1500, 4600, 8000 Da). They found that the 4600 PEG, or ~152 Å, produced optimal platelet aggregation. They further postulated that this spacing was optimal to provide enough space to prevent steric interaction with the conjugated surface, while optimizing peptide presentation.⁷³ The differences between the studies' findings may be explained by differences between bound surfaces (polyacrylonitrile beads vs. polystyrene plates)

or linker composition (polyglycine vs. PEG). Optimal spacing is therefore likely to be design specific, but the common idea is that a spacer of sufficient length is required to prevent steric hindrance of the surface, and not too long that the peptide may be presented inward.

Other groups investigating synthetic platelets have developed heteromultivalent approaches such that the hemostatic nanoparticles have the ability to not only increase platelet aggregation, but also can themselves adhere to the vessel wall.⁷⁹ Modery-Pawlowksi et al. have shown that peptide lengths must be themselves of similar presentation length so as to not prevent binding through mutual steric interference.¹¹²

Ligand Density

With other peptide targeted nanotherapeutics, optimizing ligand density has been a popular topic of research.^{98,113-116} Gu et. al. developed a method to precisely engineer targeting-ligand-tunable nanoparticles for prostate cancer drug delivery and identified the narrow conjugation ratio that optimized targeting (5% for this application).¹¹³ Fakhari et. al. varied the ligand density of Cyclo-(1,12)-PenITDGEATDSGC (cLABEL) on poly(lactic-co-glycolic acid) (PLGA) nanoparticles to optimize the targeting of intercellular adhesion molecule-1 (ICAM-1), and found that the optimal density was roughly (50:50), and that particles with higher conjugation density performed worse.¹¹⁶ In all cases, it seems that the “optimal” conjugation of targeting ligand is highly application and condition-specific. In terms of the RGD-GPIIb/IIIa interaction that our nanoparticles utilize to augment platelet-platelet aggregation, there is evidence suggesting that receptor density may play a large role in

determining the nature and strength of this interaction.⁷⁴ Coller et. al. find that platelet binding to high density fibrinogen prevents aggregation of platelets to a plate through “paradoxical loss of luminal receptors”.⁷⁴ They postulated the high density signaling of the fibrinogen (containing RGD domains) causes translocation of the GPIIb/IIIa receptors to the site of binding, and prevents platelet binding on the luminal surface.

Due to the difficulty in surface characterization of ligand density, most groups only able to report peptide conjugation in terms of mole percent used during synthesis. However, due to disparities in methodology and materials, this may lead to highly variable surface conjugation outcomes. Unfortunately, this means that each particle, even if being used for a similar application, must go through an optimization process.

IN VITRO MODELS OF COAGULATION

These models vary intrinsically in their activation reagents, dependence on preparation (whole blood, platelet rich plasma, anticoagulation), and shear environment, among other extrinsic variables sample volume, point of care, and expense. Hemostasis and its associated pathologies are complex and accordingly each test has its own merits and drawbacks. A brief review will be presented here, but the reader is directed to Michelson^{16,117} or Pakala et al.¹¹⁸ for comprehensive reviews.

Platelet aggregation

Aggregometry

Platelet aggregometry can be performed either optically or using electrical impedance measurements. The benefits of using the latter is that the test can be

performed in whole blood rather than platelet rich plasma (PRP) and platelet poor plasma (PPP) preparations. Platelet aggregometry is generally performed in citrated blood. In the optical version, PRP and PPP are isolated from two aliquots of the same blood sample and placed in a spectrophotometer capable of measuring differential light transmittance between the two samples. The PRP can then be challenged by a number of pharmacological agents and activated (e.g. ADP or collagen). As the platelets aggregate, light transmittance increases. A characteristic pattern of activated by ADP shows a first-wave and second-wave of aggregation, the latter portion being indicative of dense granule release.^{16,118}

The challenges associated with classical aggregometry include a variable sample preparation as well as insensitivity to some pharmacological agents. It also lacks a shear component and therefore does not indicate any shear-mediated (e.g. vWF) pathologies.

Verify Now

The Verify Now (Accumetrics Inc., San Diego) system is similar to classical aggregometry except utilizes fibrinogen coated polystyrene beads to produce platelet agglutination specifically through the GPIIb/IIIa interaction. As the platelets in a whole blood sample agglutinate with the fibrinogen coated beads, they fall out of solution and light transmittance through the cuvette is increased. This assay is specifically sensitive to GPIIb/IIIa antagonists, although several adaptations have been made so that it can also be used to detect non-steroidal anti-inflammatory drug (NSAID) anticoagulation and P2Y₁₂ antagonists (e.g. clopidigrel).¹⁶

Platelet adhesion/aggregation

Hemostasis occurs under flow, and it is well documented that various platelet receptor-ligand interactions occur only under specific shear stress conditions, for example the vWF-GPIb interaction.¹¹⁹ Shear rates and wall shear stresses are very different in different vessels in the body, as well as during injury conditions and stenosis (Table 3).¹⁶ Therefore for the study of coagulopathies associated with shear-dependent mechanisms, the *in vitro* modeling of shear stress is crucial. Several *in vitro* methods that incorporate shear are presented below, but only represent a fraction of the multitude available.

Table 3: Shear rates and shear stresses in the vasculature. Reproduced with permission from Michelson, A. D., Platelets. 2nd ed.; Academic Press/Elsevier: Amsterdam ; Boston, 2007; p xlii, 1343 p. Copyright 2007 Elsevier.

Vessel	Diameter (cm)	Wall Shear Rate (sec ⁻¹)	Wall Shear Stress (dyne/cm ²)
Ascending aorta	2.3-4.5	50-300	2-10
Femoral artery	0.5	350	10
Small arteries	0.03	1500	5
Capillaries	0.0006	2,000-5,000	*
Large Veins	0.5-10	200	7
Inferior vena cava	2.0	50	2
Stenosed arteries	0.025	40,000	3,000

Parallel Plates

Parallel plates are the most common perfusion-type device used to study platelet-vessel wall interactions under shear. They consist of a pump (peristaltic, roller or syringe) and a chamber containing a coated glass coverslip.

While these systems are attractive for studying particular receptor-ligand interactions under shear and particular ECM coatings, they are limited by sample

preparation (anticoagulation, intrinsic platelet activation during collection, pump activation). Furthermore, they mimic physiological shear stress, but so far have not incorporated the other properties of the endothelium such as nitrous oxide (NO) release, pulsatile flow, and vessel compliance.¹⁶ However, that being said, advances in microfluidics technologies will certainly lead to an improved *in vitro* models of blood coagulation.¹²⁰

Impact Cone and Plate(let) Analyzer

The impact cone device uses a small whole blood sample, and introduces a uniform laminar shear field using a rotating cone. The platelets adhere to a collagen or ECM-coated surface which is then washed, stained and imaged using the plate(let) analyzer which quantifies surface coverage and average size of clusters and the number of objects in the image.¹⁶ The advantages of the system include aggregation and adherence in the presence of physiological shear, automated sample and point-of-care capability.¹¹⁸ The challenges associated with this method include a large dependence on sample hematocrit and its limited use, preventing comparisons across the literature.¹⁶

Whole blood coagulation

PFA-100

The platelet function analyzer (PFA-100, Siemens Healthcare Diagnostics, Inc., Deerfield, IL) is a device that utilizes a whole blood sample and passes it through a small capillary coated with either collagen and epinephrine or collagen and ADP.¹⁶ The platelets are shear activated in the 150 micron capillary ($4000-5000 \text{ sec}^{-1}$) and form a plug in the capillary layer by layer as platelets are deposited on the collagen. Closure

time is measured, and is sensitive to a wide variety of variables including platelet count, hematocrit, function of platelet adhesion receptors, vWF, age, gender and anticoagulant concentration.¹⁶ While it has gathered acceptance as a point-of-care measurement of global hemostatic parameters, it does not specifically an individual pathway.⁵² Therefore, if an abnormality is present, further testing may be indicated to determine the mechanism.¹²¹

Hemochron

The Hemochron Signature Elite (International Technidyne Corporation, Edison, NJ) system works under a similar principle as the PFA-100, except the cartridges are specially designed to activate blood in such a way to reproduce the clinical clotting parameters, activated clotting time (ACT), prothrombin time (PT), and activated partial thromboplastin time (APTT). It is commonly used in angiocatheter procedures to monitor levels of heparinization in a patient undergoing a procedure. However, while easy to use, this point-of-care instrument is limited in research applications by the inflexibility of the proprietary cartridges.¹²²

TEG/TEM

Thromboelastometry (TEM)—and similarly thromboelastography (TEG)—uses the principle of viscoelasticity to monitor/measure the formation of a clot as it develops. A whole blood sample (usually citrated) is placed in a cup, and a slow rotation is introduced by a pin, linked to a force sensor, which correlates with the sample viscosity. The subtle difference between TEG and TEM is the cup rotates in the former while the pin rotates in the latter. The data produced is split into 3 distinct regions:

clotting time (CT,R), clot formation (CFT,K) and fibrinolysis (ly,CL) (Figure 9). Other useful parameters include the clot formation first derivative (α -angle), and the maximum clot firmness (MCF,MA).⁵² There are a wide number of reagents, activators and antagonists that can be used in this system to probe for mechanisms of clotting factor coagulopathies.¹²³

Unfortunately, these systems are rather insensitive to pathologies of primary hemostasis and are not sensitive to platelet dysfunction, shear-mediated pathologies, and receptor interactions.¹¹⁸

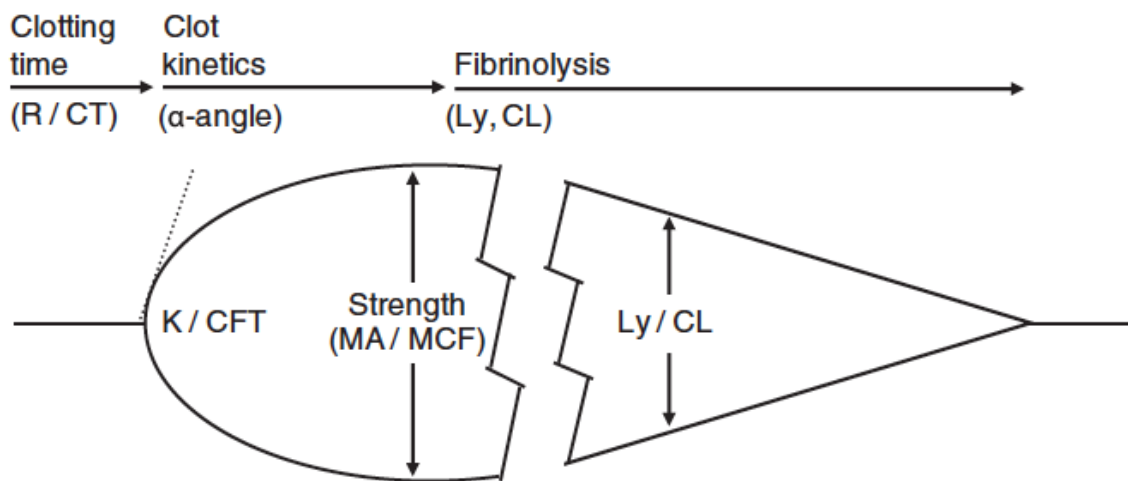


Figure 9: TEG/TEM parameters, including clotting time (R/CT), clot formation time (CFT/K), clot strength (MCF/MA), and fibrinolysis (CL/Ly). Reproduced from: Johansson, P. I.; Stensballe, J.; Ostrowski, S. R., Current management of massive hemorrhage in trauma. Scandinavian journal of trauma, resuscitation and emergency medicine 2012, 20, 47. Open Access Copyright 2012 Johansson et al.; licensee BioMed Central Ltd.

IN VIVO MODELS OF HEMOSTASIS

In vivo models of hemostasis are generally designed to assess the impact of a treatment (or knockout of a specific pathway) on clotting time, blood loss, degree of shock, and/or survival.¹²⁴ These models consist of controlled hemorrhage, uncontrolled hemorrhage, specific organ systems (e.g. CNS), or polytrauma.¹²⁴ Here, I will present a brief overview of the advantages and disadvantages of the various *in vivo* models that have been tested in uncontrolled hemorrhagic trauma, where the efficacy of a therapy such as synthetic platelets could be tested.

Mouse

Tail, Ear Bleeding Time

Murine hemorrhagic trauma models are generally limited to tail bleeding times in the literature.^{112,125-128} There are several publications looking at murine models in controlled hemorrhage, but are more utilized for examining the effects of hypovolemic shock and its rescue.¹²⁴ The advantages of using mice include their economy and wide availability, and availability of genetically-mutated strains, and the associated host of immune/biochemical assays.¹²⁴ However, the disadvantages are a limited correlation to human physiology, and an insensitivity to many coagulation defects.¹²⁵ The latter may possibly be due to the low-flow allowing vasospasm and other compensatory mechanisms to allow for normal bleeding times.¹²⁵

Rat

Tail, Ear Bleeding Times

Rat models that have been investigated include the same bleeding time models as the mouse.¹²⁹⁻¹³³ However, these studies are more often performed to look at the physiology and response to experimental treatments.¹²⁴ Surgical procedures are technically easier to perform on the rat, hemodynamics are slightly larger-scale, and they are still as widely available and relatively cheap like mice.¹²⁴

Lethal Liver Injury

There have also been a multitude of trauma models developed in the rat. One of the most widely published is a model of uncontrolled hemorrhage from a liver resection, with or without fluid resuscitation.¹³⁴⁻¹³⁷ The main outcomes studied in this model have included blood loss, survival, and blood metabolic outcomes (oxygenation) depending on the resuscitation paradigm.¹³⁵

The disadvantages of this model include a strong dependence on rat body mass and need for standardization of the liver resection.¹³⁴ Rats also tend to have a higher platelet count and a related lower clotting time compared to humans.¹³⁸ However, while there are moderate differences in hemodynamics and physiology from humans and larger animals, the coagulation cascade and associated mechanism appear to be relatively well-conserved: including platelet physiology, hepatic blood flow, and blood pressure regulation.¹³⁹⁻¹⁴²

Rabbit

Rabbit platelet counts, physiology and in-vitro clotting parameters are extremely well-correlated to humans,^{138,142} making them a viable candidate for an *in vivo* model of hemorrhage, and experimental therapies.

Thrombocytopenia

There are well-established protocols for inducing thrombocytopenia either chemically (busulfan)¹⁴³, radiation-therapy, or repeat blood draws/transfusion, and have been tested in conjunction with other synthetic platelet treatments.^{77,78,84,85}

Blood Loss and Bleeding Times

The majority of studies that have used the rabbit in a model of hemostasis have looked at bleeding times, or blood loss from surgical incisions.^{77,144-148} The limitations of bleeding times in both human and animal models is widely recognized.^{127,149} While it may produce a repeatable model, conclusions drawn must be limited to scope of isolated vascular injury, whereas the majority of clinical traumas are much more complex.^{125,127}

Lethal Liver Injury

Recently, Nishikawa et al. have published a paper investigating the use synthetic platelets to increase survival in a model of a liver trauma in thrombocytopenic rabbits.⁸⁵ This appears to be the first lethal liver trauma model developed in the rabbit, and appears to induce a repeatable injury.

Pig

Advantages

The pig is the standard model for uncontrolled hemorrhagic trauma, when investigating the physiological impact of a potential therapy.¹⁵⁰⁻¹⁵⁷ The cardiovascular system is well-correlated with human parameters and the comparable size allows for devices to be used in both clinical and research environment without modification.¹²⁴ Furthermore, the wound-healing process appears to be similar to the human due to similarities between porcine and human skin.¹²⁴

Disadvantages

The disadvantages of the porcine model include an increase in expenses due to the equipment, and need to for a technically-trained staff.¹²⁴ Furthermore, there is an increasing body of evidence that suggests pigs may be especially sensitive to complement activation and related pseudoallergy (CARPA).¹⁵⁸⁻¹⁶⁰ This latter issue will particularly be further addressed in Chapter 6, but briefly, it is a pseudoallergy observed after intravenous infusions of nanoparticles. Symptoms include severe hypotension, cardiopulmonary dysfunction, and if severe enough, death. The pathophysiological mechanisms of CARPA are still being elucidated, but it appears to be a result of acute complement system activation. Interestingly, other species are less susceptible to symptoms. However, it has been observed directly in both swine and dogs.^{158,160}

Primate

Non-human primates are the best animal analog of humans available. However, this makes their use in medical research controversial, and due to the administrative overhead, expensive. Thus, the use of primates in trauma is not well-suited for establishing efficacy in experimental therapies, except where the anatomical/physiological differences in other animals precludes their use. The majority of non-human primate studies (in hemorrhagic trauma) are for preclinical studies, where the main goal is testing safety.

Several hemorrhagic trauma models have been established.¹⁶¹⁻¹⁶⁴ Recently, of particular interest, Thrombosomes (a lyophilized hemostatic agent derived from platelets), underwent a safety study in rhesus macaques, in the presence of a hemorrhagic liver trauma.¹⁶⁴

WORKS CITED IN THIS CHAPTER

1. Krug, E.G., Sharma, G.K. & Lozano, R. The global burden of injuries. *American journal of public health* **90**, 523-526 (2000).
2. Sauaia, A., *et al.* Epidemiology of trauma deaths: a reassessment. *J Trauma* **38**, 185-193 (1995).
3. Kauvar, D.S., Lefering, R. & Wade, C.E. Impact of hemorrhage on trauma outcome: an overview of epidemiology, clinical presentations, and therapeutic considerations. *J Trauma* **60**, S3-11 (2006).
4. Champion, H.R., Bellamy, R.F., Roberts, C.P. & Leppaniemi, A. A profile of combat injury. *J Trauma* **54**, S13-19 (2003).
5. Holcomb, J.B., *et al.* Causes of death in U.S. Special Operations Forces in the global war on terrorism: 2001-2004. *Ann Surg* **245**, 986-991 (2007).
6. Schrager, J.J., Branson, R.D. & Johannigman, J.A. Lessons from the tip of the spear: medical advancements from Iraq and Afghanistan. *Respiratory care* **57**, 1305-1313 (2012).
7. Morrison, J.J. & Rasmussen, T.E. Noncompressible torso hemorrhage: a review with contemporary definitions and management strategies. *Surg Clin North Am* **92**, 843-858 (2012).

8. Kauvar, D.S. & Wade, C.E. The epidemiology and modern management of traumatic hemorrhage: US and international perspectives. *Crit Care* **9 Suppl 5**, S1-9 (2005).
9. Clifford, C.C. Treating traumatic bleeding in a combat setting. *Mil Med* **169**, 8-10, 14 (2004).
10. Kelly, J.F., *et al.* Injury severity and causes of death from Operation Iraqi Freedom and Operation Enduring Freedom: 2003-2004 versus 2006. *J Trauma* **64**, S21-26; discussion S26-27 (2008).
11. Martinowitz, U., Zaarur, M., Yaron, B.L., Blumenfeld, A. & Martonovits, G. Treating traumatic bleeding in a combat setting: possible role of recombinant activated factor VII. *Mil Med* **169**, 16-18, 14 (2004).
12. Regel, G., Stalp, M., Lehmann, U. & Seekamp, A. Prehospital care, importance of early intervention on outcome. *Acta anaesthesiologica Scandinavica. Supplementum* **110**, 71-76 (1997).
13. Acosta, J.A., *et al.* Lethal injuries and time to death in a level I trauma center. *Journal of the American College of Surgeons* **186**, 528-533 (1998).
14. Riddel, J.P., Jr., Aouizerat, B.E., Miaskowski, C. & Lillicrap, D.P. Theories of blood coagulation. *Journal of pediatric oncology nursing : official journal of the Association of Pediatric Oncology Nurses* **24**, 123-131 (2007).
15. Guyton, A.C. & Hall, J.E. *Textbook of medical physiology*, (Elsevier Saunders, Philadelphia, 2006).
16. Michelson, A.D. *Platelets*, (Academic Press/Elsevier, Amsterdam ; Boston, 2007).
17. Nievelstein, P.F. & de Groot, P.G. Interaction of blood platelets with the vessel wall. *Haemostasis* **18**, 342-359 (1988).
18. Nievelstein, P.F., D'Alessio, P.A. & Sixma, J.J. Fibronectin in platelet adhesion to human collagen types I and III. Use of nonfibrillar and fibrillar collagen in flowing blood studies. *Arteriosclerosis* **8**, 200-206 (1988).
19. Nievelstein, P.F. & Sixma, J.J. Glycoprotein IIb-IIIa and RGD(S) are not important for fibronectin-dependent platelet adhesion under flow conditions. *Blood* **72**, 82-88 (1988).
20. Hindriks, G., Ijsseldijk, M.J., Sonnenberg, A., Sixma, J.J. & de Groot, P.G. Platelet adhesion to laminin: role of Ca²⁺ and Mg²⁺ ions, shear rate, and platelet membrane glycoproteins. *Blood* **79**, 928-935 (1992).
21. Agbanyo, F.R., Sixma, J.J., de Groot, P.G., Languino, L.R. & Plow, E.F. Thrombospondin-platelet interactions. Role of divalent cations, wall shear rate, and platelet membrane glycoproteins. *J Clin Invest* **92**, 288-296 (1993).
22. Alevriadou, B.R., *et al.* Real-time analysis of shear-dependent thrombus formation and its blockade by inhibitors of von Willebrand factor binding to platelets. *Blood* **81**, 1263-1276 (1993).
23. Andrieux, A., *et al.* Amino acid sequences in fibrinogen mediating its interaction with its platelet receptor, GPIIb/IIIa. *The Journal of biological chemistry* **264**, 9258-9265 (1989).
24. Lam, S.C., *et al.* Evidence that arginyl-glycyl-aspartate peptides and fibrinogen gamma chain peptides share a common binding site on platelets. *The Journal of biological chemistry* **262**, 947-950 (1987).

25. Weisel, J.W., Nagaswami, C., Vilaire, G. & Bennett, J.S. Examination of the platelet membrane glycoprotein IIb-IIIa complex and its interaction with fibrinogen and other ligands by electron microscopy. *The Journal of biological chemistry* **267**, 16637-16643 (1992).
26. Rendu, F. & Brohard-Bohn, B. The platelet release reaction: granules' constituents, secretion and functions. *Platelets* **12**, 261-273 (2001).
27. Davie, E.W. & Ratnoff, O.D. Waterfall Sequence for Intrinsic Blood Clotting. *Science* **145**, 1310-1312 (1964).
28. Macfarlane, R.G. An Enzyme Cascade in the Blood Clotting Mechanism, and Its Function as a Biochemical Amplifier. *Nature* **202**, 498-499 (1964).
29. Davie, E.W., Fujikawa, K. & Kisiel, W. The coagulation cascade: initiation, maintenance, and regulation. *Biochemistry* **30**, 10363-10370 (1991).
30. Dahlback, B. Blood coagulation. *Lancet* **355**, 1627-1632 (2000).
31. Seligsohn, U. Factor XI in haemostasis and thrombosis: past, present and future. *Thrombosis and haemostasis* **98**, 84-89 (2007).
32. Gailani, D. & Broze, G.J., Jr. Factor XI activation in a revised model of blood coagulation. *Science* **253**, 909-912 (1991).
33. Naito, K. & Fujikawa, K. Activation of human blood coagulation factor XI independent of factor XII. Factor XI is activated by thrombin and factor XIa in the presence of negatively charged surfaces. *The Journal of biological chemistry* **266**, 7353-7358 (1991).
34. Osterud, B. & Rapaport, S.I. Activation of factor IX by the reaction product of tissue factor and factor VII: additional pathway for initiating blood coagulation. *Proceedings of the National Academy of Sciences of the United States of America* **74**, 5260-5264 (1977).
35. Vine, A.K. Recent advances in haemostasis and thrombosis. *Retina* **29**, 1-7 (2009).
36. Segers, K., Dahlback, B. & Nicolaes, G.A. Coagulation factor V and thrombophilia: background and mechanisms. *Thrombosis and haemostasis* **98**, 530-542 (2007).
37. Peyvandi, F., *et al.* Genetic diagnosis of haemophilia and other inherited bleeding disorders. *Haemophilia : the official journal of the World Federation of Hemophilia* **12 Suppl 3**, 82-89 (2006).
38. Lee, C.A., Berntorp, E. & Hoots, K. *Textbook of hemophilia*, (Wiley-Blackwell, Chichester, West Sussex, UK ; Hoboken, NJ, 2010).
39. Ljung, R. Hemophilia and prophylaxis. *Pediatric blood & cancer* **60 Suppl 1**, S23-26 (2013).
40. Wise, R.J., Dorner, A.J., Krane, M., Pittman, D.D. & Kaufman, R.J. The role of von Willebrand factor multimers and propeptide cleavage in binding and stabilization of factor VIII. *The Journal of biological chemistry* **266**, 21948-21955 (1991).
41. Akin, M. Response to low-dose desmopressin by a subcutaneous route in children with type 1 von Willebrand disease. *Hematology* (2013).
42. Arnold, D.M. Positioning new treatments in the management of immune thrombocytopenia. *Pediatric blood & cancer* **60 Suppl 1**, S19-22 (2013).

43. Falanga, A. & Marchetti, M. Anticancer treatment and thrombosis. *Thrombosis research* **129**, 353-359 (2012).
44. Hodgetts, T.J., Mahoney, P.F., Russell, M.Q. & Byers, M. ABC to <C>ABC: redefining the military trauma paradigm. *Emergency medicine journal : EMJ* **23**, 745-746 (2006).
45. Rossaint, R., *et al.* Key issues in advanced bleeding care in trauma. *Shock* **26**, 322-331 (2006).
46. Nunez, T.C. & Cotton, B.A. Transfusion therapy in hemorrhagic shock. *Curr Opin Crit Care* **15**, 536-541 (2009).
47. Blajchman, M.A. Platelet substitutes. *Vox Sang* **78 Suppl 2**, 183-186 (2000).
48. Blajchman, M.A. Novel platelet products, substitutes and alternatives. *Transfus Clin Biol* **8**, 267-271 (2001).
49. Lee, D.H. & Blajchman, M.A. Novel treatment modalities: new platelet preparations and substitutes. *British journal of haematology* **114**, 496-505 (2001).
50. Vamvakas, E.C. & Blajchman, M.A. Transfusion-related mortality: the ongoing risks of allogeneic blood transfusion and the available strategies for their prevention. *Blood* **113**, 3406-3417 (2009).
51. Hodgetts, T.J., Mahoney, P.F. & Kirkman, E. Damage control resuscitation. *Journal of the Royal Army Medical Corps* **153**, 299-300 (2007).
52. Johansson, P.I., Stensballe, J. & Ostrowski, S.R. Current management of massive hemorrhage in trauma. *Scandinavian journal of trauma, resuscitation and emergency medicine* **20**, 47 (2012).
53. Santry, H.P. & Alam, H.B. Fluid resuscitation: past, present, and the future. *Shock* **33**, 229-241 (2010).
54. Velasco, I.T., Pontieri, V., Rocha e Silva, M., Jr. & Lopes, O.U. Hyperosmotic NaCl and severe hemorrhagic shock. *The American journal of physiology* **239**, H664-673 (1980).
55. Chappell, D., Jacob, M., Hofmann-Kiefer, K., Conzen, P. & Rehm, M. A rational approach to perioperative fluid management. *Anesthesiology* **109**, 723-740 (2008).
56. Stern, S., *et al.* Resuscitation with the hemoglobin-based oxygen carrier, HBOC-201, in a swine model of severe uncontrolled hemorrhage and traumatic brain injury. *Shock* **31**, 64-79 (2009).
57. Hartog, C.S., Skupin, H., Natanson, C., Sun, J. & Reinhart, K. Systematic analysis of hydroxyethyl starch (HES) reviews: proliferation of low-quality reviews overwhelms the results of well-performed meta-analyses. *Intensive care medicine* **38**, 1258-1271 (2012).
58. Freilich, D., *et al.* HBOC-201 vasoactivity in a phase III clinical trial in orthopedic surgery subjects--extrapolation of potential risk for acute trauma trials. *J Trauma* **66**, 365-376 (2009).
59. Kauvar, D.S., Holcomb, J.B., Norris, G.C. & Hess, J.R. Fresh whole blood transfusion: a controversial military practice. *J Trauma* **61**, 181-184 (2006).
60. Achneck, H.E., *et al.* A comprehensive review of topical hemostatic agents: efficacy and recommendations for use. *Ann Surg* **251**, 217-228 (2010).

61. Seyednejad, H., Imani, M., Jamieson, T. & Seifalian, A.M. Topical haemostatic agents. *The British journal of surgery* **95**, 1197-1225 (2008).
62. Z-Medica. The Groundbreaking Technology Behind QuikClot® Hemostasis Products. Vol. 2013 (Z-Medica, WebPage, 2013).
63. Johnson, D., *et al.* The effects of QuikClot Combat Gauze on hemorrhage control in the presence of hemodilution. *U.S. Army Medical Department journal*, 36-39 (2012).
64. Rappold, J.F. & Pusateri, A.E. Tranexamic acid in remote damage control resuscitation. *Transfusion* **53 Suppl 1**, 96S-99S (2013).
65. Pusateri, A.E., *et al.* Tranexamic Acid and Trauma: Current Status and Knowledge Gaps With Recommended Research Priorities. *Shock* **39**, 121-126 (2013).
66. Boffard, K.D., *et al.* Recombinant factor VIIa as adjunctive therapy for bleeding control in severely injured trauma patients: two parallel randomized, placebo-controlled, double-blind clinical trials. *J Trauma* **59**, 8-15; discussion 15-18 (2005).
67. Duchesne, J.C., *et al.* Current evidence based guidelines for factor VIIa use in trauma: the good, the bad, and the ugly. *Am Surg* **74**, 1159-1165 (2008).
68. Morse, B.C., *et al.* The effects of protocolized use of recombinant factor VIIa within a massive transfusion protocol in a civilian level I trauma center. *Am Surg* **77**, 1043-1049 (2011).
69. Patanwala, A.E. Factor VIIa (recombinant) for acute traumatic hemorrhage. *Am J Health Syst Pharm* **65**, 1616-1623 (2008).
70. Stein, D.M. & Dutton, R.P. Uses of recombinant factor VIIa in trauma. *Curr Opin Crit Care* **10**, 520-528 (2004).
71. Benharash, P., Bongard, F. & Putnam, B. Use of recombinant factor VIIa for adjunctive hemorrhage control in trauma and surgical patients. *Am Surg* **71**, 776-780 (2005).
72. Alving, B.M., Reid, T.J., Fratantoni, J.C. & Finlayson, J.S. Frozen platelets and platelet substitutes in transfusion medicine. *Transfusion* **37**, 866-876 (1997).
73. Bertram, J.P., *et al.* Intravenous hemostat: nanotechnology to halt bleeding. *Science translational medicine* **1**, 11ra22 (2009).
74. Collier, B.S., *et al.* Studies of activated GPIIb/IIIa receptors on the luminal surface of adherent platelets. Paradoxical loss of luminal receptors when platelets adhere to high density fibrinogen. *J Clin Invest* **92**, 2796-2806 (1993).
75. Collier, B.S., *et al.* Thromboerythrocytes. In vitro studies of a potential autologous, semi-artificial alternative to platelet transfusions. *J Clin Invest* **89**, 546-555 (1992).
76. Davies, A.R., Judge, H.M., May, J.A., Glenn, J.R. & Heptinstall, S. Interactions of platelets with Synthocytes, a novel platelet substitute. *Platelets* **13**, 197-205 (2002).
77. Levi, M., *et al.* Fibrinogen-coated albumin microcapsules reduce bleeding in severely thrombocytopenic rabbits. *Nat Med* **5**, 107-111 (1999).
78. Okamura, Y., *et al.* Visualization of liposomes carrying fibrinogen gamma-chain dodecapeptide accumulated to sites of vascular injury using computed tomography. *Nanomedicine* **6**, 391-396 (2010).

79. Modery, C.L., *et al.* Heteromultivalent liposomal nanoconstructs for enhanced targeting and shear-stable binding to active platelets for site-selective vascular drug delivery. *Biomaterials* **32**, 9504-9514 (2011).
80. Ravikumar, M., Modery, C.L., Wong, T.L., Dzuricky, M. & Sen Gupta, A.P.D. Mimicking Adhesive Functionalities of Blood Platelets using Ligand-Decorated Liposomes. *Bioconjug Chem* (2012).
81. Ravikumar, M., Modery, C.L., Wong, T.L. & Gupta, A.S. Peptide-decorated liposomes promote arrest and aggregation of activated platelets under flow on vascular injury relevant protein surfaces in vitro. *Biomacromolecules* **13**, 1495-1502 (2012).
82. Agam, G. & Livne, A.A. Erythrocytes with covalently bound fibrinogen as a cellular replacement for the treatment of thrombocytopenia. *European journal of clinical investigation* **22**, 105-112 (1992).
83. Beer, J.H., Springer, K.T. & Collier, B.S. Immobilized Arg-Gly-Asp (RGD) peptides of varying lengths as structural probes of the platelet glycoprotein IIb/IIIa receptor. *Blood* **79**, 117-128 (1992).
84. Okamura, Y., *et al.* Hemostatic effects of phospholipid vesicles carrying fibrinogen gamma chain dodecapeptide in vitro and in vivo. *Bioconjug Chem* **16**, 1589-1596 (2005).
85. Nishikawa, K., *et al.* Fibrinogen gamma-chain peptide-coated, ADP-encapsulated liposomes rescue thrombocytopenic rabbits from non-compressible liver hemorrhage. *Journal of thrombosis and haemostasis : JTH* **10**, 2137-2148 (2012).
86. Bhattacharyya, S., Kudgus, R.A., Bhattacharya, R. & Mukherjee, P. Inorganic nanoparticles in cancer therapy. *Pharmaceutical research* **28**, 237-259 (2011).
87. Danhier, F., *et al.* PLGA-based nanoparticles: an overview of biomedical applications. *Journal of controlled release : official journal of the Controlled Release Society* **161**, 505-522 (2012).
88. Prabhu, P. & Patravale, V. The upcoming field of theranostic nanomedicine: an overview. *Journal of biomedical nanotechnology* **8**, 859-882 (2012).
89. Chang, T.M. From artificial red blood cells, oxygen carriers, and oxygen therapeutics to artificial cells, nanomedicine, and beyond. *Artificial cells, blood substitutes, and immobilization biotechnology* **40**, 197-199 (2012).
90. Letchford, K. & Burt, H. A review of the formation and classification of amphiphilic block copolymer nanoparticulate structures: micelles, nanospheres, nanocapsules and polymersomes. *European journal of pharmaceuticals and biopharmaceutics : official journal of Arbeitsgemeinschaft fur Pharmazeutische Verfahrenstechnik e.V* **65**, 259-269 (2007).
91. Bodmeier, R. & McGinity, J.W. The preparation and evaluation of drug-containing poly(dl-lactide) microspheres formed by the solvent evaporation method. *Pharmaceutical research* **4**, 465-471 (1987).
92. Rosca, I.D., Watari, F. & Uo, M. Microparticle formation and its mechanism in single and double emulsion solvent evaporation. *Journal of controlled release : official journal of the Controlled Release Society* **99**, 271-280 (2004).

93. Whitby, C.P., Lim, L.H., Eskandar, N.G., Simovic, S. & Prestidge, C.A. Poly(lactic-co-glycolic acid) as a particulate emulsifier. *Journal of colloid and interface science* **375**, 142-147 (2012).
94. Bahl, Y. & Sah, H. Dynamic changes in size distribution of emulsion droplets during ethyl acetate-based microencapsulation process. *AAPS PharmSciTech* **1**, E5 (2000).
95. Galindo-Rodriguez, S., Allemann, E., Fessi, H. & Doelker, E. Physicochemical parameters associated with nanoparticle formation in the salting-out, emulsification-diffusion, and nanoprecipitation methods. *Pharmaceutical research* **21**, 1428-1439 (2004).
96. Miller, C.A. Spontaneous Emulsification Produced by Diffusion - a Review. *Colloid Surface* **29**, 89-102 (1988).
97. Cheng, J., *et al.* Formulation of functionalized PLGA-PEG nanoparticles for in vivo targeted drug delivery. *Biomaterials* **28**, 869-876 (2007).
98. Gindy, M.E., Ji, S., Hoyer, T.R., Panagiotopoulos, A.Z. & Prud'homme, R.K. Preparation of poly(ethylene glycol) protected nanoparticles with variable bioconjugate ligand density. *Biomacromolecules* **9**, 2705-2711 (2008).
99. Figueroa, C.E., Reider, P., Burckel, P., Pinkerton, A.A. & Prud'homme, R.K. Highly loaded nanoparticulate formulation of progesterone for emergency traumatic brain injury treatment. *Therapeutic delivery* **3**, 1269-1279 (2012).
100. Chen, T., *et al.* Protected peptide nanoparticles: experiments and brownian dynamics simulations of the energetics of assembly. *Nano letters* **9**, 2218-2222 (2009).
101. Chen, T., Hynninen, A.P., Prud'homme, R.K., Kevrekidis, I.G. & Panagiotopoulos, A.Z. Coarse-grained simulations of rapid assembly kinetics for polystyrene-b-poly(ethylene oxide) copolymers in aqueous solutions. *The journal of physical chemistry. B* **112**, 16357-16366 (2008).
102. Gindy, M.E., Panagiotopoulos, A.Z. & Prud'homme, R.K. Composite block copolymer stabilized nanoparticles: simultaneous encapsulation of organic actives and inorganic nanostructures. *Langmuir : the ACS journal of surfaces and colloids* **24**, 83-90 (2008).
103. Liu, Y., Kathan, K., Saad, W. & Prud'homme, R.K. Ostwald ripening of beta-carotene nanoparticles. *Physical review letters* **98**, 036102 (2007).
104. Matteucci, M.E., Paguio, J.C., Miller, M.A., Williams Iii, R.O. & Johnston, K.P. Flocculated amorphous nanoparticles for highly supersaturated solutions. *Pharmaceutical research* **25**, 2477-2487 (2008).
105. Limayem, I., Charcosset, C. & Fessi, H. Purification of nanoparticle suspensions by a concentration/diafiltration process. *Sep Purif Technol* **38**, 1-9 (2004).
106. D'Addio, S.M., *et al.* Novel method for concentrating and drying polymeric nanoparticles: hydrogen bonding coacervate precipitation. *Mol Pharm* **7**, 557-564 (2010).
107. Fujiwara, M., Grubbs, R.H. & Baldeschwieler, J.D. Characterization of pH-Dependent Poly(acrylic Acid) Complexation with Phospholipid Vesicles. *Journal of colloid and interface science* **185**, 210-216 (1997).

108. Abdelwahed, W., Degobert, G., Stainmesse, S. & Fessi, H. Freeze-drying of nanoparticles: formulation, process and storage considerations. *Advanced drug delivery reviews* **58**, 1688-1713 (2006).
109. Richards, A.B., *et al.* Trehalose: a review of properties, history of use and human tolerance, and results of multiple safety studies. *Food and chemical toxicology : an international journal published for the British Industrial Biological Research Association* **40**, 871-898 (2002).
110. Varma, R.K., *et al.* Polysorbate 80: a pharmacological study. *Arzneimittel-Forschung* **35**, 804-808 (1985).
111. Jabbari, E. Targeted delivery with peptidomimetic conjugated self-assembled nanoparticles. *Pharmaceutical research* **26**, 612-630 (2009).
112. Modery-Pawlowski, C.L., Tian, L.L., Ravikumar, M., Wong, T.L. & Gupta, A.S. In vitro and in vivo hemostatic capabilities of a functionally integrated platelet-mimetic liposomal nanoconstruct. *Biomaterials* (2013).
113. Gu, F., *et al.* Precise engineering of targeted nanoparticles by using self-assembled biointegrated block copolymers. *Proceedings of the National Academy of Sciences of the United States of America* **105**, 2586-2591 (2008).
114. Garg, A., Tisdale, A.W., Haidari, E. & Kokkoli, E. Targeting colon cancer cells using PEGylated liposomes modified with a fibronectin-mimetic peptide. *International journal of pharmaceutics* **366**, 201-210 (2009).
115. Olivier, V., *et al.* Influence of targeting ligand flexibility on receptor binding of particulate drug delivery systems. *Bioconjug Chem* **14**, 1203-1208 (2003).
116. Fakhari, A., Baoum, A., Siahaan, T.J., Le, K.B. & Berkland, C. Controlling ligand surface density optimizes nanoparticle binding to ICAM-1. *Journal of pharmaceutical sciences* **100**, 1045-1056 (2011).
117. Michelson, A.D. Methods for the measurement of platelet function. *The American journal of cardiology* **103**, 20A-26A (2009).
118. Pakala, R. & Waksman, R. Currently available methods for platelet function analysis: advantages and disadvantages. *Cardiovascular revascularization medicine : including molecular interventions* **12**, 312-322 (2011).
119. Schmutz, M., Rand, M.L. & Freedman, J. Platelets and von Willebrand factor. *Transfusion and apheresis science : official journal of the World Apheresis Association : official journal of the European Society for Haemapheresis* **28**, 269-277 (2003).
120. Wong, K.H., Chan, J.M., Kamm, R.D. & Tien, J. Microfluidic models of vascular functions. *Annual review of biomedical engineering* **14**, 205-230 (2012).
121. Favalaro, E.J. Clinical utility of the PFA-100. *Seminars in thrombosis and hemostasis* **34**, 709-733 (2008).
122. Ojito, J.W., *et al.* Comparison of point-of-care activated clotting time systems utilized in a single pediatric institution. *The Journal of extra-corporeal technology* **44**, 15-20 (2012).
123. Schochl, H., *et al.* Thromboelastometric (ROTEM) findings in patients suffering from isolated severe traumatic brain injury. *J Neurotrauma* **28**, 2033-2041 (2011).

124. Frink, M., Andruszkow, H., Zeckey, C., Krettek, C. & Hildebrand, F. Experimental trauma models: an update. *Journal of biomedicine & biotechnology* **2011**, 797383 (2011).
125. Greene, T.K., Schiviz, A., Hoellriegl, W., Poncz, M. & Muchitsch, E.M. Towards a standardization of the murine tail bleeding model. *Journal of thrombosis and haemostasis : JTH* **8**, 2820-2822 (2010).
126. Broze, G.J., Jr., Yin, Z.F. & Lasky, N. A tail vein bleeding time model and delayed bleeding in hemophiliac mice. *Thrombosis and haemostasis* **85**, 747-748 (2001).
127. Dejana, E., Quintana, A., Callioni, A. & de Gaetano, G. Bleeding time in laboratory animals. III - Do tail bleeding times in rats only measure a platelet defect? (the aspirin puzzle). *Thrombosis research* **15**, 199-207 (1979).
128. De Clerck, F., Goossens, J. & Reneman, R. Effects of anti-inflammatory, anticoagulant and vasoactive compounds on tail bleeding time, whole blood coagulation time and platelet retention by glass beads in rats. *Thrombosis research* **8**, 179-193 (1976).
129. Johansen, P.B., *et al.* Automated registration of tail bleeding in rats. *Thrombosis and haemostasis* **99**, 956-962 (2008).
130. Hui, Y.H., *et al.* Pharmacokinetic comparisons of tail-bleeding with cannula- or retro-orbital bleeding techniques in rats using six marketed drugs. *Journal of pharmacological and toxicological methods* **56**, 256-264 (2007).
131. Buczko, W., Gambino, M.C. & De Gaetano, G. Prolongation of rat tail bleeding time by ketanserin: mechanisms of action. *European journal of pharmacology* **103**, 261-268 (1984).
132. Shek, P.N. & Howe, S.A. A novel method for the rapid bleeding of rats from the tail vein. *Journal of immunological methods* **53**, 255-260 (1982).
133. Butler, K.D., *et al.* Prolongation of rat tail bleeding time caused by oral doses of a thromboxane synthetase inhibitor which have little effect on platelet aggregation. *Thrombosis and haemostasis* **47**, 46-49 (1982).
134. Holcomb, J.B., *et al.* Fibrin sealant foam sprayed directly on liver injuries decreases blood loss in resuscitated rats. *J Trauma* **49**, 246-250 (2000).
135. Matsuoka, T. & Wisner, D.H. Resuscitation of uncontrolled liver hemorrhage: effects on bleeding, oxygen delivery, and oxygen consumption. *J Trauma* **41**, 439-445 (1996).
136. Matsuoka, T., Hildreth, J. & Wisner, D.H. Liver injury as a model of uncontrolled hemorrhagic shock: resuscitation with different hypertonic regimens. *J Trauma* **39**, 674-680 (1995).
137. Ryan, K.L., Cortez, D.S., Dick, E.J., Jr. & Pusateri, A.E. Efficacy of FDA-approved hemostatic drugs to improve survival and reduce bleeding in rat models of uncontrolled hemorrhage. *Resuscitation* **70**, 133-144 (2006).
138. Siller-Matula, J.M., Plasenzotti, R., Spiel, A., Quehenberger, P. & Jilma, B. Interspecies differences in coagulation profile. *Thrombosis and haemostasis* **100**, 397-404 (2008).
139. Szczepanska-Sadowska, E., *et al.* Central AVP and blood pressure regulation: relevance to interspecies differences and hypertension. *Annals of the New York Academy of Sciences* **689**, 677-679 (1993).

140. Langleben, D. & Moroz, L.A. Interspecies variation in the cellular phase of blood fibrinolytic activity. *Proc Soc Exp Biol Med* **196**, 270-272 (1991).
141. Boxenbaum, H. Interspecies variation in liver weight, hepatic blood flow, and antipyrine intrinsic clearance: extrapolation of data to benzodiazepines and phenytoin. *Journal of pharmacokinetics and biopharmaceutics* **8**, 165-176 (1980).
142. Rao, G.H.R. *Handbook of platelet physiology and pharmacology*, (Kluwer Academic, Boston, 1999).
143. Markwardt, F., Nowak, G., Glusa, E. & Hoffman, A. The influence of drugs on disseminated intravascular coagulation (dic). III. Effects of busulfan-induced thrombocytopenia and inhibition of platelet function by acetylsalicylic acid. *Thrombosis research* **15**, 79-88 (1979).
144. Blajchman, M.A. & Lee, D.H. The thrombocytopenic rabbit bleeding time model to evaluate the in vivo hemostatic efficacy of platelets and platelet substitutes. *Transfusion medicine reviews* **11**, 95-105 (1997).
145. Blajchman, M.A., Bordin, J.O., Bardossy, L. & Heddle, N.M. The contribution of the haematocrit to thrombocytopenic bleeding in experimental animals. *British journal of haematology* **86**, 347-350 (1994).
146. Blajchman, M.A., Senyi, A.F., Hirsh, J., Genton, E. & George, J.N. Hemostatic function, survival, and membrane glycoprotein changes in young versus old rabbit platelets. *J Clin Invest* **68**, 1289-1294 (1981).
147. Buchanan, M.R., *et al.* Shortening of the bleeding time in thrombocytopenic rabbits after exposure of jugular vein to high aspirin concentration. *Prostaglandins and medicine* **3**, 333-342 (1979).
148. Blajchman, M.A., *et al.* Shortening of the bleeding time in rabbits by hydrocortisone caused by inhibition of prostacyclin generation by the vessel wall. *J Clin Invest* **63**, 1026-1035 (1979).
149. Lucas, O.N. Limitations of clotting and bleeding time tests for screening haemorrhagic disorders. *Journal of the Canadian Dental Association* **32**, 599-602 (1966).
150. Alam, H.B., *et al.* Hemostatic and pharmacologic resuscitation: results of a long-term survival study in a swine polytrauma model. *J Trauma* **70**, 636-645 (2011).
151. Alam, H.B., *et al.* Testing of blood products in a polytrauma model: results of a multi-institutional randomized preclinical trial. *J Trauma* **67**, 856-864 (2009).
152. Dong, F., *et al.* Immune effects of resuscitation with HBOC-201, a hemoglobin-based oxygen carrier, in swine with moderately severe hemorrhagic shock from controlled hemorrhage. *Shock* **25**, 50-55 (2006).
153. Philbin, N., *et al.* A hemoglobin-based oxygen carrier, bovine polymerized hemoglobin (HBOC-201) versus hetastarch (HEX) in a moderate severity hemorrhagic shock swine model with delayed evacuation. *Resuscitation* **66**, 367-378 (2005).
154. Gurney, J., *et al.* A hemoglobin based oxygen carrier, bovine polymerized hemoglobin (HBOC-201) versus Hetastarch (HEX) in an uncontrolled liver injury hemorrhagic shock swine model with delayed evacuation. *J Trauma* **57**, 726-738 (2004).

155. Velmahos, G.C., *et al.* Abdominal insufflation for control of bleeding after severe splenic injury. *J Trauma* **63**, 285-288; discussion 288-290 (2007).
156. Sava, J., *et al.* Abdominal insufflation for prevention of exsanguination. *J Trauma* **54**, 590-594 (2003).
157. Jaskille, A., *et al.* Abdominal insufflation decreases blood loss and mortality after porcine liver injury. *J Trauma* **59**, 1305-1308; discussion 1308 (2005).
158. Szebeni, J., *et al.* A porcine model of complement-mediated infusion reactions to drug carrier nanosystems and other medicines. *Advanced drug delivery reviews* **64**, 1706-1716 (2012).
159. Szebeni, J., *et al.* Prevention of infusion reactions to PEGylated liposomal doxorubicin via tachyphylaxis induction by placebo vesicles: a porcine model. *Journal of controlled release : official journal of the Controlled Release Society* **160**, 382-387 (2012).
160. Johnson, R.A., *et al.* Histamine release associated with intravenous delivery of a fluorocarbon-based sevoflurane emulsion in canines. *Journal of pharmaceutical sciences* **100**, 2685-2692 (2011).
161. Deitch, E.A., *et al.* Lymph from a primate baboon trauma hemorrhagic shock model activates human neutrophils. *Shock* **25**, 460-463 (2006).
162. Deitch, E.A., *et al.* The role of lymph factors in lung injury, bone marrow suppression, and endothelial cell dysfunction in a primate model of trauma-hemorrhagic shock. *Shock* **22**, 221-228 (2004).
163. Miller, D.L., Rayner, A.A., Girton, M. & Doppman, J.L. CT evaluation of hepatic and splenic trauma with EOE-13. An experimental study in monkeys. *Investigative radiology* **20**, 68-72 (1985).
164. Fitzpatrick, G.M., Cliff, R. & Tandon, N. Thrombosomes: a platelet-derived hemostatic agent for control of noncompressible hemorrhage. *Transfusion* **53 Suppl 1**, 100S-106S (2013).

Chapter 3: Synthetic Platelets in Lethal Liver Trauma*

* THE MATERIAL IN THIS CHAPTER HAS BEEN PUBLISHED: SHOFFSTALL, A. J.; ATKINS, K. T.; GROYNOM, R. E.; VARLEY, M. E.; EVERHART, L. M.; LASHOF-SULLIVAN, M. M.; MARTYN-DOW, B.; BUTLER, R. S.; USTIN, J. S.; LAVIK, E. B., INTRAVENOUS HEMOSTATIC NANOPARTICLES INCREASE SURVIVAL FOLLOWING BLUNT TRAUMA INJURY. BIOMACROMOLECULES 2012, 13 (11), 3850-7.

INTRODUCTION

There is a dearth of tools to address internal bleeding, and a tremendous opportunity to improve survival after trauma if one were able to staunch it.¹⁻⁶ Methods that have been pursued include blood and blood product transfusions, and treatment with clotting factors such as recombinant factor VIIa (RFVIIa).⁷ Resuscitative strategies with blood components such as fibrinogen or platelets are limited by their necessity for donor sources, immunocompatibility, need for refrigeration and risk of loss of activity during storage or preservation methods.⁷ These complications limit their use to hospital settings. The administration of recombinant factor VIIa intravenously to reduce bleeding after acute trauma has been a topic of debate.^{4,8-10} Several studies have shown that perioperative administration of RFVIIa reduces the volume of blood transfusion. However, it is unclear whether the benefit is large enough to have any associated effect on mortality after hemorrhagic trauma.^{11,12} Its potential use in the prehospital phase is further diminished due to its high cost, potential for adverse effects, and necessity to be stored at 2-8° C.^{8,13}

Intravenous administration of hemostatic nanoparticles that target activated platelets have been investigated by a number of groups with some promise and a range of challenges.¹⁴⁻¹⁶ RGD conjugated red blood cells (RBCs) called thromboerythrocytes showed promise *in vitro* but did not significantly reduce prolonged bleeding times in thrombocytopenic primates.^{14,17} Fibrinogen-coated albumin microparticles, “Synthocytes”¹⁸ and liposomes carrying the fibrinogen γ chain dodecapeptide (HHLGGAKQAGDV)^{19,20} showed success in bleeding models in thrombocytopenic rabbits. However, Synthocytes were ineffective in treating bleeding in normal rabbits¹⁸, and the liposomes from Okamura et al.^{19,20} do not appear to have yet been studied for this purpose.

From this work, several things are clear. First, if particles are too large or carry immunogenic materials, they may trigger non-specific thrombosis. Second, what works *in vitro* may not translate to *in vivo* conditions, or to the general (non-thrombocytopenic) trauma population. No single species, model or experimental outcome seem to robustly predict a treatment’s clinical efficacy. Because trauma and the coagulation system is complex, multiple *in vitro* and *in vivo* models are needed to corroborate a potential treatment.²¹

We have developed novel hemostatic nanoparticles (GRGDS-NPs) that can be administered intravenously to reduce bleeding times by ~ 50% in a model of rat femoral artery injury, performing better than saline or RFVIIa controls.²² These nanoparticles are made of biodegradable polymers, reducing the risk of long-term immunological and inflammatory reactions. The salient features of these nanoparticles

include a 400 nm core made of biodegradable block copolymer of poly(lactic-co-glycolic acid) (PLGA) and poly- ϵ -L-lysine (PLL) with poly(ethylene glycol) (PEG) arms terminated with arginine-glycine-aspartic acid (**GRGDS**)-based targeting ligands (Figure 12a). GRADSP ligands are used as a scrambled peptide to control for nonspecific actions of the particles (Scrambled-NPs). For research purposes, the nanoparticles have been loaded with coumarin-6, a fluorescent dye that allows us to track their biodistribution.²²

In this study, we investigated the impact of intravenous delivery of the GRGDS-NPs on blood loss and survival in a clinically relevant model of blunt trauma. We investigated the nanoparticles in a lethal liver injury model to determine 1) whether the nanoparticles had an effect in a complex solid organ injury, 2) if that effect produced any functional impact on blood loss and mortality outcomes, and 3) to investigate the effects of the nanoparticles on clotting time and clot firmness parameters using rotational thromboelastometry (ROTEM), to better understand the mechanism by which the nanoparticles augment hemostasis. The data from these studies is a critical step in determining the clinical potential of these particles and gaining insight into nanomedicine more broadly.

MATERIALS AND METHODS

Materials

PLGA (Resomer 503H) was purchased from Evonik Industries. Poly-L-lysine and PEG (~4600 Da MW) were purchased from Sigma Aldrich. All reagents were ACS grade and were purchased from Fisher Scientific.

Particle synthesis

A PLGA-PLL-PEG triblock polymer was synthesized using stepwise conjugation reactions, starting with PLGA (Resomer 503H) and poly(ϵ -cbz-L-lysine) (PLL-cbz) PLL with carbobenzoxy-protected side amine side groups (Sigma P4510) as previously described (Figure 10).^{22,23} This conjugation reaction was confirmed using UV-Vis to check for a signature triple peak corresponding to the cbz groups. After deprotecting the PLGA-PLL-cbz with HBr, the free amines on the PLL-NH₃ were reacted with CDI-activated PEG in a 5:1 molar excess.²⁴ The conjugated triblock copolymer PLGA-PLL-PEG (with CDI activated PEG endgroups) was dissolved to a concentration of 20 mg/ml in acetonitrile containing coumarin-6 (C6), a fluorescent dye is used to track the nanoparticles after injection (loaded at 1% w/w). However, this concentration can be varied to tune the nanoparticle size (Figure 11). This solution was added dropwise to a volume of stirring PBS, twice that of the acetonitrile.²⁵ Precipitated nanoparticles form as the water-miscible solvent is displaced. The nanoparticles were then conjugated with GRGDS or the conservatively substituted GRADSP peptide and stir-hardened for 3 hours in a single step. Nanoparticles were then collected using the coacervate precipitation method described below.

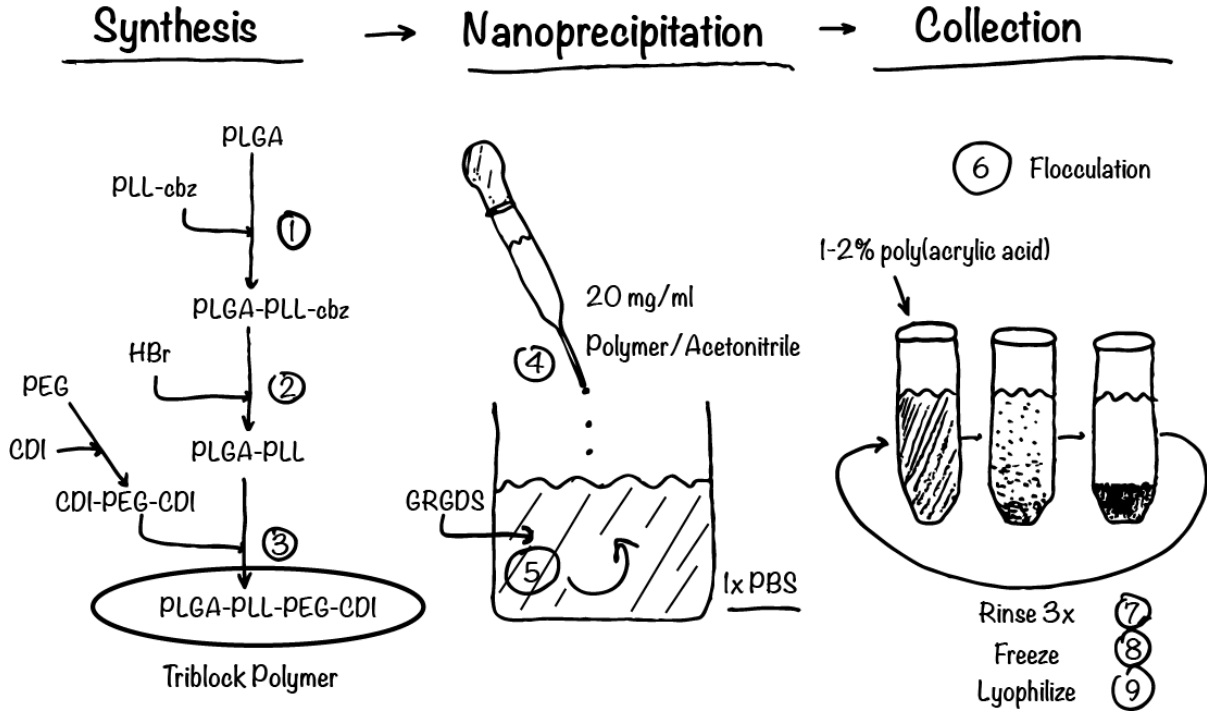


Figure 10: Particle synthesis, nanoprecipitation and collection methods. 1) PLGA-PLL-cbz conjugation (DCC/DMAP), 2) Carbobenzoxy (Cbz) group deprotection (HBr/Chloroform), 3) Pegylation (CDI diactivated PEG), 4) Nanoprecipitation, 5) GRGDS conjugation (to CDI-activated PEG), 6) Flocculation (poly(acrylic acid)), 7-9) Rinsing and lyophilization.

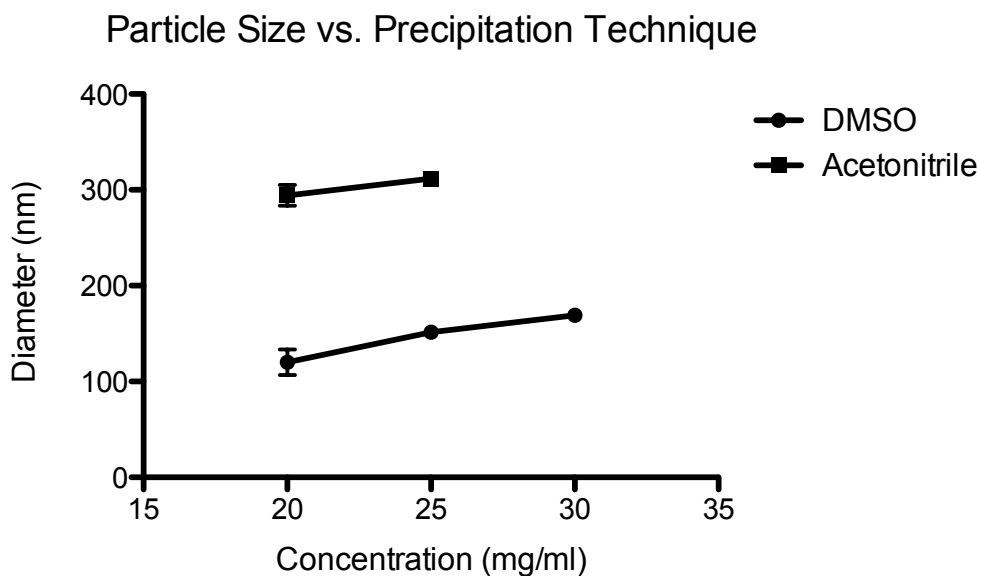


Figure 11: Varying nanoparticle size by changing polymer:solvent ratios during nanoprecipitation

Coacervate precipitation and resuspension

The method for nanoparticle collection was adapted from D’Addio et al. ²⁶. One mass equivalent of dry poly(acrylic acid) (pAA) (Sigma, MW = 1,800) was added to the stirring particle suspension. 1% w/v pAA was then added to the stirring suspension until flocculation occurred, approximately 10 ml. After 5 minutes, the flocculated nanoparticles were collected by centrifugation and rinsed 3 times. Nanoparticles were resuspended to approximately 10 mg/ml with deionized water, snap-frozen in liquid nitrogen and lyophilized for 3 days. Nanoparticles were resuspended to a concentration of 20 mg/ml in 1x PBS and briefly sonicated (VCX-130, Sonics & Materials, Inc.).

Characterization

Nanoparticles were characterized for size distribution and polydispersity using dynamic light scattering (90Plus, Brookhaven Instruments Corporation) and scanning

electron microscopy (Hitachi S4500). DLS data was represented as the effective diameter as calculated by the 90Plus software. SEM images were analyzed in ImageJ software. Successful conjugation of PLL, PEG and peptide ligands was confirmed using UV-spectroscopy, ¹H-NMR and amino acid analysis with high pressure liquid chromatography (HPLC) (BioRad, Varian and Shimadzu respectively). ¹H-NMR is performed with chloroform for analyzing the triblock structure and deuterated water to verify the PEG coronal shell.²⁷ Amino acid analysis was performed by W.M. Keck Foundation Biotechnology Resource Laboratory (New Haven, CT).

In vitro coagulation assay (ROTEM)

Coagulation assays, using Sprague Dawley rat blood, were performed using the ROTEM's NATEM test in the presence of either saline, GRGDS-NPs, or scrambled GRADSP-NPs. The blood collection method (cardiac puncture) was rigidly followed to minimize variability in the highly sensitive NATEM test. A 5 ml syringe is loaded with 0.5 ml of 3.8% disodium citrate prepared in 1x PBS. Rats were anesthetized with a ketamine:xylazine rodent cocktail (90:10 mg/kg, i.p.). 4.5 ml of blood is collected to mix with the anticoagulant solution at a 1:9 ratio (soln:blood). For a given run, the cup of blood consisted of: 300 µl citrated blood, 20 µl starTEM reagent (0.2 mM calcium chloride), 20 µl nanoparticles (1.25 or 2.5 mg/ml), totaling a 340 µl sample. To account for time dependency on coagulation tests, a block of 4 NATEM tests were run simultaneously on a single ~1.2 cc aliquot of blood, where saline was always included as one of the four tests. The raw data was analyzed using a generalized linear model, with run time as blocks and with Tukey comparisons between groups. The main

outcomes we considered include the standard ROTEM parameters clotting time (CT), clot formation time (CFT), the sum of the two (CT+CFT), and maximum clot firmness (MCF). CT is defined as the time from the start of the assay until the initial clotting is detected (thickness = 2mm). CFT is defined as the time between the initial clot (thickness = 2mm) until a clot thickness of 20 mm is detected. MCF is defined as the maximum thickness (in mm) that a clot reaches during the duration of the test.

In vivo liver injury model

In order to assess the efficacy of the nanoparticles to augment survival in a lethal injury model, a liver injury model was adapted from Ryan et al.²⁸ and Holcomb et al.²⁹ and is described below. The injury model was approved and undertaken according to the guidelines set by Case Western Reserve University's institutional animal care and use committee. The main outcomes recorded for this study include survival at 1 hour and blood loss as measured with pre-weighed gauze.

Surgical procedure

Sprague Dawley rats (225-275 g, Charles River) were anesthetized with intraperitoneal ketamine:xylazine (90:10 mg/kg, respectively) cocktail, chosen for being a standard rodent anesthetic with minimal cardiovascular effects. Ketamine alone can act like a sympathetic system stimulant. However, co-administration of xylazine mitigates these effects.³⁰ After 10 minutes, rats were shaved and placed in a supine position on a heatpad. The abdomen was accessed and the medial lobe of the liver was marked with an arch radius 1.3 cm from the suprahepatic vena cava using a handheld cautery device. Once marked, the tail vein was exposed, and catheterized with a saline-

flushed 24G x 3/4" Excel Safelet Catheter. The medial liver lobe was then resected along the marked lines, the abdomen was closed with wound clips, and 0.5 cc bolus treatment solution was immediately administered followed by 0.2 cc saline flush to clear the catheter dead-volume.

The rats were allowed to bleed for 1 hour or until death, as confirmed by lack of both breathing and a palpable heartbeat. Before measuring blood loss, all rats were injected with a lethal dose of sodium pentobarbital (i.v.). The abdomen was then reopened and blood collected with pre-weighed gauze. The clot adherent to the liver was collected last as this usually caused additional bleeding to occur. The resected liver was weighed and fixed in 10% buffered formalin solution. Remaining liver, kidney, spleen, lungs and adherent clot were harvested and similarly preserved in 10% buffered formalin.

Procedure and statistics

Treatments included no injection (n=3), saline (n=17), scrambled-NPs (n=15), and hemostatic GRGDS-NPs (n=20). Particle treatments were resuspended to 20 mg/ml in PBS. The surgeon was blinded to the treatments and all blood loss measurements and death were independently recorded by a second person also blinded to the treatment. The no injection group (n=3) was included as a reference, but was not included in the statistics. ANOVA with Tukey comparisons was used to analyze blood loss data (Minitab). Survival was analyzed with a binomial logistic regression with chi-squared tests between odds-ratios (SAS). A power analysis based on preliminary studies

suggested an n=15 per group for significance for survival data ($\alpha = 0.05$, $\beta = 0.2$, odds ratio = 3).

Biodistribution

Liver, kidney, spleen, lung and adherent clots were harvested and lyophilized for the biodistribution assay. The dry weight of the whole organ was recorded and 100-200 mg of dry tissue was homogenized (Precellys 24) and incubated overnight in acetonitrile at 37 C. This dissolved any nanoparticles present in the tissue and left the C6 in the organic solvent solution. Tubes were then centrifuged at 15,000 g for 10 minutes to remove solid matter and supernatant was tested on the HPLC. Mobile phase was 80% acetonitrile, and 20% aqueous (8% acetic acid). Stationary phase was a Waters Symmetry C18 Column, 100Å, 5 μ m, 3.9 mm X 150 mm with fluorescence detection (450/490 nm ex/em). Based on the known C6 loading and injection volume of particles, data is represented as percent (%) of particles injected.

Imaging injury surface and adherent clots

Resected portions of the liver were rinsed and placed directly on a high-resolution (1200 dpi) flatbed scanner (Cannon CanoScan LiDE 700F) to image the surface of the injury. Adherent clots, still attached to livers were fixed in 10% formalin, soaked overnight in sucrose, frozen and cryosectioned to 20-micron thickness. Sections were then stained with VectaShield DAPI to stain hepatocyte nuclei and imaged with an inverted fluorescence microscope (Zeiss Axio Observer.Z1). Several clots per group were fixed in 10% formalin, and dehydrated in serial steps with ethanol to prepare them for imaging with a scanning electron microscope (SEM). These were then dried

overnight in anhydrous hexamethyldisilazane and sputter coated. Samples were mounted and imaged with a Hitachi S4500 field emission SEM at 5kx magnification.

RESULTS

Particle synthesis and characterization

The PLGA-PLL-PEG triblock polymer is synthesized using stepwise conjugation reactions, starting with PLGA (Resomer 503H) and poly(ϵ -cbz-L-lysine) PLL with carbobenzoxy-protected side amine side groups following Bertram et al.^{22,23,31} However, batch sizes and synthesis times were optimized to shorten the synthesis procedure from one that took 3 weeks to produce ~60mg to one that produced in a week (Table 4).

Table 4: Synthesis scale-up. Reaction times were optimized and batch sizes increased, to produce nearly 8x the polymer mass in one-third the time as previously reported by Bertram et al.²² Shoffstall method (1) forms nanoparticles with the triblock polymer PLGA-PLL-PEG and then conjugates the RGD peptide to nanoparticles. Shoffstall (2) forms nanoparticles from the previously RGD-conjugated quaddblock polymer PLGA-PLL-PEG-GRGDS.

Product	Days of Synthesis		
	Bertram et al.	Shoffstall et al. (1)	Shoffstall et al. (2)
PLGA-PLL-cbz	4.0	1.5	1.5
PLGA-PLL	2.5	1.5	1.5
PLGA-PLL-PEG	4.5	1.5	1.5
Nanosphere	4.0	1.5	2.0
GRGDS-conj.	3.5	0.5	2.5
	Totals		
	Bertram et al.	Shoffstall et al. (1)	Shoffstall et al. (2)
Time (Days)	18.5	6.5	9.0
Yield (%)	2%	5%	2%
Product Mass (mg)	60	500	200

Conjugation efficiency for the PLGA-PLL-cbz conjugation step is approximately ~30-40% molar ratio PLL:PLGA, as determined by UV-vis. After deprotection of side groups, the free amines on the PLL are reacted with CDI-activated PEG. This PEG creates a hydrophilic shell around the nanoparticles that allow them to have a longer residence time in blood circulation²⁷ (Figure 12a). ¹H-NMR in deuterated chloroform and deuterated water is performed to verify the expected surface-pegylated structure (Figure 12c, and larger in Figure 13). Peaks a, b, and d confirm the composition of PLGA (50:50), and peak c confirms the presence of PEG. From this spectrum, percent pegylation is calculated to be 1:10 (PEG:PLGA) molar ratio. In deuterated water, the PEG peak becomes much larger in relation to the other peaks and confirms the PEG-coronal structure of the nanoparticles in an aqueous environment. The size and distribution of the nanoparticles cores (by SEM) and in the aqueous environment (by DLS) is homogenously distributed around 400 nm and 420 nm respectively (Table 5). The increase in size from SEM to DLS can be accounted for by the hydration shell, created by the PEG arms. There appears to be a slight increase in size as a result of C6 loading (approximately 5-10%), with no significant change in size depending on the GRGDS or GRADSP peptide conjugated.

Table 5: Particle characterization: size, polymer composition, and amino acid content.

Nanoparticle Formulation (PLGA-PLL-PEG-X)	SEM – Core dia. [nm] (Mean +/- SD)	DLS – effective dia. [nm] (Mean +/- Polydispersity)	DLS – num. avg. dia. [nm] (Mean +/- SD)	PLL:PLGA (mol:mol)	PEG:PLGA (mol:mol)	Surface Amino Acid X:PEG (mol:mol)
X=GRGDS + C6	391.1 +/- 90.5	419.3 +/- 0.049	431.9 +/- 19.3	0.3:1	0.10:1	0.053:1
X=GRADSP + C6	420.5 +/- 81.7	431.0 +/- 0.005	424.3 +/- 13.4	0.3:1	0.14:1	0.054:1

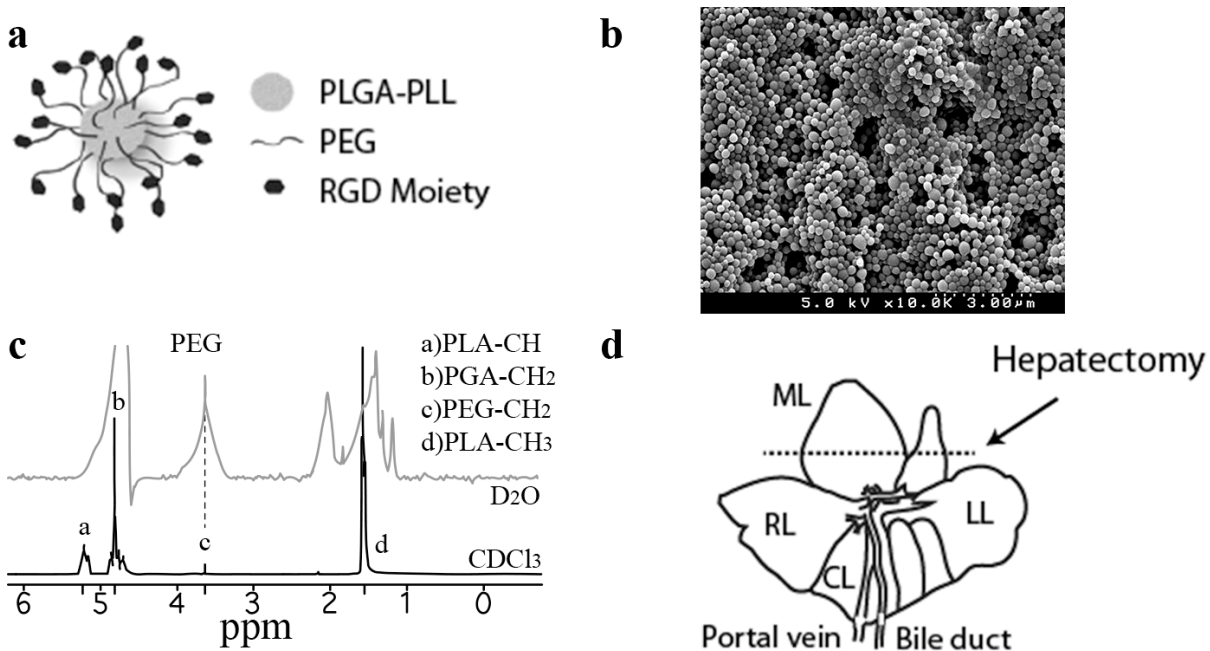


Figure 12: Nanoparticle Schematic and Characterization. a) Hemostatic nanoparticles (GRGDS-NPs) consist of PLGA-PLL biodegradable polymer cores, with PEG arms that expose the GRGDS moiety for targeting activated platelets. b) SEM shows nanoparticle size distribution and morphology. c) $^1\text{H-NMR}$ spectral analysis confirms the pegylation of the co-block-polymer and the PEG-coronal structure of the nanoparticles. Deuterated water (top, gray overlay) and deuterated chloroform (bottom, black overlay). d) These are administered intravenously via the tail vein after a partial hepatectomy in the rat. The medial lobe (ML) is transected in this model. Right (RL), left (LL) and caudate lobes (CL) are labeled for reference.

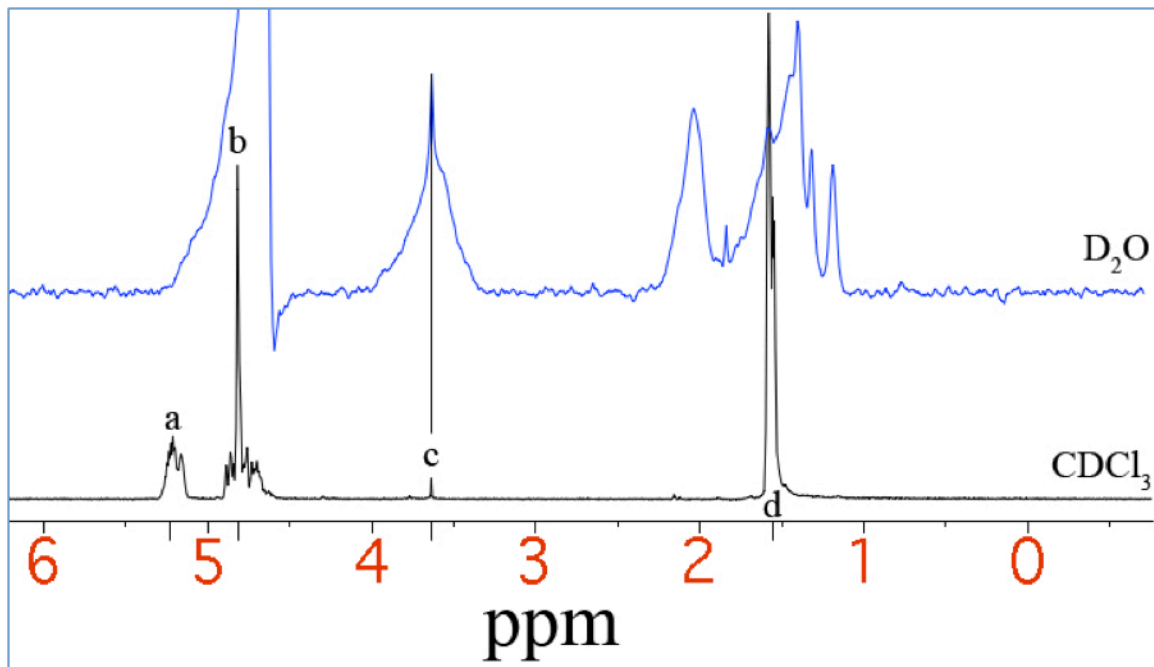


Figure 13: NMR tracing of nanoparticles in deuterated water (blue) and deuterated chloroform (black), showing increased relative PEG content in water, confirming the PEG-coronal structure of nanoparticles.

In vivo injury model development

Following injury of the medial lobe (Figure 12d), rats were administered either saline, scrambled (GRADSP), or hemostatic (GRGDS-conjugated) nanoparticles. Saline is used as the baseline control because the administration of fluids can impact bleeding.³² Based on our preliminary results, we found that resected liver mass and body mass were well-correlated with bleeding outcomes, and similar to Holcomb et al.²⁹, we chose to strictly adhere to inclusion criteria for rat body mass (225-275 g) and liver resection (0.8-1.2% of body mass) (Figure 14). At the conclusion of the study, this inclusion criteria was found to reduce rat-to-rat variability based on body mass. However, liver resection mass was still significantly correlated with bleeding outcomes ($p=0.0004$).

When resected liver mass and treatment are included in the ANOVA model, the treatment is still not significantly correlated with bleeding outcomes ($p=0.113$).

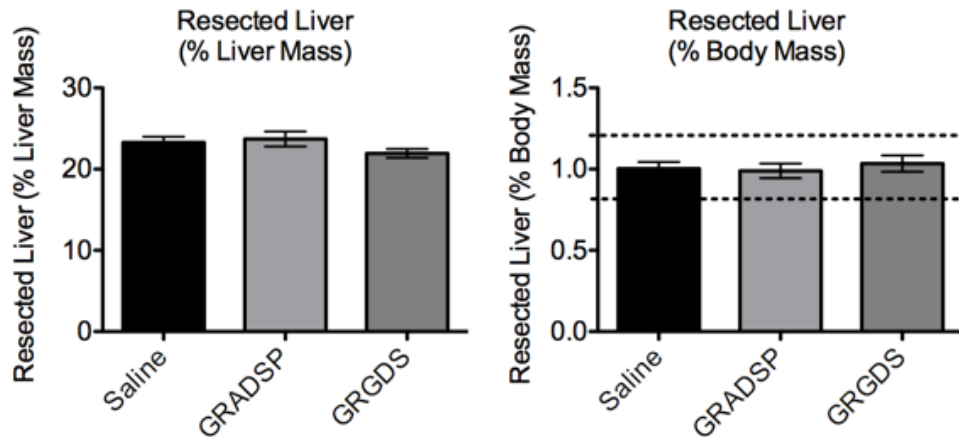


Figure 14: Injury reproducibility. Resected liver mass normalized by total liver mass (left) and body mass (right). The liver mass is tightly controlled in this injury model and is extremely reproducible in size, both in ratio to body mass (1.00% +/- 0.13% S.D.) and in ratio to the remaining liver (22.8 % +/- 2.8% S.D.). The dotted lines on the resected liver graph show the inclusion criteria for this study. Error bars represent SEM.

1-Hour survival

One of the most critical parts of this work was to determine whether administration of the nanoparticles led to improved survival following blunt trauma injury. Administration of the hemostatic, GRGDS nanoparticles significantly improves survival following the lethal liver injury. Specifically, the GRGDS-NPs increases the odds of survival to 80% (Figure 15). This is compared to 47% in the saline group ($p=0.040$, odds ratio (OR)=4.5, 95% CI 1.1-19.2) and 40% in the scrambled-NP group ($p=0.019$,

OR=6, 95% CI 1.3-27.0). Administering the GRGDS-NPs almost doubles the chances of survival from this lethal injury.

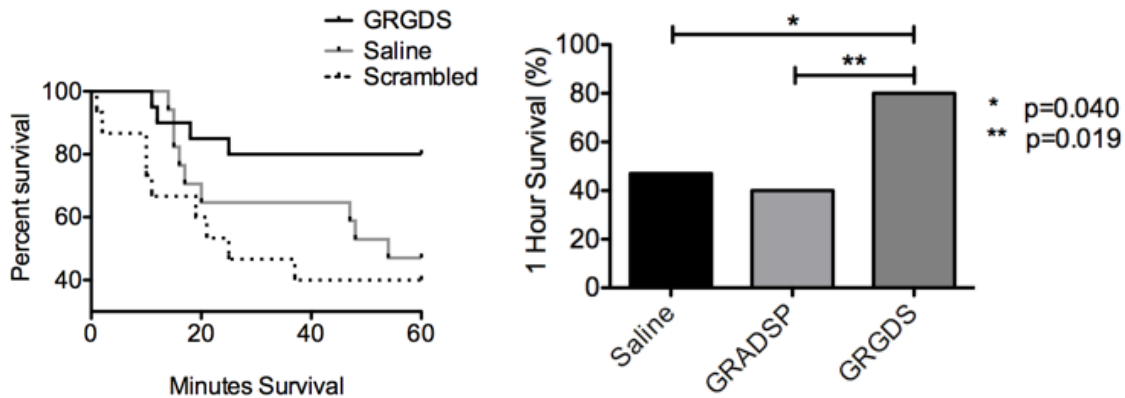


Figure 15: 1-hour survival. Survival is significantly increased by treatment with the hemostatic GRGDS-functionalized nanoparticles. Error bars represent SEM.

Blood loss

We know from our previous work ²² that the GRGDS-NPs reduce bleeding. In this work, we measured blood loss through the weight change in gauze used to adsorb the blood in the body cavity at the end of the experiment. This method gives data on blood loss but lacks the fine resolution permitted in the previous study. Measuring total blood loss in this model is complicated by the impact of survival time. The rate of blood loss may be a better indicator of survival for this model, but since the injury model is maintained in the small, closed cavity of rats, blood loss could not be dynamically measured. Nevertheless, we saw a trend in blood loss that correlates with survival with the GRGDS-NPs exhibiting the least blood loss. This trend towards reduction in blood loss is not statistically significant ($p=0.0552$), but it suggests that the GRGDS-NPs are improving survival through mitigation of bleeding (Figure 16). There also appears to be

a critical threshold around 35% blood volume loss, above which there is rapidly increasing proportion of mortality (Figure 16).

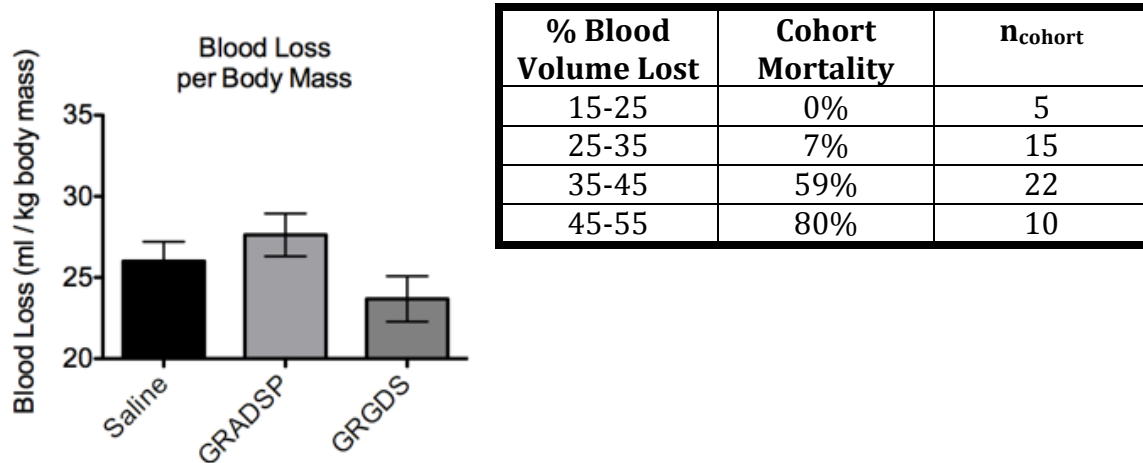


Figure 16: Blood loss outcomes. There is a trend toward a reduction in blood loss with the GRGDS-NP group, but is not significantly significant. 100% of animals with a blood volume loss less than 32% survive, but rapidly increases above this threshold. Error bars represent SEM.

Imaging injury surface

To help validate that our GRGDS-NPs are targeting the injury site, and accumulating within the clot, we imaged the injury surface using several modalities including fluorescent microscopy and SEM. Nanoparticles loaded with the fluorescent compound coumarin-6 (C6) are found within the injury surface, integrated with the clot (Figure 17). The injury surface is also characterized using a flatbed scanner to help depict the nature of the injury. From visual observation of the injury during model development, it is apparent that the majority of bleeding occurs through the 2-4 major blood vessels that are transected in the medial lobe injury.

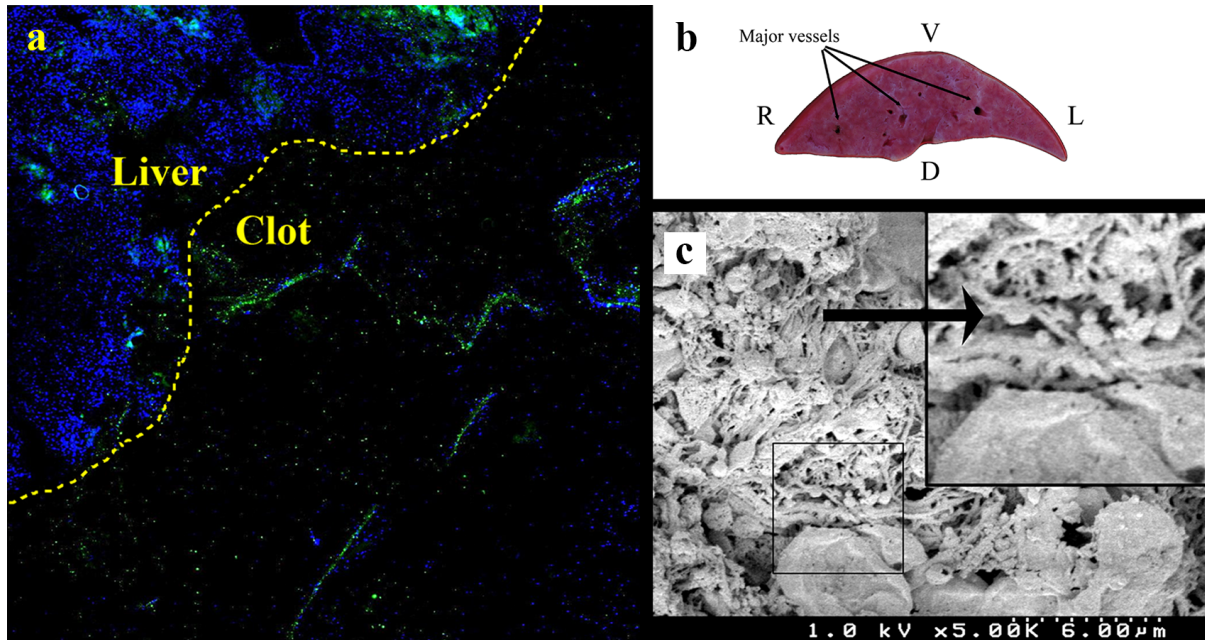
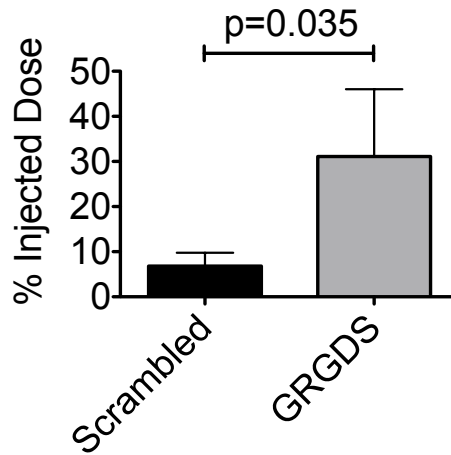


Figure 17: Injury Surface Characterization. a) Hemostatic nanoparticles loaded with C6 (green) are found integrated with the adherent clot after it is removed and examined under fluorescent microscopy. b) The majority of bleeding appears to occur from the 2-4 major transected blood vessels in this injury model. c) Scanning electron microscopy is used to verify the presence of the nanoparticles (black arrow) and their integration with the fibrin mesh.

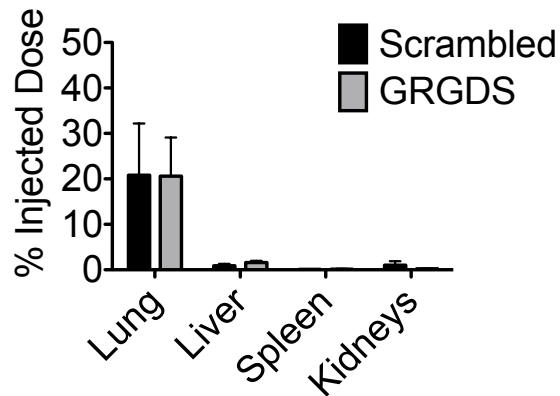
Biodistribution

For the GRGDS-NPs, 31.1% of the injected dose is found in the clot versus only 6.8% for the scrambled-NP group. Total recovery of the nanoparticles between the clot and organs tested was 53.7% and 29.6% for the GRGDS-NPs and scrambled-NP groups, respectively; the unrecovered proportion is most likely located in the shed blood, not actively participating in the clot, or remaining in plasma circulation. There was a relatively large percentage of nanoparticles found in the lungs for each group, 20.8% and 20.6% (GRGDS and Scrambled, respectively), and a small percentage found in the other organs tested (<2%).

a Adherent Clot Biodistribution



b Organ Biodistribution



n=	LIV	LNG	KDY	SPL	CLOT
Scrambled	n=12	n=14	n=14	n=14	n=8
GRGDS	n=16	n=17	n=17	n=17	n=7

Figure 18: Biodistribution. a) 31% of hemostatic GRGDS-NPs locate in the clot, versus 7% for the scrambled-NP control group. Total mean nanoparticle recovery is 53.7% of total injected dose for GRGDS and 29.6% for scrambled. b) The “Liver” group is representative of the particle distribution to the uninjured lower left lobe of the liver. Minimal particle distribution is found in the spleen and kidneys. Approx. 20% is found in the lungs for each formulation. This may be indicative of microemboli in the lung or nanoparticles still in pulmonary circulation.

In vitro coagulation model

A dosing study was performed using rotational thromboelastometry (ROTEM), with citrated rat. In this assay, a 20 μ l volume of PBS containing a varying concentration of nanoparticles was added to a 300 μ l volume of blood immediately before starting the assay. In addition to saline, concentrations of nanoparticles tested included 0.625, 1.25, 2.5, 5.0, and 20 mg/ml for GRGDS and scrambled nanoparticle groups. In all concentrations tested in the scrambled group, the CT+CFT increased and the MCF decreased compared to saline. In GRGDS-NP 1.25 and 2.5 mg/ml concentrations, MCF increased. Similarly, the clotting time is decreased in 1.25 mg/ml, and 5.0 mg/ml groups, but was increased otherwise. This is indicative of a clot forming faster and thicker when treated with the nanoparticles at an optimal dose, approximately 73.5-294 μ g/ml in the blood or a 5.2-20 mg/kg dose for a 250 g male rat, assuming 68.6 ml/kg blood volume.³³

We then further investigated 1.25 and 2.5 mg/ml concentrations as these had the most favorable effects on clotting parameters. We used a randomized block experimental method, using saline as the control for each test-block. The 2.5 mg/ml GRGDS-NP dose reduced clotting time compared to saline controls ($p=0.0437$) and had a trend toward increasing MCF although the difference was not significant ($n=3$ rats, with triplicate measurements at each treatment-dose level). The 2.5 mg/ml GRGDS-NP dose significantly reduced clotting time compared to saline controls ($p=0.0437$) and had a trend toward increasing MCF although not statistically significant. Interestingly, the scrambled-NP groups also appeared to reduce clotting times and increase MCF, but

the differences were not significantly different from either saline or GRGDS treatments (Figure 19).

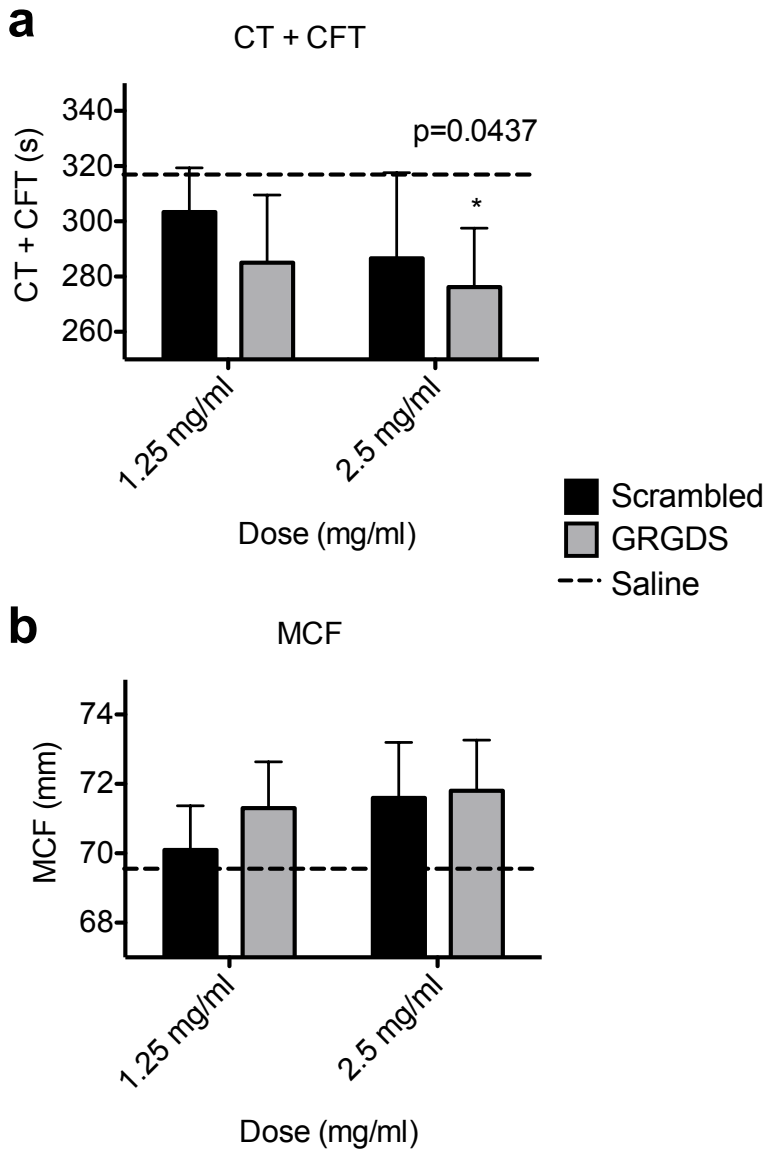


Figure 19: In vitro Testing. Outcomes include CT+CFT (a) and MCF (b). The GRGDS group had a lower (faster) clotting time and a higher clot firmness compared to saline. Error bars represent SEM.

DISCUSSION

Administration of hemostatic nanoparticles increased 1-hour survival

Early intervention is critical to improve chances of survival following trauma, and we see the effects of early intervention in this work. For all groups tested, there was a window of 20 minutes, after which, the odds of survival improved, as well as a critical blood volume loss of approximately 35% blood volume, below which 95% of rats survived.

Nearly twice as many rats survive one hour with administration of the hemostatic nanoparticles compared to controls. This result is statistically significant and clinically tremendous. We have seen previously that these hemostatic nanoparticles are stable at room temperature and reduce bleeding in a controlled injury model, but one of the major questions was whether this reduction in blood loss would impact survival in lethal trauma models of bleeding. The liver injury model is one of the most reproducible and comparable in the field.^{28,29,34} Seeing an almost two fold increase in survival with the GRGDS-NPs confirms that they not only reduce bleeding but do so at a level that impacts survival in the critical prehospital window.

There is a 4.5-fold higher amount of GRGDS-NPs found in the adherent liver clot compared to the scrambled-NP group, with very small quantities of nanoparticles found in the kidney, spleen and uninjured liver, confirming their injury-targeting capability. Nearly 20% of injected nanoparticles have been found in the lungs regardless of the treatment group. While some basal level of nanoparticles in the lungs is expected due to the pulmonary perfusion still present in the organ at the time of collection, previous

studies in naïve rats estimate this to account for only 5-10% of the injected dose.²² These findings may indicate that the nanoparticles could be accumulating in thromboemboli in the lungs, concomitant with the massive hemorrhagic nature of this injury model.³⁵ However, it is of particular interest to note that survival does not appear to be deleteriously impacted—rather the opposite. It therefore reasons to argue that these thrombi are also present in the saline control, and may be present as microemboli that may not have any clinical presentation.^{35,36} Future studies may be aimed at assessing the risk of particle aggregation in the lungs and determining what functional impacts they may have, for example, by monitoring lung perfusion, tissue oxygenation, or blood gas levels. The ease of intravenous administration of these nanoparticles, coupled with their effective injury-targeting without deleterious functional outcomes bodes well for translation of this therapy to the clinic.

We observed a trend toward reduction in blood loss with the functionalized treatment versus controls. However, the methods for blood collection in trauma models in rats are limited, and the sensitivity is modest at best. Therefore, it is not surprising that we were not able to resolve the differences between the groups in this area to statistical significance. A power analysis to determine the number of animals needed to see differences suggests that an unethically large number of animals would be needed. While this model is not acutely sensitive to differences in blood loss, the trend regarding blood loss correlates well with the survival outcomes, the key point of this study.

One of the questions that plays an important role in the safety and efficacy of a technology like this is the mechanism by which the nanoparticles reduce bleeding. We successfully titrated the optimal whole-blood dosing of the nanoparticles using this *in vitro* model by using rotational thromboelastometry (ROTEM). This confirmed that their effect on clotting times was dose dependent and the optimal dose tested was the 2.5 mg/ml group, corresponding to a blood concentration of 147 ug/ml (particle mass/blood volume). Based on our *in vitro* findings, where the nanoparticles reduce clotting time and tend to increase clot firmness, we hypothesize the mechanism for increased survival is more rapid clot formation and increase in clot strength, leading to the reduction in blood loss and increase in survival.

CONCLUSION

Trauma is the leading cause of death among young people, and blood loss plays a major role in those deaths.¹ We have developed a hemostatic nanoparticle that can be administered easily following injury that reduces bleeding and significantly increases survival following a blunt trauma injury. This is a clinically relevant result as this suggests that this treatment could be used in the field to expand the window of treatment and reduce mortality after hemorrhagic injury. This has the potential to fundamentally impact trauma care and patient outcomes. Further work is indicated to assess the long-term risks associated with hemostatic particle administration and further characterize their efficacy in large animal models where the hemodynamic conditions of flow may have drastic effects on dosing and blood loss outcomes.

WORKS CITED IN THIS CHAPTER

1. Kauvar, D.S., Lefering, R. & Wade, C.E. Impact of hemorrhage on trauma outcome: an overview of epidemiology, clinical presentations, and therapeutic considerations. *J Trauma* **60**, S3-11 (2006).
2. Kauvar, D.S. & Wade, C.E. The epidemiology and modern management of traumatic hemorrhage: US and international perspectives. *Crit Care* **9 Suppl 5**, S1-9 (2005).
3. Champion, H.R., Bellamy, R.F., Roberts, C.P. & Leppaniemi, A. A profile of combat injury. *J Trauma* **54**, S13-19 (2003).
4. Clifford, C.C. Treating traumatic bleeding in a combat setting. *Mil Med* **169**, 8-10, 14 (2004).
5. Morrison, J.J. & Rasmussen, T.E. Noncompressible torso hemorrhage: a review with contemporary definitions and management strategies. *Surg Clin North Am* **92**, 843-858 (2012).
6. Holcomb, J.B., *et al.* Causes of death in U.S. Special Operations Forces in the global war on terrorism: 2001-2004. *Ann Surg* **245**, 986-991 (2007).
7. Nunez, T.C. & Cotton, B.A. Transfusion therapy in hemorrhagic shock. *Curr Opin Crit Care* **15**, 536-541 (2009).
8. Martinowitz, U., Zaarur, M., Yaron, B.L., Blumenfeld, A. & Martonovits, G. Treating traumatic bleeding in a combat setting: possible role of recombinant activated factor VII. *Mil Med* **169**, 16-18, 14 (2004).
9. Patanwala, A.E. Factor VIIa (recombinant) for acute traumatic hemorrhage. *Am J Health Syst Pharm* **65**, 1616-1623 (2008).
10. Stein, D.M. & Dutton, R.P. Uses of recombinant factor VIIa in trauma. *Curr Opin Crit Care* **10**, 520-528 (2004).
11. Boffard, K.D., *et al.* Recombinant factor VIIa as adjunctive therapy for bleeding control in severely injured trauma patients: two parallel randomized, placebo-controlled, double-blind clinical trials. *J Trauma* **59**, 8-15; discussion 15-18 (2005).
12. Duchesne, J.C., *et al.* Current evidence based guidelines for factor VIIa use in trauma: the good, the bad, and the ugly. *Am Surg* **74**, 1159-1165 (2008).
13. Morse, B.C., *et al.* The effects of protocolized use of recombinant factor VIIa within a massive transfusion protocol in a civilian level I trauma center. *Am Surg* **77**, 1043-1049 (2011).
14. Alving, B.M., Reid, T.J., Fratantoni, J.C. & Finlayson, J.S. Frozen platelets and platelet substitutes in transfusion medicine. *Transfusion* **37**, 866-876 (1997).
15. Blajchman, M.A. Platelet substitutes. *Vox Sang* **78 Suppl 2**, 183-186 (2000).
16. Blajchman, M.A. Novel platelet products, substitutes and alternatives. *Transfus Clin Biol* **8**, 267-271 (2001).
17. Coller, B.S., *et al.* Thromboerythrocytes. In vitro studies of a potential autologous, semi-artificial alternative to platelet transfusions. *J Clin Invest* **89**, 546-555 (1992).
18. Levi, M., *et al.* Fibrinogen-coated albumin microcapsules reduce bleeding in severely thrombocytopenic rabbits. *Nat Med* **5**, 107-111 (1999).

19. Okamura, Y., *et al.* Hemostatic effects of phospholipid vesicles carrying fibrinogen gamma chain dodecapeptide in vitro and in vivo. *Bioconjug Chem* **16**, 1589-1596 (2005).
20. Okamura, Y., *et al.* Visualization of liposomes carrying fibrinogen gamma-chain dodecapeptide accumulated to sites of vascular injury using computed tomography. *Nanomedicine* **6**, 391-396 (2010).
21. Poindexter, B. & Vostal, J.G. Guidance for Industry: For Platelet Testing and Evaluation of Platelet Substitute Products. (ed. FDA) (U.S. Department of Health and Human Services, Bethesda, MD, 1999).
22. Bertram, J.P., *et al.* Intravenous hemostat: nanotechnology to halt bleeding. *Science translational medicine* **1**, 11ra22 (2009).
23. Bertram, J.P., *et al.* Functionalized poly(lactic-co-glycolic acid) enhances drug delivery and provides chemical moieties for surface engineering while preserving biocompatibility. *Acta biomaterialia* **5**, 2860-2871 (2009).
24. Hermanson, G. *Bioconjugate Techniques*, (Academic Press, San Diego, CA, 2008).
25. Cheng, J., *et al.* Formulation of functionalized PLGA-PEG nanoparticles for in vivo targeted drug delivery. *Biomaterials* **28**, 869-876 (2007).
26. D'Addio, S.M., *et al.* Novel method for concentrating and drying polymeric nanoparticles: hydrogen bonding coacervate precipitation. *Mol Pharm* **7**, 557-564.
27. Hrkach, J.S., Peracchia, M.T., Domb, A., Lotan, N. & Langer, R. Nanotechnology for biomaterials engineering: structural characterization of amphiphilic polymeric nanoparticles by 1H NMR spectroscopy. *Biomaterials* **18**, 27-30 (1997).
28. Ryan, K.L., Cortez, D.S., Dick, E.J., Jr. & Pusateri, A.E. Efficacy of FDA-approved hemostatic drugs to improve survival and reduce bleeding in rat models of uncontrolled hemorrhage. *Resuscitation* **70**, 133-144 (2006).
29. Holcomb, J.B., *et al.* Fibrin sealant foam sprayed directly on liver injuries decreases blood loss in resuscitated rats. *J Trauma* **49**, 246-250 (2000).
30. Kohn, D.F. *Anesthesia and analgesia in laboratory animals*, (Academic Press, San Diego, 1997).
31. Lavik, E.B., Hrkach, J.S., Lotan, N., Nazarov, R. & Langer, R. A simple synthetic route to the formation of a block copolymer of poly(lactic-co-glycolic acid) and polylysine for the fabrication of functionalized, degradable structures for biomedical applications. *J Biomed Mater Res* **58**, 291-294 (2001).
32. Matsuoka, T. & Wisner, D.H. Resuscitation of uncontrolled liver hemorrhage: effects on bleeding, oxygen delivery, and oxygen consumption. *J Trauma* **41**, 439-445 (1996).
33. Probst, R.J., *et al.* Gender differences in the blood volume of conscious Sprague-Dawley rats. *J Am Assoc Lab Anim Sci* **45**, 49-52 (2006).
34. Matsuoka, T., Hildreth, J. & Wisner, D.H. Liver injury as a model of uncontrolled hemorrhagic shock: resuscitation with different hypertonic regimens. *J Trauma* **39**, 674-680 (1995).
35. Knudson, M.M., Ikossi, D.G., Khaw, L., Morabito, D. & Speetzen, L.S. Thromboembolism after trauma: an analysis of 1602 episodes from the

- American College of Surgeons National Trauma Data Bank. *Ann Surg* **240**, 490-496; discussion 496-498 (2004).
36. Guo, G., *et al.* Trauma and pulmonary thromboembolism: an experimental study on their correlation. *Chin J Traumatol* **10**, 237-241 (2007).

Chapter 4: Varying Peptide Concentration: Effects on Hemostasis*

* THE MATERIAL IN THIS CHAPTER WILL BE THE OBJECT OF A MANUSCRIPT (IN PREPARATION). SHOFFSTALL A.J., EVERHART L.M., VARLEY M.E., SOEHNLEN E.S., USTIN J.S., LAVIK E.B., "TUNING TARGETING LIGAND DENSITY ON INTRAVENOUS HEMOSTATIC NANOPARTICLES IMPACTS HEMOSTASIS FOLLOWING BLUNT TRAUMA INJURY."

INTRODUCTION

Intravenous hemostatic nanoparticles have been developed to address internal hemorrhage.¹ There are a multitude of design parameters that could affect the hemostatic properties of these nanoparticles. For our hemostatic nanoparticles, Bertram et al. determined the optimal PEG chain length for allowing peptide-receptor interaction.² Bertram et al. also looked at RGD flanking peptides that increase the activity of the RGD peptide to the GPIIb/IIIa receptor.² However, it is well known that other factors such as size^{3,4}, shape⁴, and material can have dramatic effects on nanoparticle clearance from the blood circulation, margination to the vessel wall, and biocompatibility. Furthermore, heteromultivalent ligand approaches as those taken by Modery et al. allow the hemostatic nanoparticles the ability to not only increase platelet aggregation, but also can themselves adhere to the vessel wall.⁵ With such a large number of factors to test, that likely have significant interaction with one another, one must temporarily limit one's scope.

With other peptide targeted nanotherapeutics, optimizing ligand density (and clustering) has been popular topic of research.⁶⁻¹² Gu et al. developed a method to precisely engineer targeting-ligand-tunable nanoparticles for prostate cancer drug

delivery and identified the narrow conjugation ratio that optimized targeting (5% for this application).⁸ Fakhari et al. varied the ligand density of cLABL on PLGANanoparticles to optimize the targeting of ICAM-1, and found that the optimal density was roughly (50:50), and that higher conjugated particles performed worse.¹² In all cases, there it seems that the “optimal” conjugation of targeting ligand is highly application and condition-specific. In terms of the RGD-GPIIb/IIIa interaction that our nanoparticles utilize to augment platelet-platelet aggregation, there is evidence suggesting that receptor density may play a large role in determining the nature and strength of this interaction.¹³ Coller et al. find that platelet binding to high density fibrinogen prevents aggregation of platelets to a plate through “paradoxical loss of luminal receptors”.¹³ Theoretically, the high density signaling of the fibrinogen (containing RGD domains) causes translocation of the GPIIb/IIIa receptors to the site of binding, and prevents platelet binding on the luminal surface.

Here, our challenge was to develop a method for reproducibly controlling surface ligand conjugation and determine the impact of this change on hemostasis. We tested this change in both an in vivo model of lethal liver trauma as well as an in vitro assay, rotational thromboelastometry (ROTEM). A dose-response study was undertaken after lethal liver trauma in the rat to determine optimal dose of highly conjugated NPs and further utilized ROTEM to titrate an optimal peptide conjugation density. This work demonstrates the impact of changing synthetic platelet ligand density on hemostasis, and lays the foundation for methods to determine optimal ligand

concentration parameters, providing a critical step toward translation of this technology.

MATERIALS AND METHODS

Nanoparticle Synthesis

PLGA (Resomer 503H) was purchased from Evonik Industries. Poly-l-lysine and PEG (~4600 Da MW) were purchased from Sigma Aldrich. All reagents were ACS grade and were purchased from Fisher Scientific. PLGA-PLL-PEG coblock polymer was made using standard bioconjugation techniques as previously described.^{1,2,14,15}

PLGA-PLL-PEG (1 g) is dissolved in anhydrous DMSO to a concentration of 100 mg/ml. Oligopeptides (25 mg GRGDS or GRADSP) is dissolved in 1 ml DMSO and added to the stirring polymer solution. This is reacted for 3 hours, and then transferred to dialysis tubing (SpectraPor 2 kDa MWCO). Dialysis water is changed every half hour for 4 hours with Type I D.I. water. The product is then snap-frozen in liquid nitrogen and lyophilized for 2-5 days.

The resulting quaddblock copolymer PLGA-PLL-PEG-GRGDS (or a blend with PLGA-PLL-PEG) is then dissolved to a concentration of 20 mg/ml in acetonitrile (120 mg / 6 ml). This solution is added dropwise to a stirring volume of PBS. Precipitated nanoparticles form as the water-miscible solvent dissipates. Particles are collected using a coacervate precipitation method. Briefly, one mass equivalent of dry poly(acrylic acid) is added to the stirring particle suspension. 15ml of 1% w/v pAA is then added slowly to the stirring suspension until flocculation occurs. After 5 minutes,

the flocculated particles are collected by centrifugation at 500g, and rinsed 3 times with 1% pAA (centrifuging @ 500 g, 2m, 4C between rinses). On the final rinse, particles are resuspended with D.I. water, snap-frozen and lyophilized for 2-5 days. Particles are resuspended in PBS and briefly sonicated at 4W to a total energy of 50 J using a probe sonicator (VCX-130, Sonics & Materials, Inc.) prior to use.

Characterization

Successful conjugation of PLL, PEG and peptide ligands was confirmed using UV-spectroscopy, ¹H-NMR and amino acid analysis HPLC (BioRad, Varian and Shimadzu respectively). Nanoparticles were characterized for size distribution and polydispersity using dynamic light scattering (90Plus, Brookhaven Instruments Corporation) and scanning electron microscopy (Hitachi S4500).

Amino acid analysis (AAA) was used to quantify the GRGDS peptide conjugation to the triblock polymer PLGA-PLL-PEG. The outcome arg:lys ratio is used to measure this relative conjugation efficiency. Briefly, a 5 mg aliquot of polymer is hydrolyzed for 24 h in a hydrolysis/derivitization workstation (Eldex Laboratories, Inc., Napa, CA). The hydrolysate was then neutralized with a redrying solution (ethanol: water: triethylamine in a 2:2:1 ratio) and derivitized with 6-aminoquinolyl-N-hydroxysuccinimidyl carbamate, using the Waters' AccQ-Tag system. These samples were run on an HPLC (Shimadzu, with Water's PicoTag Column) and measured using a fluorescence detector. Standard addition of known quantities of arg and lys to hydrolyzed samples was used to correct for polymer hydrolysate background.

Liver Trauma Model

Sprague Dawley rats (225-275g, Charles River) were anesthetized with intraperitoneal ketamine/xylazine, and injured according to the previously established liver injury model.^{1,16-19} Treatments were administered immediately after injury and included saline, scrambled particles, and functionalized particles. All particle treatments were resuspended in a 0.5 cc PBS carrier solution.

The rats were allowed to bleed for 1 hour or until death, as confirmed by lack of both breathing and a palpable heartbeat. Before measuring blood loss, all rats were injected with a 1cc lethal dose of sodium pentobarbital. The abdomen was then reopened and blood collected with pre-weighed gauze. The clot adherent to the liver was collected last as this usually caused additionally bleeding to occur. The resected liver was weighed and fixed in 10% buffered formalin solution. Remaining liver, kidney, spleen and lungs were harvested and similarly preserved in 10% buffered formalin.

Biodistribution

Liver, kidney, spleen, lung and adherent clots were harvested and lyophilized for the biodistribution assay. The dry weight of the whole organ was recorded and 100-200 mg of dry tissue was homogenized (Precellys 24) and incubated overnight in acetonitrile at 37 C. This dissolved any nanoparticles present in the tissue and left the C6 in the organic solvent solution. Tubes were then centrifuged at 15,000 g for 10 minutes to remove solid matter and supernatant was tested on the HPLC. Mobile phase was 80% acetonitrile, and 20% aqueous (8% acetic acid). Stationary phase was a Waters Symmetry C18 Column, 100Å, 5 µm, 3.9 mm X 150 mm with fluorescence

detection (450/490 nm ex/em). Based on the known C6 loading and dosage, data is represented as percent (%) of particles injected.

Histology

Tissue samples from the left lobe of the liver (uninjured), medial lobe (injured) with adherent clot, lung, kidney, and spleen were fixed in formalin, soaked overnight in sucrose, frozen and cryosectioned to 20-micron thickness. Sections were imaged with an inverted fluorescence microscope (Zeiss Axio Observer.Z1). The DsRed filter was used to image tissue background fluorescence as a reference channel since staining with VectaShield DAPI, or H&E displaced nanoparticles from the tissue.

In vitro Assay

Coagulation assays, using Sprague Dawley rat blood, were performed using the ROTEM's NATEM test in the presence of either saline, GRGDS-NPs, or scrambled GRADSP-NPs as previously described.¹ The outcomes we considered include the standard ROTEM parameters clotting time (CT), clot formation time (CFT), the sum of the two (CT+CFT), and maximum clot firmness (MCF). CT is defined as the time from the start of the assay until the initial clotting is detected (thickness = 2mm). CFT is defined as the time between the initial clot (thickness = 2mm) until a clot thickness of 20 mm is detected. MCF is defined as the maximum thickness (in mm) that a clot reaches during the duration of the test.

Statistics

ANOVA with ad-hoc Tukey comparisons was used to analyze blood loss and ROTEM data (Minitab). 1-hour survival was analyzed with a binomial logistic regression with chi-squared tests between odds-ratios (SAS), and survival curves with a log-rank (Mantel-Cox) test. Quantification of histology was analyzed with two sample t-tests with Welch's correction.

RESULTS

GRGDS conjugation density

Polymer characteristics were the same as previously described¹, except for the higher conjugation efficiency of RGD peptide to the activated PEG groups (Figure 20).

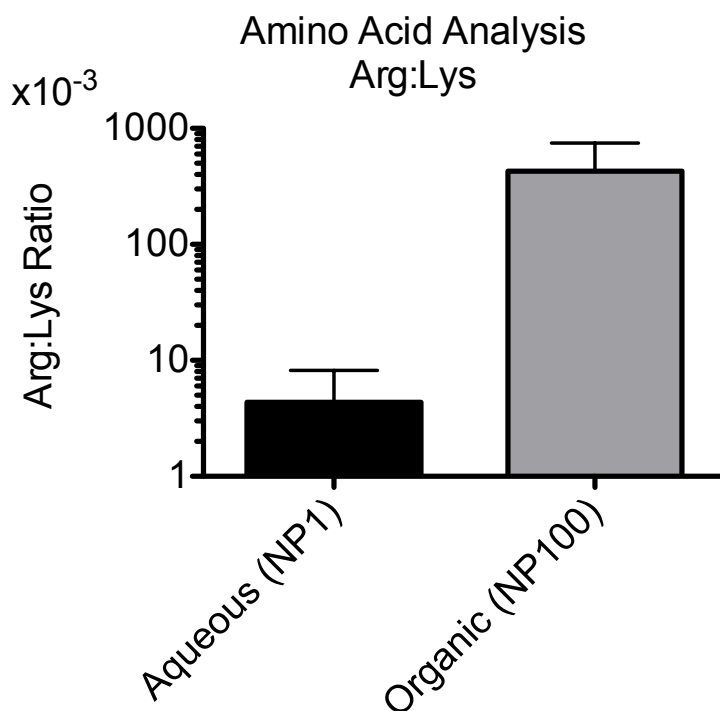


Figure 20: AMINO ACID ANALYSIS. Peptide conjugation efficiency Arg:Lys ratio. Peptide conjugation levels are approximately 100-fold higher when the conjugation reaction is performed in DMSO instead of aqueous phase. This leads to the nomenclature, NP100 and NP1 for the organic and aqueous phase polymers respectively. Interestingly the scrambled peptide, GRADSP, had a slightly higher conjugation efficiency in aqueous phase relative to GRGDS, while the GRGDS peptide had a slightly higher conjugation efficiency in aqueous relative to the scrambled GRADSP, possibly suggesting an interaction of the hydrophobic proline residue during this reaction in the different phases. Error bars denote SEM.

This was accomplished primarily by performing the peptide conjugation before nanosphere formation and allowing this reaction to take place in organic phase (anhydrous DMSO) rather than aqueous to form what we term the quadblock polymer (PLGA-b-p(lys)-b-PEG-b-GRGDS). After nanoparticle formation, peptide loading levels were measured with amino acid analysis and the arginine to lysine ratio was

determined to obtain the percentage of polymer chains with the GRGDS peptide. The nanoparticles made from the quadblock polymer has 2 orders of magnitude more GRGDS than the nanoparticles made from triblock polymer (and then conjugated with GRGDS in aqueous) used in the hemostatic nanoparticles tested previously (Arg:Lys ratio 4.35×10^{-3} compared to 0.428).¹ The high-RGD-loaded nanoparticles based on the quadblock polymer are referred to as GRGDS-NP100 and Scrambled-NP100, while the previously used triblock nanoparticles are referred to as GRGDS-NP1 and Scrambled-NP1.

In vitro test of GRGDS NP100

A dosing study with anticoagulated whole rat blood was performed to titrate the optimal dose of the NP100 nanoparticles (Figure 21). Rotational thromboelastometry (ROTEM) was used to determine clotting time (CT), clot formation time (CFT), and maximum clot firmness (MCF). Each sample consisted of 300 ul of anticoagulated blood, 20 ul of a particle dosing solution, and 20 ul of CaCl solution to replace the calcium in the blood and initiation coagulation. Previously, using the GRGDS-NP1 particles, we found that a particle dosing concentration of 2.5 mg/ml (blood concentration = 147 ug/ml) reduced clotting time in this *in vitro* model. When testing the GRGDS-NP100 particles at this same concentration, we observed an increase in total clotting time (CT+CFT), and a decrease in MCF, demonstrating an anticoagulant-like effect (Figure 21a). A dose response was then performed to titrate down to the optimal dose for the GRGDS-NP100 particles (Figure 21a-b). We found that the optimal dose was 10-fold lower, at 0.25 mg/ml (blood concentration = 14.7 ug/ml). Further testing at this

concentration yielded a reduced total clotting time (CT+CFT, $p=0.0346$), with no adverse impact on MCF (Figure 21c-d).

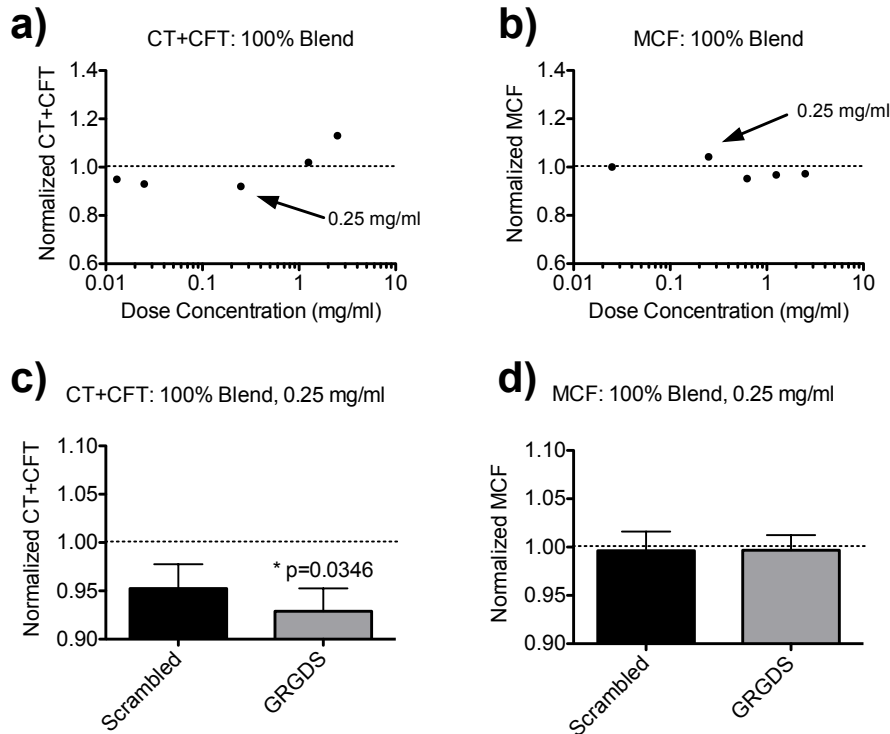


Figure 21: *IN VITRO* DOSE RESPONSE GRGDS-NP100. a-b) Total clotting time (CT+CFT) and maximum clot firmness (MCF) dose-responses, recapitulates the *in vivo* response observed: high doses have adverse impact on clotting parameters. This is observed until dosing down to 0.25 mg/ml. (n=1) C-D) 0.25 mg/ml is then further tested (n=6) to show that CT+CFT is reduced compared to saline ($p=0.0346$), with no significant impact on MCF. Dotted lines represent the normalization of clotting outcomes to saline-treated baseline sample. Error bars denote SEM.

NP100 particles in liver injury model

Previous experiments with the low-peptide conjugated nanoparticles (GRGDS-NP1) at 20 mg/ml concentration in a 0.5 cc carrier solution (40mg/kg) led to increased

1 hour survival (80% compared to 47% saline control) in a model of lethal liver trauma.¹ When this experiment was repeated with high-peptide conjugated nanoparticles (GRGDS-NP100) at the same dose concentration (20 mg/ml, 40 mg/kg) and ½ dose (10 mg/ml, 20 mg/kg), survival time was drastically reduced from a mean time of 43 minutes (saline) to 28 minutes (GRGDS 20 mg/ml) and 34 minutes (GRGDS 10 mg/ml), suggesting an adverse effect on the injury model (Figure 22d). The effects of the particles appeared to be harmful until dosing down to 2.5 mg/ml (5 mg/kg), at which, 1 hour survival increased to 100% for the pilot study with n=3 animals (Figure 22b).

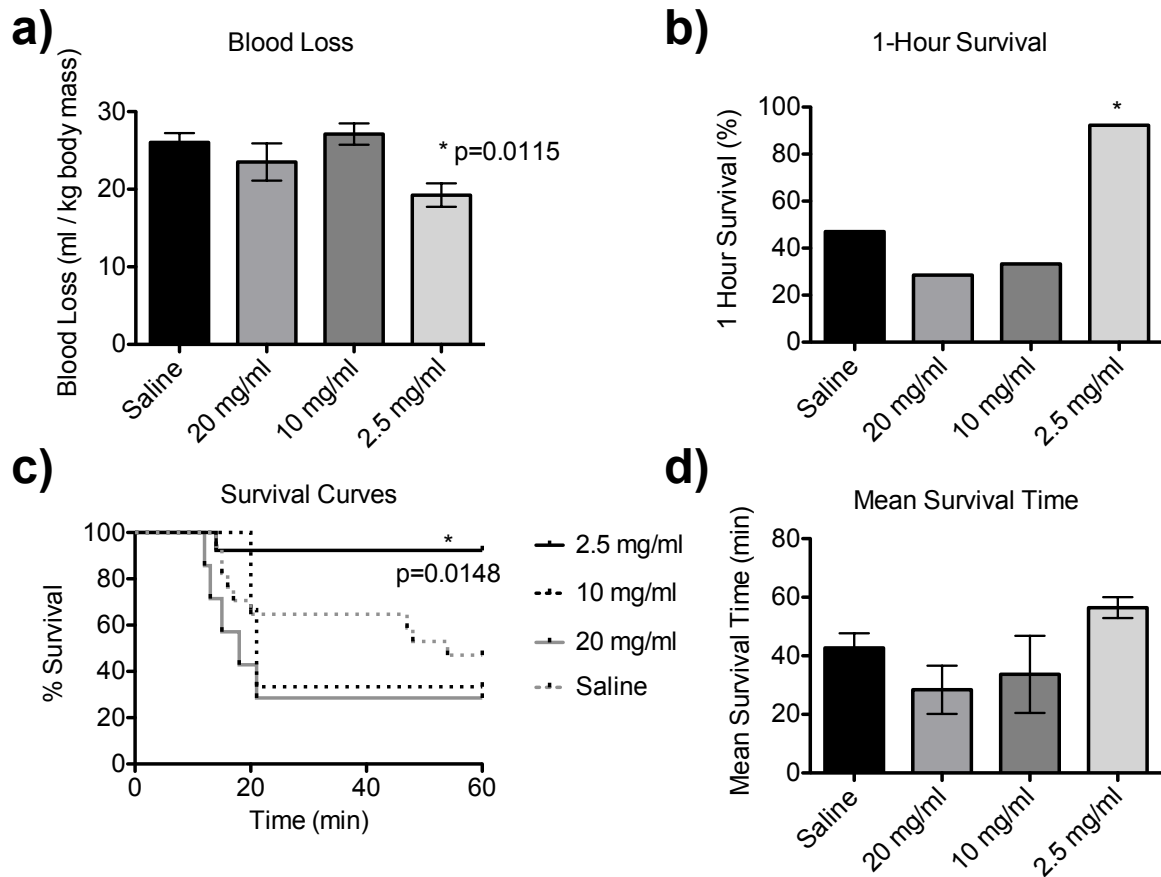


Figure 22: *IN VIVO* DOSE RESPONSE GRGDS-NP100. Dose response with GRGDS-NP100 in rat liver injury model (n=3 for pilot study). a) Blood loss is significantly reduced in the 2.5 mg/ml dose, and not significantly changed with either 20 mg/ml or 10 mg/ml doses compared to the saline control. b) Percentage of animals surviving to 1-hour is reduced in the 20 mg/ml and 10 mg/ml groups, but increased in the 2.5 mg/ml dose. c) Survival curves, showing 2.5 mg/ml is significantly improved compared to saline, log-rank (Mantel-Cox) test, p=0.0148. D) Mean survival time is reduced with the 20 mg/ml and 10 mg/ml doses, suggesting an adverse “overdose” effect. Error bars denote SEM.

We then scaled up the study (n=13) at this new dosage, 2.5 mg/ml. 1-h survival was increased to 92.3% compared to a scrambled peptide control 45% (OR=14.4, 95%

CI=[1.36, 143], power=0.836) a saline control 47% (OR=13.5, 95% CI=[1.42, 125], power=0.888) and the previously reported hemostatic nanoparticles 80% (OR=1.3, n.s., Figure 23a). Blood loss, as measured by collecting intra-abdominal blood with pre-weighed gauze, was significantly decreased from a mean of 26.0 ml/kg (saline) to 19.25 ml/kg (GRGDS-NP100, $p=0.0067$, Figure 23b).

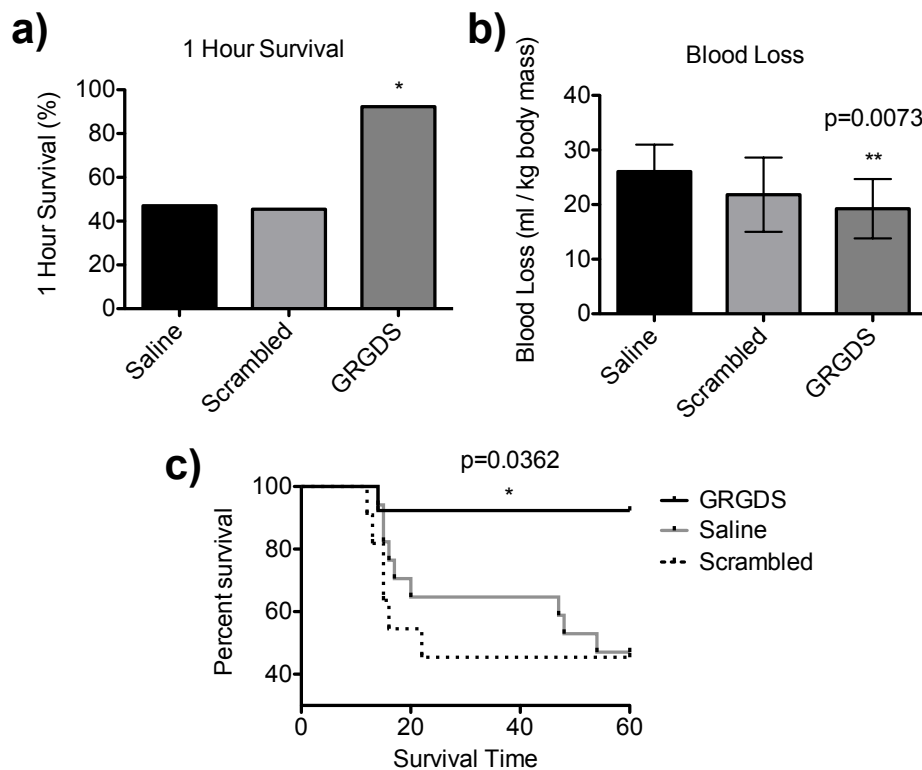


Figure 23: LIVER INJURY RESULTS NP100. Rat medial liver injury model at 2.5 mg/ml dose. a) 1-hour survival was increased to 92%, compared to a scrambled peptide control, 45% (OR=14.4, 95% CI=[1.36, 143]), a saline control, 47% (OR=13.5, 95% CI=[1.42, 125]), and GRGDS-NP1, 80% (OR=1.30, n.s.). b) Blood loss was significantly reduced in the GRGDS-NP100 group compared to saline ($p=0.0073$). c) Survival curves display increased survival with GRGDS-NP100 compared to the scrambled and saline groups, log-rank (Mantel-Cox) test, $p=0.0362$. Error bars denote SEM.

The higher peptide-conjugated particles, GRGDS-NP100, led to significantly increased survival and significantly reduced blood loss at a concentration that is one-eighth of the dose required for the previous GRGDS-NP1 formulation. This finding is incredibly important because it suggests that peptide concentration is a critical variable, and demonstrates the significant impact on the dosing of these particles by modulating targeting ligand concentration.

Biodistribution

Compared to the previous liver injury study¹, where 40 mg/kg of GRGDS-NP1 particles were injected, the present study only used 5 mg/kg of GRGDS-NP100 particles, 1/8 the previous mass. We find that similar proportions of the injected dose are found in the tissues, with the majority of particles being cleared through the liver (7.5-10.5%) or becoming entrapped in the clot (11%) or lungs (2-46%) as measured using an HPLC fluorescence assay for C6 (Figure 24). Less than 1% is found in the kidney and spleen, and the particles are rapidly cleared from the blood plasma, with only 2% remaining in circulation at the end of the one hour experiment.

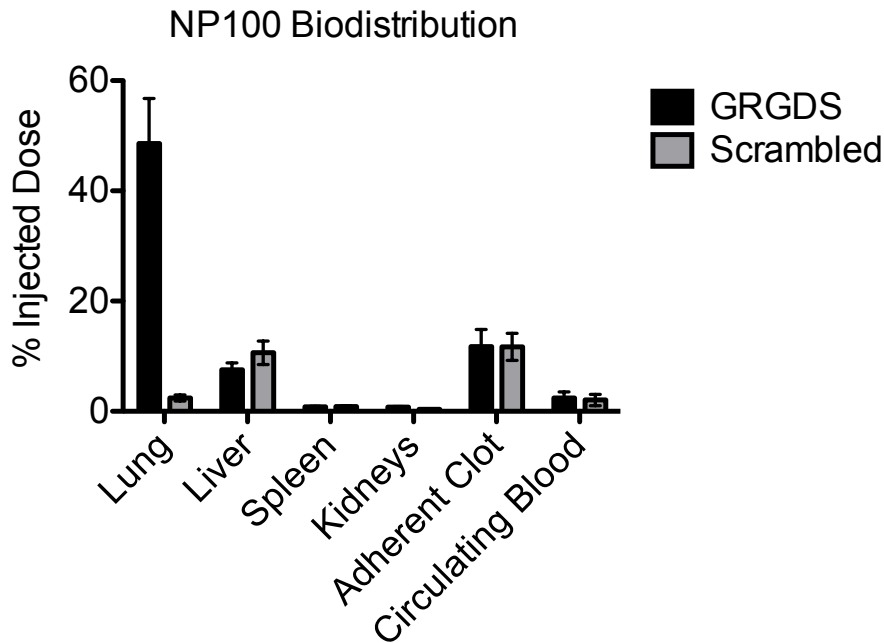


Figure 24: BIODISTRIBUTION (HPLC ASSAY). An assay for fluorescent C6 was performed using HPLC. Data is normalized to dry organ mass to reflect amount of nanoparticles found as a percent of the injected dose. There is a large proportion of the injected dose of nanoparticles accumulating in the lung tissue with the GRGDS group compared to the previous study and to the scrambled peptide group. However, it should be noted that since the total mass of particles injected is 8x less than the previous study,¹ The liver accumulates 7.5-10.5% of the injected dose (GRGDS, scrambled respectively), while ~11% becomes entrapped in the adherent clot found in the abdominal cavity post-mortem, regardless of the peptide group. Less than 1% is found in the kidney and spleen, and the particles are rapidly cleared from the blood plasma, with only 2% remaining in circulation at the end of the 1-hour experiment. Error bars denote SEM.

While the percentage of the injected dose accumulating in the lungs is greater for the GRGDS group than the scrambled group, one must note that the total dose of particles in the lungs is significantly lower than we recorded in the previous study with NP1 nanoparticles, because of the 8x lower dose needed with NP100 nanoparticles

(Figure 25: BIODISTRIBUTION (HPLC) COMPARISON BETWEEN NP1 AND NP100. There is a total of 8x fewer particles in the tissues overall, equating to approximately 2 mg in the lungs from the NP1 study versus 0.57 mg for the present study with GRGDS-NP100 particles.). Pulmonary complications were not observed in either study.

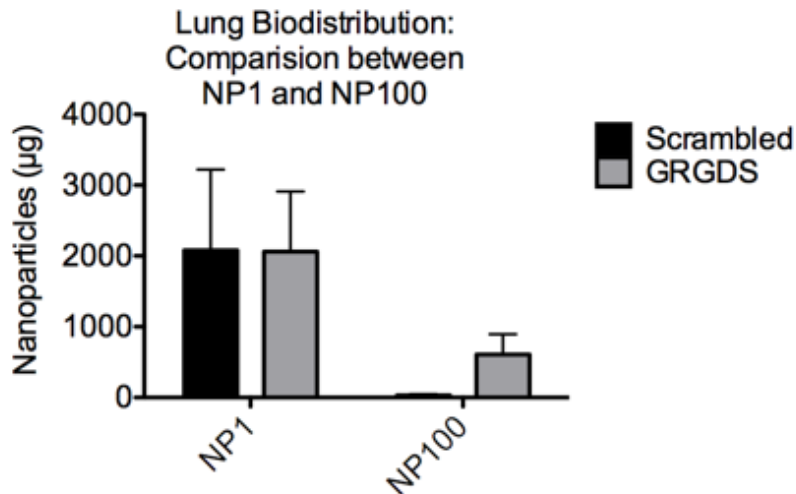


Figure 25: BIODISTRIBUTION (HPLC) COMPARISON BETWEEN NP1 AND NP100. There is a total of 8x fewer particles in the tissues overall, equating to approximately 2 mg in the lungs from the NP1 study versus 0.57 mg for the present study with GRGDS-NP100 particles.

Since biodistribution within anisotropic organs can have a heterogeneous distribution, a histological investigation was conducted, looking at the kidney, capillary beds of the deep lung, the uninjured left lobe of the liver, and the adherent clot attached to the injured medial lobe of the liver (Figure 26). We found that while the proportion of particles accumulating in the clot was similar between the GRGDS and scrambled particles (by HPLC), the GRGDS particles appeared in clusters rather than individual satellite particles (by histology), suggesting that they may be actively participating in platelet aggregation (Figure 26d). This means that for the scrambled group, the

particles may just be merely present at the injury site from the process of shedding blood. However the functionally targeted GRGDS group is not only present in the adherent clot, but could be playing an active role in platelet aggregation.

The distribution of particles to the capillary beds of the lung was significantly smaller than expected for the GRGDS group (Figure 26b), suggesting that the large quantity of particles found in the GRGDS-NP100 group, by the HPLC assay of the whole lung tissue, is not collected in the capillary beds, and must be accumulating in higher order branches.

NP100 Biodistribution (Histology)

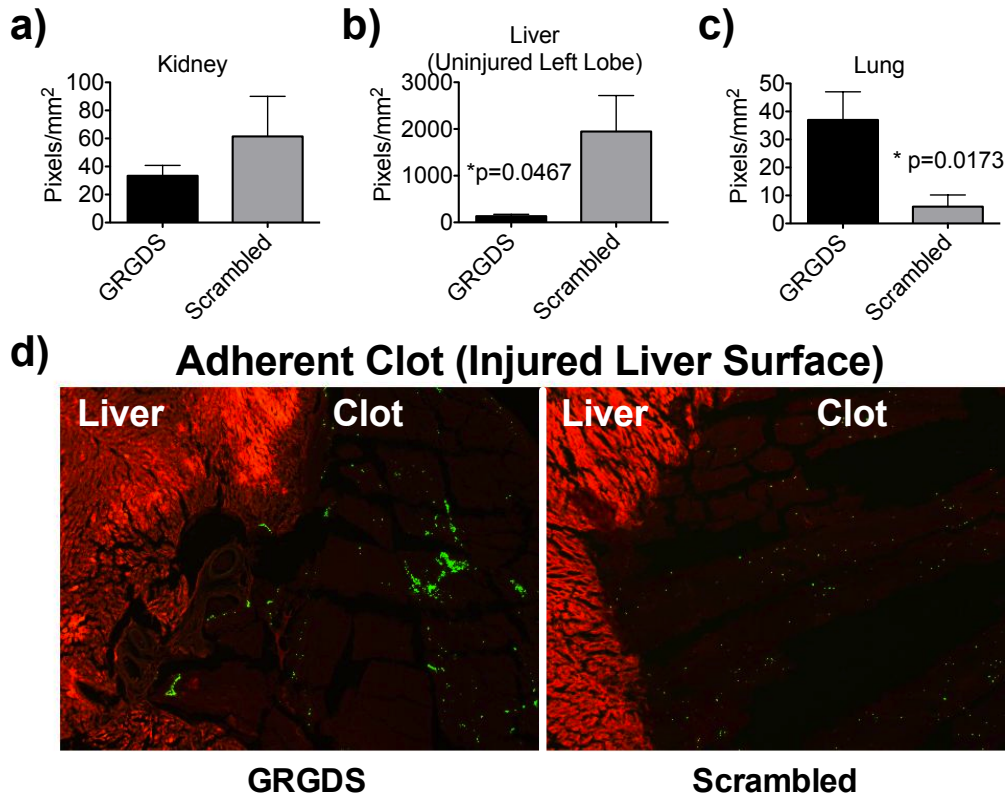


Figure 26: HISTOLOGY AND QUANTIFICATION. Histology was performed on the kidneys, uninjured left lobe of the liver, lungs, and injured medial lobe of the liver with adherent clot intact. Sections are 20 μ m, and were not stained to prevent displacement of the nanoparticles. Quantification of the particles is measured in triplicate for n=3 rats per group, and represented as pixels/mm². a) Kidneys show no significant differences between treatment groups, b) Uninjured liver (left lobe), contains higher density of particles in the scrambled group compared to GRGDS (p=0.0467). c) Lungs show a larger proportion of particles accumulating in the GRGDS group compared to scrambled, but at an average of 37 pixels/mm², this does not reflect the large proportion of particles suggested by the biodistribution determined by HPLC. The portion of the lung sampled for histology consisted of the deep lung (capillary beds), while the HPLC sample, consisted of the whole lung, including higher order vasculature, potentially explaining this discrepancy. d) Clot adherent to remaining liver. Green = coumarin-6 (C6) loaded hemostatic nanoparticles; Red =

Tissue background fluorescence (DsRed filter) used as reference channel. While the concentration of particles in the adherent clot is equal between groups, the particles in the GRGDS group appear as clusters, while the scrambled particles appear evenly dispersed. Error bars denote SEM.

In vitro test of GRGDS-NP blends

After observing the critical impact of the peptide concentration on the dose in vivo, we wanted to further explore the role of peptide density on clot formation. ROTEM provides one of the most efficient methods to look at this and requires the use of the least number of animals. First, we experimented with a platelet aggregation assay, where blends of the PLGA-b-p(lys)-b-PEG-b-GRGDS and PLGA-b-p(lys)-b-PEG to vary the peptide density were coated on a 96-well plate, and ADP-activated platelet aggregation was measured. Blends of 0%, 25%, 50%, 75% and 100% PLGA-b-p(lys)-b-PEG-b-GRGDS were tested. We observed that more peptide (higher % blends) led to more aggregation (Figure 27). However, this first experiment utilized platelet-rich-plasma and a film of the polymer blend rather than the nanoparticles tested in vivo, and we were next interested in a more physiologically relevant model of coagulation.

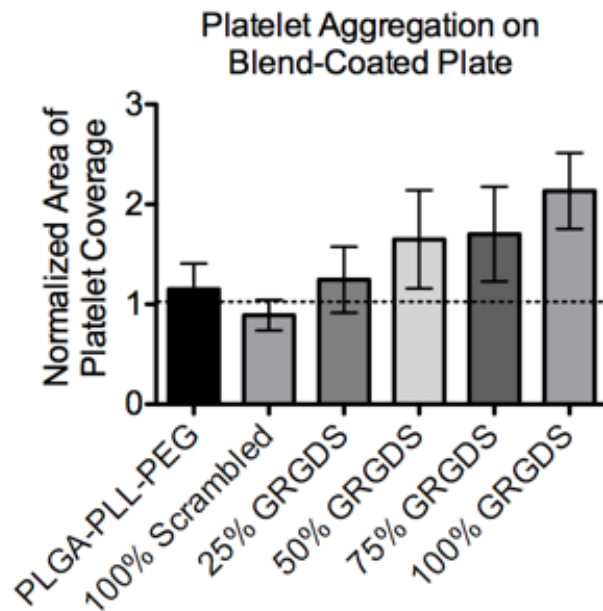


Figure 27: BLEND-COATED PLATE; PLATELET AGGREGATION ASSAY. ADP activated platelet aggregation assay, shows that higher GRGDS-loaded blends are associated with a larger amount of platelet aggregation. Error bars denote SEM.

We therefore used ROTEM, as described above, to test a series of blends of PLGA-b-p(lys)-b-PEG and PLGA-b-p(lys)-b-PEG-b-GRGDS to vary the peptide density. We investigated blends of 1%, 10%, 100% PLGA-b-p(lys)-b-PEG-b-GRGDS at three concentrations of 0.2 mg/ml, 2.0 mg/ml and 20 mg/ml using the ROTEM assay. An ANOVA (GLM) test of blend, concentration and the interaction term blend*concentration was run. This test showed that blend had a significant impact on clotting parameters ($p=0.002$, CT+CFT and $p=0.001$, MCF), while concentration did not. However it also yielded significant interaction on the blend*concentration term ($p=0.021$, MCF and $p=0.064$, CT+CFT). This is consistent with our in vivo test where we saw that the amount of peptide has a strong impact on the optimal particle dose.

However, the overall optimal dosage occurred at 20 mg/ml (GRGDS-NP10, 20 mg/ml), and we therefore focused our attention on this concentration to make comparisons between blends (Figure 28). At this dose, CT+CFT is increased by 31% for the GRGDS-NP1 blend compared to saline ($p=0.020$), decreased by 15% for the GRGDS-NP10 blend (n.s.) and unchanged for the 100% blend compared to saline (Figure 28a). MCF follows an inverse pattern, where the GRGDS-NP1 blend is reduced by 8%, the GRGDS-NP10 blend is increased by 7%, and the GRGDS-NP100 blend is unchanged compared to saline (Figure 28b). This suggests that, of the blends tested, adjusting the peptide concentration to 10% will lead to the most rapidly forming, strongest clots.

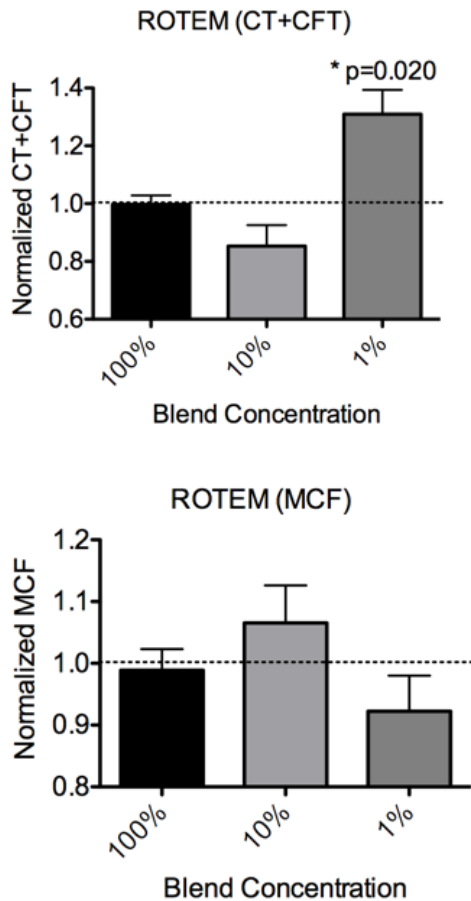


Figure 28: *IN VITRO* DOSE RESPONSE GRGDS-NP_x BLENDS. ROTEM was used to titrate the dose responses of GRGDS-NP blends (100%, 10%, 1%) with the high dose of 20 mg/ml was chosen as it produced the largest impact on clotting parameters in the ROTEM assay. However, there is significant interaction of the blend*concentration term which may be further exploited to optimize this treatment in the future. a) CT+CFT, showing no effect of the GRGDS-NP100, a decrease of 15% compared to saline for the GRGDS-NP10, and an adverse increase of 31% (p=0.020) for the GRGDS-NP1 blend compared to saline. b) This is mirrored in the MCF values, showing no effect with the GRGDS-NP100, an increase of 7% with the GRGDS-NP10, and an adverse decrease of 8% with the GRGDS-NP1 particles compared to saline. This data demonstrates the utility of the ROTEM to assay relative efficacy of these blended formulations of intravenous hemostatic nanoparticles.

DISCUSSION

We previously showed that administration of GRGDS-NP1 nanoparticles can improve survival after lethal liver trauma.¹ Here, we have increased the targeting ligand concentration on our nanoparticles 100-fold and achieved a 92% survival rate when administering GRGDS-NP100 (5 mg/kg) compared to 80% from the previous work. We found that they were efficacious at an 8-fold lower dosage compared to GRGDS-NP1 (40 mg/kg).¹ We also found blood loss was significantly reduced with the GRGDS-NP100 at 5 mg/kg. This is a significant finding as it continues to show that intravenous hemostatic nanoparticles can augment the clotting process, and that this can produce a large impact on survival.

However, at higher doses (>5 mg/kg), it is evident that the GRGDS-NP100 particles have an adverse effect, substantially reducing mean survival time in the lethal liver trauma. These *in vivo* findings are recapitulated by our *in vitro* observations, that higher doses of the GRGDS-NP100 hemostatic nanoparticles actually adversely impact hemostasis. Specifically, we find that higher doses appear to inhibit the standard ROTEM parameters of clotting time and, to a lesser degree, maximum clot firmness. These observations may potentially be explained by a saturation effect of the endogenous platelets. Too many platelet-bound nanoparticles could theoretically sterically hinder platelet-platelet interactions, leading to an inhibition of their aggregation. Another potential mechanism could be one similar to that proposed by Coller et. al.,¹³ who observed a decrease in platelet aggregation when activated on plates coated with high-density fibrinogen, compared to a low-density. They cite the

potential for translocation of GPIIb/IIIa receptors within the platelet membrane, which could then prevent the further binding interactions at the luminal surface. Together, these findings suggest that titrating the correct dosing *in vitro* will be crucial as this technology moves forward into large animal and potentially clinical trials.

We previously found that accumulation of particles in the lungs was dose, but not targeting peptide dependent, showing ~20% dose accumulation in the lung for both the GRGDS-NP1 and Scrambled-NP1 particles.¹ We have now observed peptide dependence as well, showing that we have ~46% dose accumulation in the lungs for GRGDS-NP100, but ~2% for Scrambled-NP100 particles. However, due to the discrepancies in total dose injected, there is still less total particle accumulation in the lungs with the GRGDS-NP100 (~0.57 mg total) formulation compared to GRGDS-NP1 (~2mg total).

Lung accumulation was further investigated histologically, but practically no particles were found in the capillary beds of the deep lung tissue. This tissue was isolated and saved for histology because it was where the adverse impact of intravenous nanoparticle administration was expected.²⁰⁻²² However, it is apparently not where these particles are going; only sparsely distributed single nanoparticles may be found in sections of the deep capillary beds of the lungs. It is possible that if particles are associating with clots, as has been previously suspected^{1,23,24}, and are subsequently being thrown from the injury site, these may be too large to reach the deep lung and are likely being incorporated in the higher order vasculature of the lung. The increased number of GRGDS-NP100 particles found in the lung in this study would therefore

suggest a stronger clot-targeting effect compared to the scrambled-NP100, but has the disadvantage of accumulating in what appears to be clots in the lung. It may be possible to ameliorate these effects by changing the route of administration to one that directly feeds the injury site. Regardless, the question to answer will be whether or not these particles exacerbate pulmonary function (e.g. pulmonary artery pressure) or increase risk for further embolization. It is clear that the uptake of particles in the various tissues can be widely heterogeneous, and further investigations are required to determine the impact of nanoparticles on pulmonary function and assess the risk for pulmonary embolism development.

Optimizing targeting ligand conjugation densities to increase targeting potential of nanotherapeutics is a field that is gaining more and more attention.⁶⁻¹¹ It is clear that more is not always better.^{8,11,12} Here, we presented a method to tune the density of targeting ligands presented on the surface of the intravenous hemostatic nanoparticles, by producing them with blends of the GRGDS-NP100 and the nonfunctionalized pegylated polymer, PLGA-PLL-PEG. While we developed our methods independently in our lab, other groups have taken similar approaches previously.^{8,25} Unsurprisingly, this method is more efficient, repeatable, and allows for greater control over peptide conjugation than other potential approaches such as tuning the stoichiometry or other reaction conditions of the conjugation chemistry.⁸ One potential challenge of this method is that it is possible to encapsulate unconjugated peptide within the polymer matrix upon precipitation from the organic phase. This can be mitigated by multiple

precipitation and washing steps after the GRGDS conjugation reaction to produce the quadblock polymer, PLGA-PLL-PEG-GRGDS.

Of the blends tested, we found that the 10% blend led to the most beneficial impact on clotting parameters in whole blood. However, this was not corroborated by our platelet aggregation study, using polymer-coated plates, which suggested that the 100% blend led to the highest aggregation. However, we only tested the single concentration of 500 ug-polymer/well, and may have been below the threshold for this phenomenon to occur. Additionally, the 96-well plate assay utilized a film of the polymer rather than a solution of nanoparticles, and it is therefore reasonable that the same saturation effect was not observed, since at most the platelets would only interact with the single surface, leaving the luminal surface available for additional platelet binding. While the plate assay may be potentially useful in identifying and comparing the activity of different targeting ligands and the effect of the polymer structure on platelet binding², it lacks dose-sensitivity, which appears to be a paramount factor *in vivo*. As documented by Gu et. al.⁸ the “optimal” window can be extremely narrow, and further research is indicated to fully determine optimal blend and dose parameters. We have shown here that ROTEM is a potential assay for elucidating the effects of these changes in an *in vitro* system using whole blood, and that the same dose-relationship trends are observed in an *in vivo* model of lethal liver trauma.

CONCLUSION

Here, our challenge was to develop a method for reproducibly controlling surface ligand conjugation and determine the impact of this change on hemostasis. We

tested this change in both an *in vivo* model of lethal liver trauma as well as an *in vitro* assay, rotational thromboelastometry (ROTEM). A dose-response study was undertaken after lethal liver trauma in the rat to determine optimal dose of highly conjugated NPs and further utilized ROTEM to test the effects of peptide conjugation density. This work demonstrates the impact of changing synthetic platelet ligand density on hemostasis, and lays the foundation for methods to determine optimal ligand concentration parameters, providing a critical step toward translation of this technology. Moving this technology in to clinical trials will require validation of the initial dose before proceeding. *In vitro* ROTEM testing with human blood may be one method for ascertaining this information as well as provides a mechanism for optimizing surface ligand concentrations.

WORKS CITED IN THIS CHAPTER

1. Shoffstall, A.J., *et al.* Intravenous hemostatic nanoparticles increase survival following blunt trauma injury. *Biomacromolecules* **13**, 3850-3857 (2012).
2. Bertram, J.P., *et al.* Intravenous hemostat: nanotechnology to halt bleeding. *Science translational medicine* **1**, 11ra22 (2009).
3. Merkel, T.J., *et al.* The effect of particle size on the biodistribution of low-modulus hydrogel PRINT particles. *Journal of controlled release : official journal of the Controlled Release Society* **162**, 37-44 (2012).
4. Toy, R., Hayden, E., Shoup, C., Baskaran, H. & Karathanasis, E. The effects of particle size, density and shape on margination of nanoparticles in microcirculation. *Nanotechnology* **22**, 115101 (2011).
5. Modery, C.L., *et al.* Heteromultivalent liposomal nanoconstructs for enhanced targeting and shear-stable binding to active platelets for site-selective vascular drug delivery. *Biomaterials* **32**, 9504-9514 (2011).
6. Ng, Q.K., *et al.* Engineering clustered ligand binding into nonviral vectors: alphavbeta3 targeting as an example. *Molecular therapy : the journal of the American Society of Gene Therapy* **17**, 828-836 (2009).
7. Sancey, L., *et al.* Clustering and internalization of integrin alphavbeta3 with a tetrameric RGD-synthetic peptide. *Molecular therapy : the journal of the American Society of Gene Therapy* **17**, 837-843 (2009).

8. Gu, F., *et al.* Precise engineering of targeted nanoparticles by using self-assembled biointegrated block copolymers. *Proceedings of the National Academy of Sciences of the United States of America* **105**, 2586-2591 (2008).
9. Garg, A., Tisdale, A.W., Haidari, E. & Kokkoli, E. Targeting colon cancer cells using PEGylated liposomes modified with a fibronectin-mimetic peptide. *International journal of pharmaceuticals* **366**, 201-210 (2009).
10. Gindy, M.E., Ji, S., Hoye, T.R., Panagiotopoulos, A.Z. & Prud'homme, R.K. Preparation of poly(ethylene glycol) protected nanoparticles with variable bioconjugate ligand density. *Biomacromolecules* **9**, 2705-2711 (2008).
11. Olivier, V., *et al.* Influence of targeting ligand flexibility on receptor binding of particulate drug delivery systems. *Bioconjug Chem* **14**, 1203-1208 (2003).
12. Fakhari, A., Baoum, A., Siahaan, T.J., Le, K.B. & Berkland, C. Controlling ligand surface density optimizes nanoparticle binding to ICAM-1. *Journal of pharmaceutical sciences* **100**, 1045-1056 (2011).
13. Collier, B.S., *et al.* Studies of activated GPIIb/IIIa receptors on the luminal surface of adherent platelets. Paradoxical loss of luminal receptors when platelets adhere to high density fibrinogen. *J Clin Invest* **92**, 2796-2806 (1993).
14. Lavik, E.B., Hrkach, J.S., Lotan, N., Nazarov, R. & Langer, R. A simple synthetic route to the formation of a block copolymer of poly(lactic-co-glycolic acid) and polylysine for the fabrication of functionalized, degradable structures for biomedical applications. *J Biomed Mater Res* **58**, 291-294 (2001).
15. Bertram, J.P., *et al.* Functionalized poly(lactic-co-glycolic acid) enhances drug delivery and provides chemical moieties for surface engineering while preserving biocompatibility. *Acta biomaterialia* **5**, 2860-2871 (2009).
16. Holcomb, J.B., *et al.* Fibrin sealant foam sprayed directly on liver injuries decreases blood loss in resuscitated rats. *J Trauma* **49**, 246-250 (2000).
17. Ryan, K.L., Cortez, D.S., Dick, E.J., Jr. & Pusateri, A.E. Efficacy of FDA-approved hemostatic drugs to improve survival and reduce bleeding in rat models of uncontrolled hemorrhage. *Resuscitation* **70**, 133-144 (2006).
18. Matsuoka, T. & Wisner, D.H. Resuscitation of uncontrolled liver hemorrhage: effects on bleeding, oxygen delivery, and oxygen consumption. *J Trauma* **41**, 439-445 (1996).
19. Matsuoka, T., Hildreth, J. & Wisner, D.H. Liver injury as a model of uncontrolled hemorrhagic shock: resuscitation with different hypertonic regimens. *J Trauma* **39**, 674-680 (1995).
20. Grislain, L., *et al.* Pharmacokinetics and Distribution of a Biodegradable Drug-Carrier. *International journal of pharmaceuticals* **15**, 335-345 (1983).
21. Martin, F.J., *et al.* Acute toxicity of intravenously administered microfabricated silicon dioxide drug delivery particles in mice: preliminary findings. *Drugs in R&D* **6**, 71-81 (2005).
22. Decuzzi, P., *et al.* Size and shape effects in the biodistribution of intravascularly injected particles. *Journal of controlled release : official journal of the Controlled Release Society* **141**, 320-327 (2010).
23. Guo, G., *et al.* Trauma and pulmonary thromboembolism: an experimental study on their correlation. *Chin J Traumatol* **10**, 237-241 (2007).

24. Knudson, M.M., Ikossi, D.G., Khaw, L., Morabito, D. & Speetzen, L.S. Thromboembolism after trauma: an analysis of 1602 episodes from the American College of Surgeons National Trauma Data Bank. *Ann Surg* **240**, 490-496; discussion 496-498 (2004).
25. Ali, M.M. & Zale, S.E. Cancer cell targeting using nanoparticles. (ed. USPTO) (Bind Biosciences, Inc, USA, Mar 30, 2007).

Chapter 5: Porcine Liver Trauma Model

INTRODUCTION

Several groups have developed intravenous hemostatic particles, to address noncompressible hemorrhage in the acute phase after injury.¹⁻⁶ With a few exceptions¹, the majority of these experimental therapeutics have been limited to *in vitro* and small animal studies. Clinical translation of any intravenous hemostat requires both scaling material synthesis and the investigation of safety and efficacy in larger species. While at a molecular level, hemostasis appears to be well-conserved, there is a significant difference in hemodynamics and blood coagulation parameters that may not be fully conserved from rodents to humans.⁷⁻¹⁰ Porcine hemorrhagic injury models have been developed for vascular trauma (femoral vessels)^{11,12}, solid organ injury (liver, spleen)¹³⁻¹⁶, thoracic injury (lung)¹⁷, and polytrauma (solid organ/femur).¹⁸⁻²⁰ Pigs are often used as a preclinical model of uncontrolled hemorrhage, as their hemodynamics and size are relatively well-scaled to humans.⁷

The pig is the standard model for uncontrolled hemorrhagic trauma, when investigating the physiological impact of a potential therapy.^{14-16,18,19,21-23} The cardiovascular system is well-correlated with human parameters and the comparable size allows for devices to be used in both clinical and research environment without modification.⁸ Furthermore, the wound-healing process appears to be similar to humans, resulting from similarities between porcine and human skin.⁸

The disadvantages of the porcine model include an increase in expenses due to the equipment, and need to for a technically-trained staff.⁸ Furthermore, there is an increasing body of evidence that suggests pigs may have heightened immune responses compared to small animal models and perhaps even humans, due to selective breeding practices in the meat industry, where disease susceptibility is strongly selected against.¹⁰

We have previously investigated the use of intravenous hemostatic agents, and shown that they can reduce bleeding times both in vitro and in vivo (rat), as well as lead to significant increases in survival after a lethal liver trauma in rats.^{24,25} In order to address the difference in hemodynamics between small and large animal, we studied the efficacy of the hemostatic nanoparticles in a large animal, porcine model of hemorrhage. Here, we investigated the use of intravenous hemostatic nanoparticles to reduce blood loss and increase survival after a solid organ injury, as this appears to be one of the most consistently cited models to study resuscitative and novel treatments for noncompressible hemorrhage.¹⁶

METHODS

Liver resection model

Animal protocols were developed based on Gurney et al.¹⁶, and were adapted in conjunction with the Trauma Research Laboratory at Massachussettes General Hospital, and approved by the Case Western Reserve Unviersity IACUC. The goal of the liver injury study was to determine safe and efficacious dose levels of the experimental

nanoparticle treatment. The initial dose was started at roughly 20 mg/kg and dosed down by a factor of 10 until a safe dosage was reached, followed by a factor of 2 until no effect was observed (~0.03 mg/kg).

Yorkshire pigs (30-35 kg) were anesthetized with telazol (6-8 mg/kg i.m.), intubated, placed on a ventilator, and maintained on isoflurane (2-2.5%). Catheters were placed in the carotid artery for arterial sampling and invasive blood pressure monitoring, as well as in the internal jugular vein for drug administration and saline infusions. A laparotomy was performed, and the left lobe of the liver isolated from the underlying anatomy with a malleable retractor (Figure 29). This provides a collection surface for suctioning blood, after injury. The left lobe was resected 2" from the apex (measured from the most distal part of the lobe) with a #15 scalpel blade. Treatments were administered i.v. 5 minutes after the injury was created, and consisted of active intravenous hemostat (GRGDS-NP), scrambled particles (Scrambled-NP) and saline (lactated ringers).

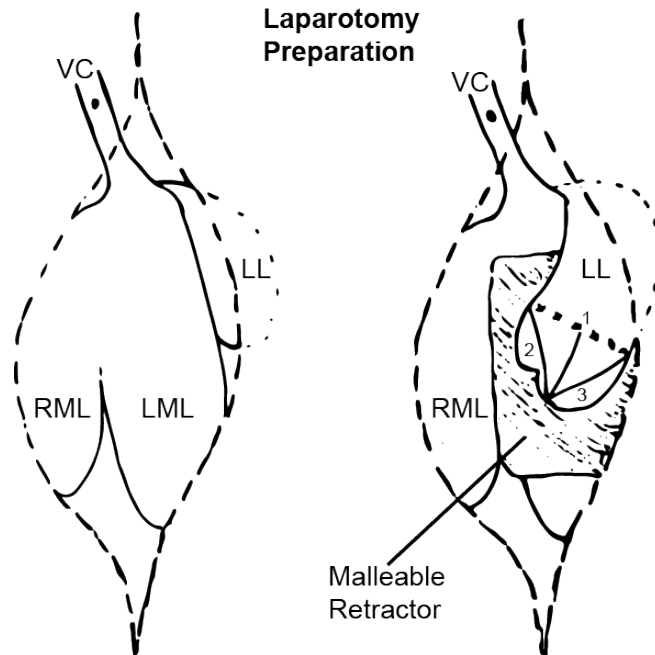


Figure 29: Making a reproducible liver injury. The left lobe (LL) is isolated from the underlying anatomy and medial lobe (left LML; right RML) with a malleable retractor, and measured and marked with cautery 2" from the apex (1). Two additional measurements are made from the apex to the lateral aspects of the resection line to ensure consistent equilateral angles (2 & 3). Ring clamps are used to hold the liver while the injury is made. The liver is resected to the left lobe midline (1), starting from patient-right. This is allowed to bleed for 1 minute with ring clamps still holding proximal to the injury line, and then the remaining liver is cut. After the injury is made, the left lobe is placed back in its natural resting place to prevent alteration of normal hepatic blood flow. VC=hepatic inferior vena cava.

Blood loss was measured directly by suctioning blood immediately from the abdominal cavity, but maintaining a sweep radius of approximately 1cm to prevent removal of clot from the injury surface. Arterial blood samples were collected at baseline, 15, 30, 60, 120, 180, and 240 minutes after injury, and were immediately followed by lactated ringers infusions: 400 ml @ 40 ml/min for the first time point (15

min) and 200 ml @ 20 ml/min for all subsequent time points that the MAP is below baseline.

Outcomes considered include physiological parameters: heart rate (HR), mean arterial pressure (MAP), SpO₂, and ETCO₂. Blood samples are analyzed for platelet counts, blood gas, and diagnostic clotting times (ROTEM and Hemochron). The animal was monitored for 4 hours after injury or death, at which point pigs were euthanized with an overdose of sodium pentobarbital.

Naïve administration/response model

Our initial results with this pig model indicated an adverse impact of the experimental nanoparticle therapeutic when dosed higher than ~0.15 mg/kg. This adverse response was characterized by rapid hemorrhage from the induced liver injury. We therefore, developed a naïve administration model to determine the impact of the nanoparticles in the absence of an injury. Here, the formulation of the nanoparticles was varied to look at the influence of 2 factors: excipient (+/- polyacrylic acid), and zeta potential (-30mV, neutral, and +20mV).

The surgery was performed as described above to introduce catheters for invasive blood pressure monitoring, arterial blood sampling and venous infusions. A dose of 2 mg/kg of nanoparticles was injected, denoting time=0. The pig was then monitored for 1 hour, with regards to physiological parameters: heart rate (HR), mean arterial pressure (MAP), SpO₂, and ETCO₂. Blood samples were analyzed for platelet counts, blood gas, and diagnostic clotting times (ROTEM and Hemochron).

After 1 hour, a second formulation of the nanoparticles was injected, and the naïve administration model experiment repeated. N=2 pigs were used in this experiment. The first pig received 2 doses of PLA-PEG-NP's (zeta=-30 mV) with (t=0 min) and without the PAA excipient (t=85 min). The second pig received 2 doses of PLGA-PEG-NP's (with PAA), comparing zeta potentials of -1.29 mV (t=0) and +20 mV (t=65 min).

RESULTS

Making a reproducible injury

Creating a reproducible liver injury was crucial to producing a consistent injury model. The initial, and only criteria, during our initial experiments is that we resect the left lobe of the liver, measuring 2" from the apex. When comparing the blood loss in the pre-administration time (0-5 minutes), it was observed that there was a very large variation between pigs. This was reduced to a consistent ~300-400 ml, after the liver injury was standardized as described (Figure 29). This was primarily achieved by establishing a consistent degree of injury as well as the angle of the cut, measuring 2" from the left lobe apex (1), and ensuring that measurements (2 and 3) were equivalent (Figure 29). Replacement of the injured left lobe in its natural resting place, was also critical to prevent tension/torsion from altering normal hepatic blood flow. Ring clamps were held in place placed during the injury, and proximal, to maintain consistency with the previously established injury protocol.¹⁶

In our initial work, the pre-administration blood loss (0-5 minutes) was highly variable, indicating an irreproducible injury model. This was later ameliorated by tightly standardizing the injury. The comparison of cumulative blood loss (Figure 30), or blood loss at relevant experimental times points (Figure 31) before and after particle administration appears to be one metric that may be able to be used to measure hemostatic efficacy of these particles, and minimize the impact of the disparity in pre-administration blood loss between pigs.

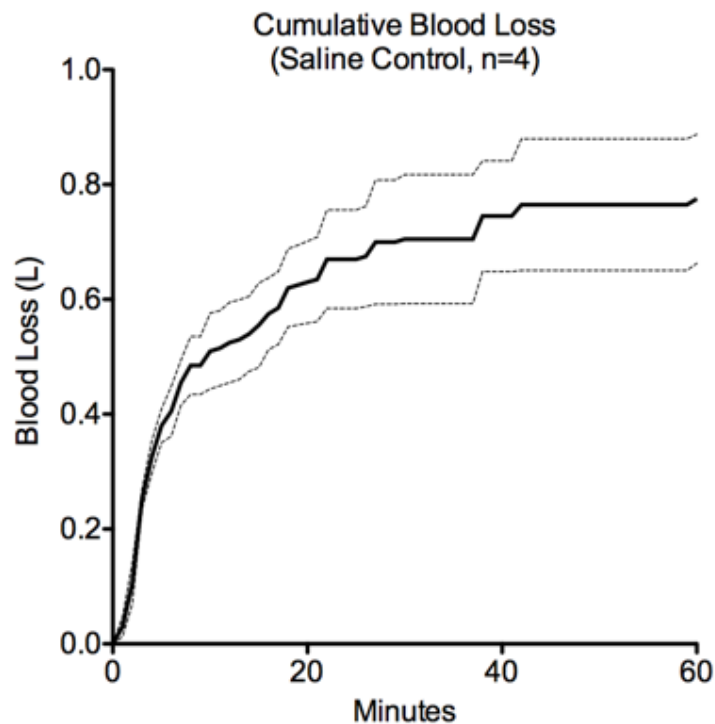


Figure 30: CUMULATIVE BLOOD LOSS, LACTATED RINGERS CONTROL. The liver injury is made at time = 0, and allowed to bleed freely. Blood is collected via suction. This curve represents cumulative blood loss averaged from 4 experiments. The majority of blood loss occurs in the first 5 minutes. The dotted lines denote SEM.

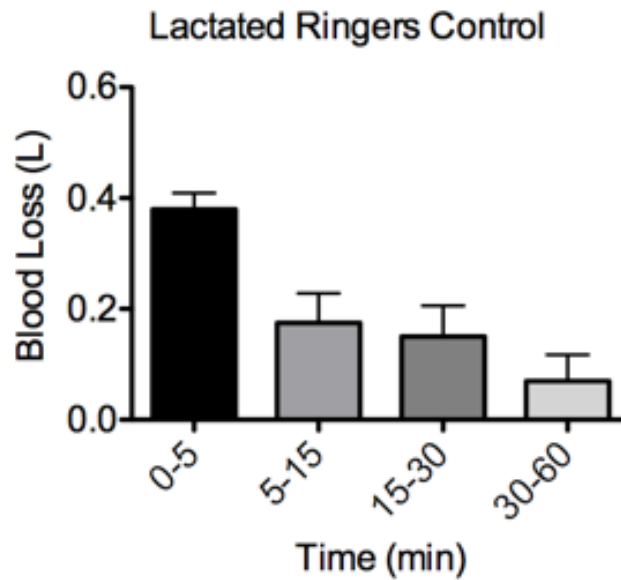


Figure 31: BLOOD LOSS, divided into 4 time ranges, pre-administration (0-5 min, 380+/-59 ml), post-administration (5-15 min, 174+/-106 ml), post-infusion 1 (15-30 min, 150+/-111 ml), and post-infusion 2 (30-60 min, 70+/-95 ml). +/- represents S.D.

Nanoparticle administration exacerbates bleeding during liver injury

One of the interesting outcomes of this work is that administration of our particles caused an unexpected, massive bleed-out at doses ≥ 2 mg/kg, independent of the peptide attached. This occurred with the NP100 and NP1 particles (varying peptide density), and it occurred regardless of the peptide attached (GRGDS, GRADSP, or none). This is readily seen in survival time, and total blood loss, where control groups given lactated ringers (n=4/4) survived the entire duration of the 240 minute experiment, with a mean 775 ml blood loss +/- 225 S.D., whereas the particle treatment groups fared considerably worse (Table 6).

Table 6: SURVIVAL TIME AND BLOOD LOSS grouped by dose (mg/kg). All 4/4 lactated ringers control pigs survived the entire 240 minutes, with a mean blood loss of 775 ml +/- 225 S.D. The optimal dosing appears to be between 0.1-0.2 mg/kg, where the adverse impact appears to be minimized. Interestingly, dosing down to 0.03 mg/kg, appears to also exacerbate the injury model, however, not as drastically as was observed with doses >2.0 mg/kg. Rather, animals are susceptible to prolonged bleeding times instead of induction of rapid hemorrhage.

Dose (mg/kg)	Survival Time (min)			Blood Loss (ml)		
	Mean	S.D.	N	Mean	S.D.	N
Saline Control	240	0	4	775	224.7	4
NP1						
<i>Scrambled</i>						
0.03	210		1	1260		1
0.10	26	28.3	3	920	408.4	3
0.20	7		1	880		1
2.00	8		1	1040		1
<i>GRGDS</i>						
0.03	30		1	1240		1
0.10	144	93.1	3	853	391.1	3
0.20	240		1	1020		1
2.00	9	0.0	2	890	14.1	2
NP100						
<i>Scrambled</i>						
0.10	73	77.6	5	1335	168.6	5
0.20	87		1	820		1
<i>GRGDS</i>						
0.10	172	81.4	6	1086	545.6	6
0.20	87	132.2	3	992	246.0	3

Our initial hypothesis for this adverse response was that the particles may have been causing saturation of platelet receptors, as would be seen with administration of

free RGD peptide, causing platelet inhibition. We therefore proceeded with our dosing study as planned, and found 0.1-0.2 mg/kg to be the “optimal” dose which did not elicit an adverse response. However, upon further analysis, the particles still appear to prolong bleeding times in the pigs, demonstrating increased amounts of bleeding post-treatment (5-60 min). This held true for both NP1 particles (Figure 32) and NP100 particles (Figure 33).

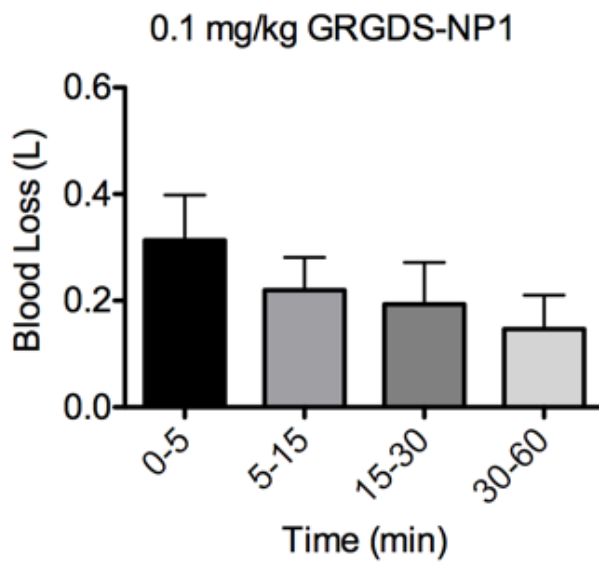
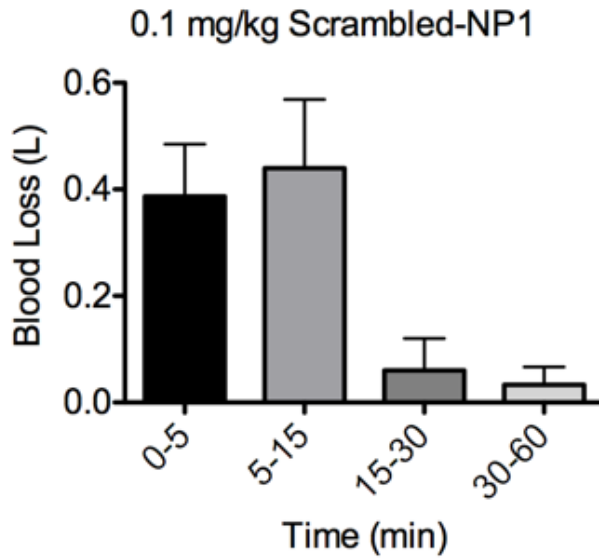


Figure 32: NP1 RATE OF BLOOD LOSS (0.1 mg/kg dose at 5 min post-injury). While blood loss in the pre-administration (0-5 min) window was consistent between groups, the post-administration (5-60 min) blood loss was exacerbated greatly in the both the GRGDS (560 +/-118 ml) and scrambled (533 +/- 146 ml) groups compared to the saline control (395 +/-104 ml). Mean survival time was 26 min for scrambled and 144 min for GRGDS, compared to 240 min for the saline control. +/- represents S.D.

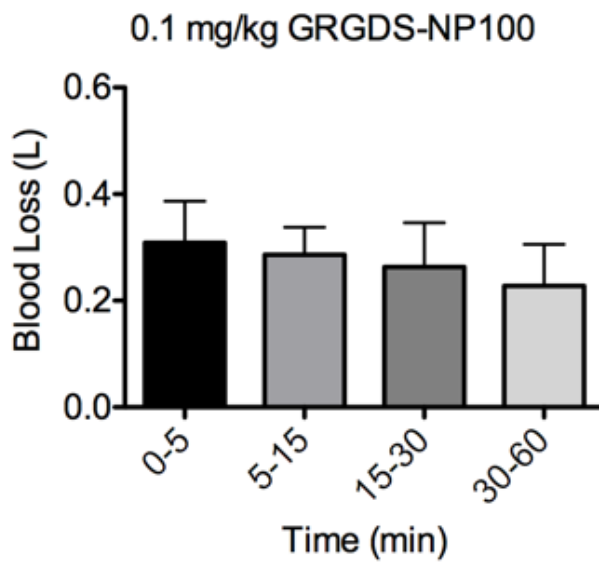
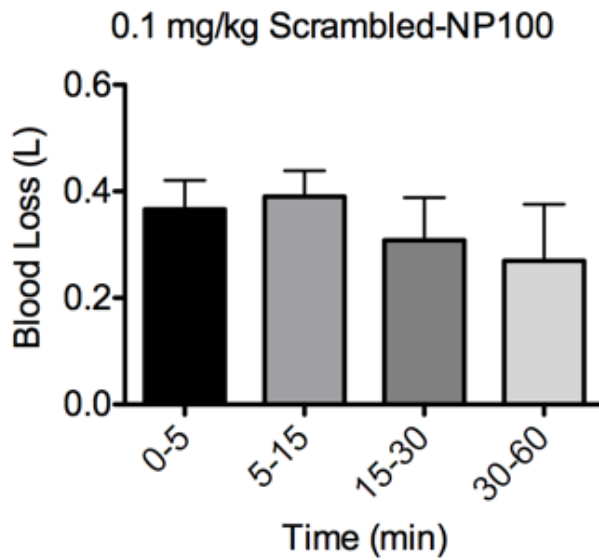


Figure 33: NP100 RATE OF BLOOD LOSS. (0.1 mg/kg dose at 5 min post-injury). While blood loss in the pre-administration (0-5 min) window was consistent between groups, the post-administration (5-60 min) blood loss was exacerbated greatly in the both the GRGDS (777 \pm 177 ml) and scrambled (968 \pm 183 ml) groups compared to the saline control (395 \pm 104 ml). Mean survival time was 73 min for scrambled and 172 min for GRGDS, compared to 240 min for the saline control. \pm represents S.D.

We then tested several particle controls (2 mg/kg) that contained no targeting peptide, suspecting that even the GRADSP peptide may still be interacting with platelet receptors. However, we again observed that the nanoparticles induced a hemorrhagic response, regardless of the fact they contained no-peptide. We were then led to believe that the adverse effect must be from a nonspecific interaction of the nanoparticles' material itself, leading to the development of a naïve administration model to further investigate the phenomenon.

Nanoparticle administration in naïve pig induces CARPA

Within 1 minute of administration of hemostatic nanoparticles (2 mg/kg, no-peptide control NP's) in an uninjured (naïve) pig, cardiopulmonary issues are present, and consistent with those previously reported with complement activation related pseudoallergy (CARPA).²⁶⁻²⁸ The symptoms of CARPA include: increase in heart rate, hypotension, flushing of the skin (erythema), decreased cardiac output, decreased pulmonary pressures, and decreased blood gas levels.²⁷ Surprisingly, these issues spontaneously resolve within minutes. However, we noticed recurrent episodes of these acute symptoms, concomitant with arterial blood sampling from the carotid artery, which has not been previously reported. For the purposes of this first experiment, blank (no peptide, no coumarin-6), pegylated nanoparticles were utilized, comprised of the copolymer poly(l-lactic acid)-poly(ethylene glycol) (PLA-PEG-NP's). We injected 2 mg/kg nanoparticles (-pAA) at t=0 min, and another 2 mg/kg nanoparticles (+pAA) at t=85 min, to test the effect of the pAA excipient on the CARPA

response. 2 mg/kg was selected as we were sure this dose produced a strong effect from experiments with the liver injury model.

Fig 1: First administration 2 mg/kg PLA-PEG-NP's -PAA (zeta = -30.04 mV)

Symptoms presented 1.5 minutes after the first injection at t=0, and included a profoundly decreased arterial pressure, end-tidal CO₂ and paO₂ (Figure 34). The pulse-oximeter failed during the episode likely due to limited perfusion of the extremities during hypotension. However the arterial blood gas sample corroborated the decrease in pO₂, changing from 680-700 mmHg baseline to 269 mmHg during the episode.

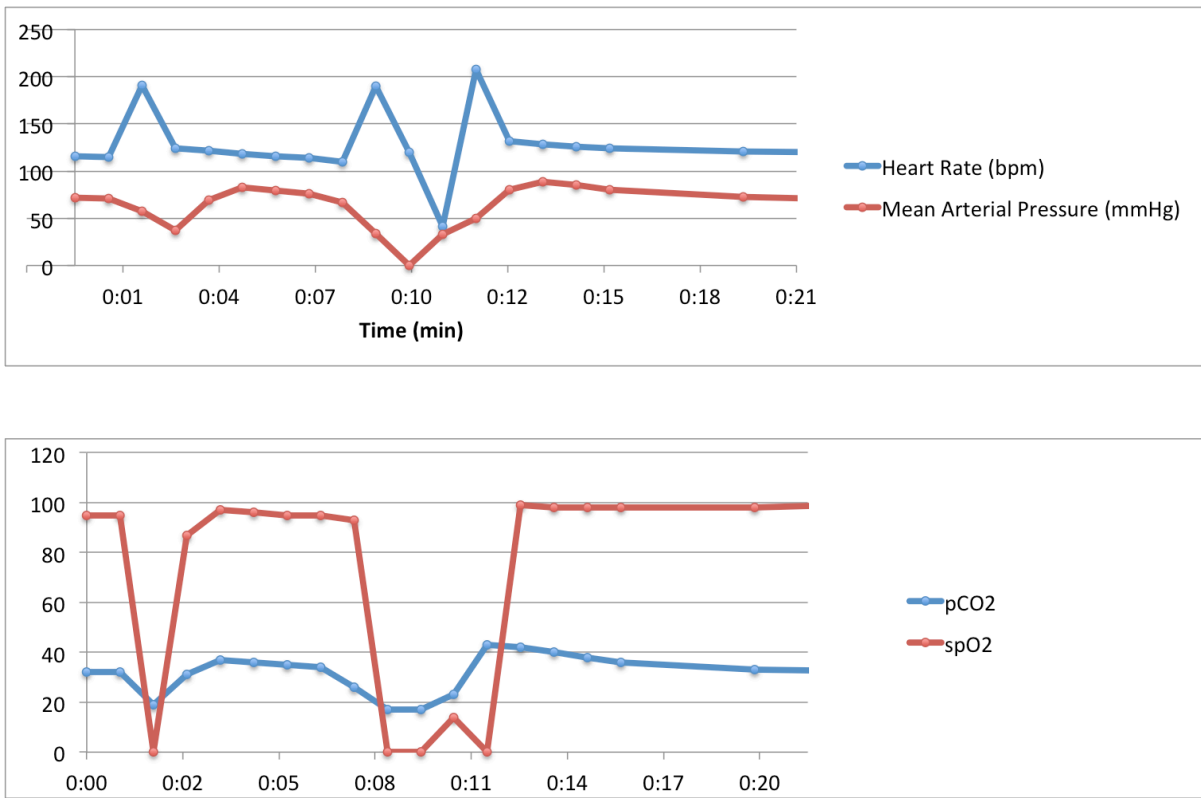


Figure 34: Fig 1: First administration of 2 mg/kg PLA-PEG-NP's -PAA (zeta=-30mV). CARPA is present immediately after injection at t=1-2 min, 8-12 min, and 61-65 min after initial injection at t=0 min.

A red flushing of the skin was present (erythema) immediately following recovery from these cardiopulmonary episodes, lasting approximately 1 minute each (episodes occurring at t=1-2 min, 8-12 min, and 61-65 min after initial injection). The subsequent episodes appeared to have been linked to blood, as they occurred immediately after collections.

Pig 1: Second administration 2 mg/kg PLA-PEG-NP's +PAA (zeta = -31.64 mV)

The pig was allowed to stabilize up to 88 minutes after the initial injection, at which time, a second injection of 2 mg/kg PLA-PEG-NP's + pAA was injected. This initiated another CARPA response, from which the pig did not recover (Figure 35). This may indicate that the pAA elicited a stronger response, or just be a result of sequential dosing.

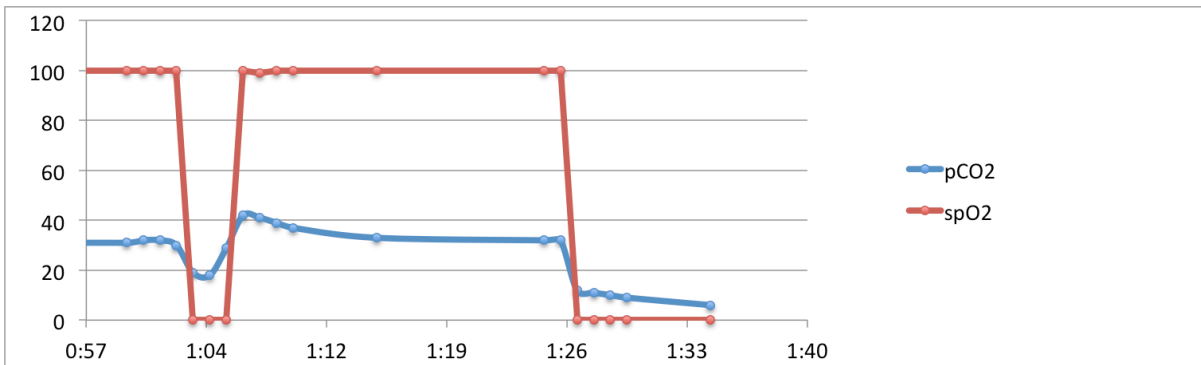
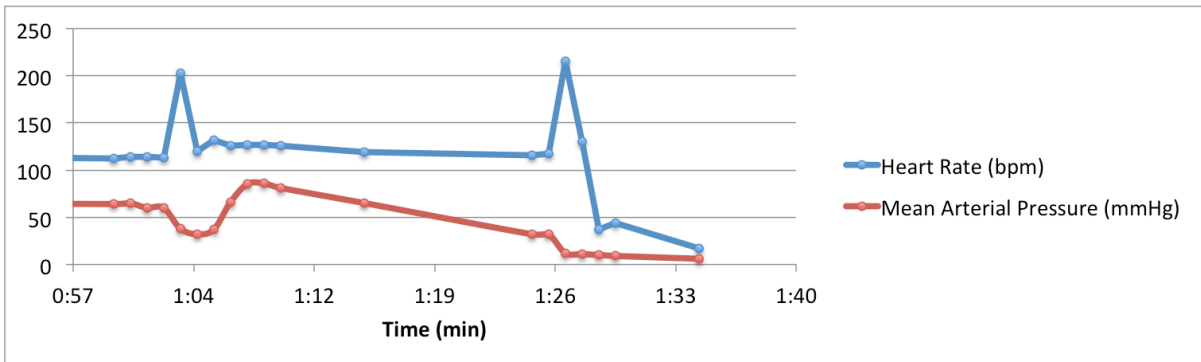


Figure 35: Pig 1: Second administration of PLA-PEG nP +PAA ($\zeta=-30$ mV) at 85 minutes after initial particle injection.

Clotting times during naïve particle administration do not appear to be adversely affected. On the final blood draw ($t=90$ min), the pig was in severe shock and died shortly after, which may account for the apparently reduced clotting time (Figure 36).

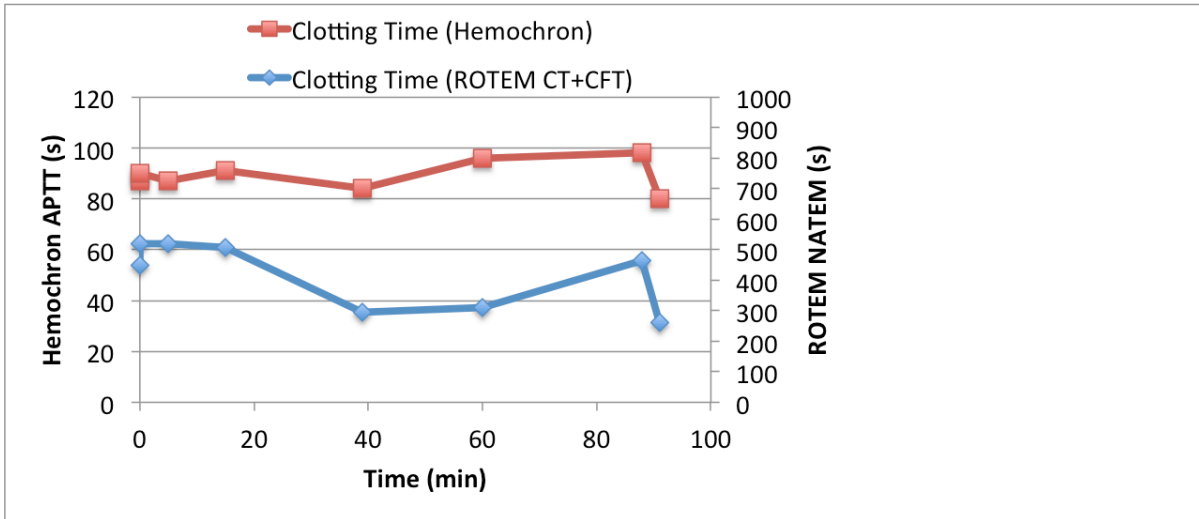


Figure 36: Clotting times during naive particle administration. Coagulopathy does not appear to be innately present.

Varying nanoparticle charge (zeta potential) mitigates CARPA

This study consisted of a pig injected at t=0 with neutral particles (zeta potential = -1.29 mV), followed by a second injection at t=65 min with positively charged particles. Both particle formulations contained poly(acrylic acid).

First administration 2 mg/kg PLGA-PLL-PEG-NP's +PAA (zeta = -1.29 mV)

There were no adverse effects following injection of neutrally charged particles (Figure 37). Physiological parameters HR, MAP, pO₂, pCO₂, and coagulation profile as measured by ROTEM (NATEM) and Hemochron Jr. (APTT) remained within range of their baseline values. The pig was observed up to 1 hour before proceeding with the second injection (t=65 min).

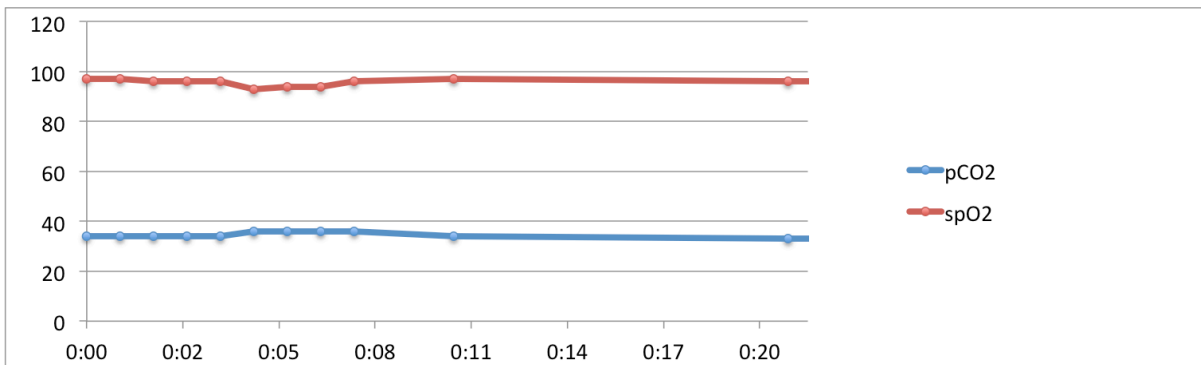
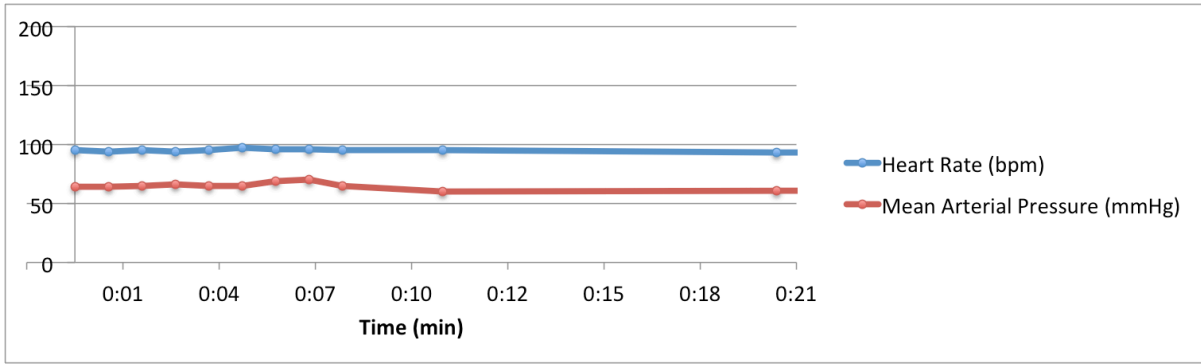


Figure 37: First administration 60mg PLGA-PLL-PEG -pAA (zeta=-1.29 mV). No adverse effects were seen, including coagulation profiles measured by ROTEM (NATEM) and Hemochron (APTT).

Second administration 2 mg/kg PLGA-PLL-PEG-NP's +pAA (zeta=+22.97 mV)

Onset of symptoms, consistent with CARPA, was observed within 1.5 minutes of injection. These symptoms included an erratic heart rate, a decreased MAP, EtCO₂, pO₂, which spontaneously recovered within 7 minutes. Erythema, as well as a characteristic overshoot was then observed as physiological parameters returned to baseline over the following 20 minutes.

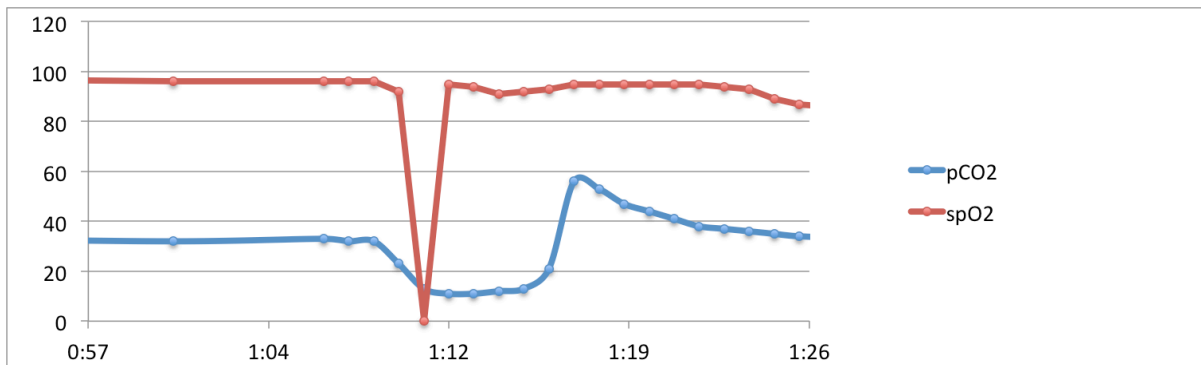
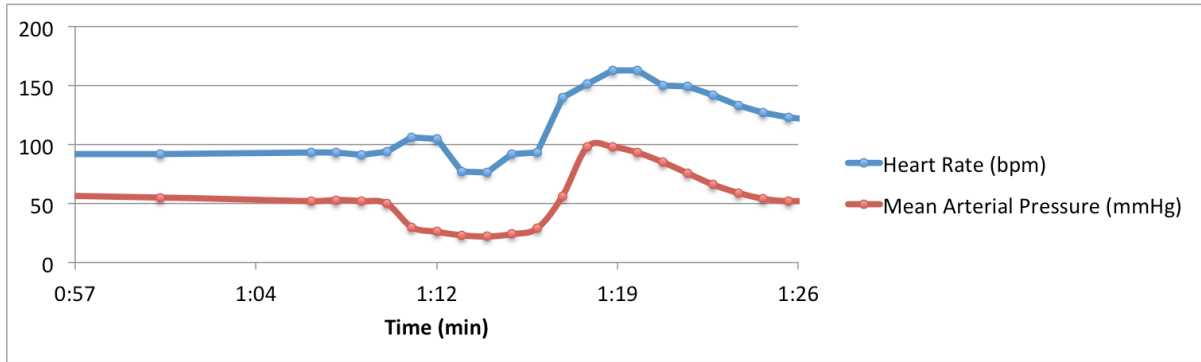


Figure 38: Second administration 2 mg/kg PLGA-PLL-PEG-NP's +pAA (zeta=+22.97 mV)

Injury after nanoparticle-induced CARPA

Once baseline physiological readings of HR, MAP, CO₂ and O₂ had returned to baseline, the liver injury model was performed (t=88 min, or 10 minutes after the resolution of CARPA induced by the +20 mV particles) to investigate the impact of CARPA on hemostasis following hemorrhagic trauma.

Immediate bleed-out was not observed, as in the previous study, where CARPA was induced 5 minutes after creating the liver injury. Instead, however, there appeared to be an increased amount of blood loss over a prolonged time period, compared to the previous control groups which only received saline (Figure 39).

**Injury Post-CARPA Episode
Induced by PLGA-NP (no-peptide, +20 mV)**

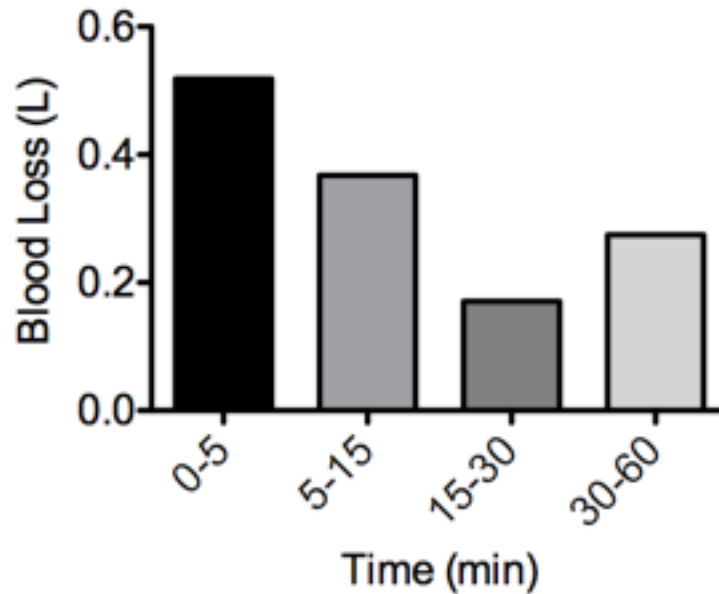


Figure 39: Blood loss after liver injury induced post-CARPA episode. There is an apparent coagulopathy, compared to the saline-treated pigs. Particles were administered at time=0min. Blood loss in the acute phase (0-5 min) is exacerbated to 519 ml from 380ml +/-59 ml (S.D.) in the saline control group. This coagulopathy continues in the 5-60 min time range, exacerbating bleeding to 814 ml compared to 395 ml in the saline control group. Survival in the CARPA (+injury) experiment was 82 minutes, compared to 240 minutes for (n=4/4) pigs treated with saline.

Total 1-hour blood loss for this study was 1330 ml compared to a mean of 775 ml in the control group (or an equivalent of ~2.5 standard deviations above the control). Total survival time was 82 minutes, compared to the saline control group, where all (n=4) pigs survived to at least 240 minutes (the end of the experiment).

DISCUSSION

Our initial hypothesis was that the nanoparticles could be causing platelet receptor saturation. However, the half-maximal inhibitory concentration (IC50) of GRGDS for fibrinogen binding to GPIIb/IIIa is 205 nM.²⁹, and the amount of nanoparticles injected at the lowest dosage of GRGDS-NP1 at 0.03 mg/kg is orders below this threshold. The results are also contradictory to this hypothesis since scrambled-NP's and no-peptide-NP's elicited equivalent (if not worse) adverse effects.

Upon further testing in the naïve administration model, we found that the results are consistent with the induction of CARPA, a pseudoallergy that has just recently begun to be characterized, and appears to be elicited readily in pigs.^{26,27} CARPA, to my knowledge, has never been studied in the presence of an active hemorrhage. The surprisingly lethal result is one that may have significant implications moving this technology forward.

Possible causes of CARPA in this model

Excipient usage: poly (acrylic acid)

Our experiments in the naïve pig model have shown that poly(acrylic acid) alone is not responsible for initiating the CARPA response, as the injection of neutrally charged particles (+PAA) did not itself induce a response. However, the pig in the first experiment showed a more severe reaction to the particles with the PAA. While it is possible, that the PAA is directly responsible for increasing the severity, it is also likely that the response was increased due to an already heightened and active complement

system. Subclinical reactions to PAA may still exist, and as suggested in the literature should be tested with inflammatory marker/cytokine assays in future experiments.³⁰

Endotoxemia (bacterial/fungal origin)

Complement activation is classically induced by the endotoxin lipopolysaccharide (LPS). Pigs are especially sensitive to endotoxemia and sepsis, which make them good models for those pathologies.¹⁰ However, the spontaneous resolution of symptoms as observed in the present study is not consistent with the prolonged symptoms usually seen with endotoxemia and sepsis.^{31,32}

Nanoparticle surface charge (zeta potential)

Szebeni et al. have postulated that zeta potential is one potential mediator of CARPA induced by intravenous nanoparticle systems.³³ While the mechanism is currently not fully understood, both the results presented by Szebeni et al. and our experience with the neutral particles, suggest that neutrally charged nanoparticles may mitigate the initiation of CARPA in pigs. Additional research is needed to elucidate this mechanism so that the parameters to minimize CARPA may be identified.

Inherent species difference

Interestingly, however, we do not see any drastic response of the nanoparticles in the rat liver injury model. It is most likely, as has been previously reported, that the pig species simply has a heightened immune response to pathogens. This is potentially due to their selective breeding in the meat industry, where susceptibility to disease has been strongly selected against.¹⁰

Potential causes for apparent coagulopathy during liver injury model

CARPA

The mechanism of CARPA and its relation to the coagulation cascade have not yet been fully elucidated. However, there are prior indications that biomaterials in contact with blood have the potential to elicit complement activation, which are mediated by FXII activation, and its fragments (factor XII_f).^{34,35} These papers have shown that charged, or hydrophilic materials, tend to adsorb proteins and produce FXII fragments as well as kallikrein (which in turn cause bradykinin formation – a strong vasodilator). While these previous studies have looked at macroscopic devices which contact blood for long periods of time, there have been no similar studies of biomaterial interactions with nanoparticles in vivo, which may produce more transient responses as they are cleared or endocytosed.

If CARPA is indeed mediated by factor XII activation by adsorption to the charged nanoparticle surface, then its fragments may well induce coagulopathy by activating plasminogen, and further cause additional hemorrhage due to bradykinin (or histamine) vasodilation.³⁶ While long-term coagulopathy was not observed clotting time and APTT assays, it is possible that this coagulopathy is transient, and only catastrophic when occurring simultaneously with an injury.

The link from coagulation cascade activation to complement activation (FXII_f → complement C1 activation) is well documented.³⁶ However, the link between nanoparticle-induced CARPA and factor XII does not appear to have been studied. However, the charge dependence of both biomaterial interactions (which produce XII_f)

and CARPA may suggest that the mechanisms are linked. Future studies may be aimed at testing this hypothesis.

Excipient usage: poly (acrylic acid)

While we did not see any effect of this excipient in the rat liver injury model, it is possible it was contributing to our coagulopathy observations in the pig. Deng, et al. ³⁰ describes poly(acrylic acid) conjugated nanoparticles that induce MAC-1 inflammatory activation, through fibrinogen denaturation. Monien and Desai ³⁷ describe the role of poly(acrylic acid) in direct anti-coagulation through a mechanism similar to that of heparin. Furthermore, PAA's chemical structure is similar to that of citric acid, a commonly used anticoagulant, for its calcium chelating ability.

In vivo, citric acid is rapidly metabolized in the citric acid cycle and the calcium recovered, leading to an ineffective in vivo anticoagulant therapy. PAA, on the other hand would not be metabolized as quickly, and may lead to a reduction in free calcium ions in the blood. However, due to the tightly controlled blood calcium levels in the blood, the quantity of poly(acrylic acid) being injected is likely not able to impact bleeding as drastically as has been observed. At maximum 60 milligrams of PAA is injected (assuming it constitutes 100% of the injected dose, when it is actually <50%).

$$0.06g * \frac{1}{1800} \frac{mol - PAA}{g} * 25 \frac{mol - A}{mol - PAA} * \frac{mol - A - Ca}{2 mol - A} = 416 \mu mol A - Ca$$

$$1 mM Ca * 2.5 L = 2.5 mmol Ca$$

This would predict that optimally 16.6% of the ionized calcium could be chelated in an injection to a pig (2.5L blood volume). This could make a large difference, except that ionized calcium only comprises ~50% of the total calcium in the blood, the other 50% is bound to serum proteins (40%) or anions such as citrate (10%), acting as a buffering mechanism. Additionally, the polyanion PAA polymer is rapidly coated by proteins in serum plasma (albumin, fibrinogen) and only a fraction of the acrylic acid residues would be available for binding calcium.³⁸ The dose would also (at most) be half that suggested above, since the particle injection contains less than 50% poly(acrylic acid). Therefore, it is unlikely that calcium chelation alone can explain the anticoagulation observed experimentally.

Monien et al.^{37,39} performing both in vitro complexation studies of PAA with antithrombin as well as computational modeling of their interaction, suggests that PAA has a direct activation of antithrombin, acting as a bridge, similar to heparin, to form the ternary antithrombin-protease complex that inhibits thrombin.^{37,39} They show with competitive binding studies with low-affinity heparin and a heparin tetrasaccharide, that PAA binds to antithrombin in both the pentasaccharide and extended heparin-binding sites through the formation of 5 ionic interactions. Depending on the MW of the pAA used, the acceleration of the antithrombin enzyme is between 118-1,109 fold higher (k_{act}/k_{uncat}) in its thrombin-inhibiting activity. This is comparable to heparin which has a (k_{act}/k_{uncat}) of roughly 2,500 fold. However, the authors note that compared to the sulfated heparin which has both ionic and nonionic bond formations with antithrombin, PAA only has the salt-dependent linkages, leading to a relatively low

affinity at physiological osmolarity and pH. This leads to a dissociation constant $k_d = 34\text{-}180 \text{ uM}$ for PAA (MW 6200-1500 respectively) compared to a $k_d = 1.4 \cdot 10^{-3} \text{ uM}$ for the heparin DEFGH binding site. However, when considering how much we inject, $\sim 13.3 \text{ uM}$ (estimated from a 60 mg dose of PAA and 2.5 L pig), one can calculate the estimated AT-bound pAA from the k_d .

$$k_d = 150 \text{ uM} = \frac{[pAA] * [AT]}{[pAA - AT]}$$

$$\frac{[pAA - AT]}{[AT]} = \frac{13.3}{150} = 0.088$$

This yields $\sim 8\%$ of AT being bound to PAA. Depending on the activity of the activated enzyme, this may be a substantial enough amount of activation to cause anticoagulation, although unlikely.

The final theory comes from Deng et al.³⁰ who observed that PAA coated gold nanoparticles induced an inflammatory response via Mac-1 receptor activation.³⁰ They show that their GNP-PAA particles tightly bind serum fibrinogen and cause the protein to unfold, exposing its C/D domain, which signals activation of the MAC-1 pathway. In vitro, particle binding reaches equilibrium within 5 minutes and remains stable over 4 hours. They go on to show that particle size and fibrinogen binding density greatly impacts the degree of inflammatory pathways activated. They show that TNF-alpha as well as IL-8 are greatly upregulated in the presence of both GNP-PAA and fibrinogen, but that neither is observed when one of those is missing, strongly implying the

interaction between GNP-PAA and fibrinogen. Fibrinogen sequestration and presentation to macrophages may induce a coagulopathy.

While high doses of PAA may induce coagulopathy, the amount proposed here, does not appear as though it would cause an issue. If there were a direct coagulopathic effect on ionized calcium, fibrinogen denaturation or its sequestration, one would expect to see these coagulopathies reflected in prolonged ROTEM (NATEM CT) or Hemochron (APTT) assays. However, these values are normal, even during these transient CARPA episodes (Figure 36).

Mitigation of response

Prophylaxis

Szebeni et al.^{26,27} describes the nonspecific complement activation (CARPA) to infusions of nanoparticle drug carrier systems similar to ours and its prevention. They discuss that the reaction can be prevented with preconditioning with low doses of the nanoparticle carrier or pharmacologically with indomethacin (a potent complement inhibitor).

Diphenhydramine, phenylephrine, epinephrine and steroids may also be used in conjunction to reverse the anaphylaxis induced by CARPA.²⁸ Unfortunately for the application of intravenous hemostatic agents to be administered during trauma, co-administration with additional pharmaceuticals should be avoided if possible.

One potential method for reducing the onset of CARPA is to infuse the nanoparticles slowly (or with multiple small doses) (tachyphylaxis)²⁶ This appeared to

prevent the onset of CARPA and reduce the severity of any symptoms. It relies on a desensitization mechanism. However, since the present therapy will rely on rapid administration after hemorrhagic injury, tachyphylaxis does not appear to be a viable option.

Tuning particle charge

Currently, the most viable option for prevention of CARPA appears to be tuning the zeta potential of the targeted nanoparticles to be close to neutral. The GRGDS targeting ligand is inherently negatively charged due to the presence of Arg (+), Asp (-) and the carboxylic acid terminus (-). One potential mitigation for this study would be to substitute the GRGDS targeting peptide for one with a neutral charge, such as a cyclic RGD, which has both a higher specificity for activated platelet GPIIb/IIIa and a net neutral charge.⁴⁰

While the symptoms appear to be exaggerated in pigs, there does appear to be a large population of individuals that experience CARPA symptoms, when administered the novel liposomal chemotherapeutic Doxil.⁴¹ In one particular study, a post-hoc analysis demonstrated that 45% of patients receiving Doxil showed symptoms of CARPA (grade 2 and 3), where grade 2 is symptomatic but does not require intervention, and grade 3 is a severe reaction requiring anti-allergic medication and cessation of the infusion. The responding population received infusions at a mean rate of 0.51 mg/min, with a mean total 151.8 mg, compared to those that showed no symptoms, receiving a mean infusion rate of 0.23 mg/min, total 70.1 mg.⁴¹ However, it's important to note that even in patients not showing symptoms, complement activation

(SC5b-9 elevation) is present, which may aggravate other pathways during trauma.⁴¹ While the infusion rate of 0.2 mg/min (or tachyphylaxis) may be an acceptable method to mitigate the induction of CARPA for chemotherapy, this is not an acceptable practice for intravenous hemostat applications, where a large bolus (e.g. 60 mg), must be infused as quickly as possible to prevent blood loss. At a rate of 0.2 mg/min, this would take 300 minutes, rendering the treatment ineffective for treating acute trauma.

CONCLUSION

This study has shown that CARPA induced by nanoparticle administration produces massive hemorrhage when administered during a large hemorrhagic injury. We have further shown that coagulopathy may still be present, even after an episode of CARPA (characterized by cardiopulmonary dysfunction) has passed. However, we have also shown that this response is transient and can be modulated by tuning the parameters of intravenous hemostatic nanoparticles, specifically by neutralizing their charge (zeta potential).

The mechanisms of CARPA are currently poorly understood, and are exaggerated in the pig model compared to humans, as evidenced by the clinical administration of Doxil (a liposome-based chemotherapeutic nanoparticle, zeta potential = -13.3 mV³³), with relatively few severe adverse reactions. However, consequences of CARPA during administration of this intravenous hemostat could be catastrophic, and the mitigation by pharmaceutical prophylaxis is likely contraindicated. Therefore, the use of a porcine model to ensure a minimized risk for

CARPA, and elucidating its mechanisms so that patient-exclusion criteria, based on heightened risk factors, will be paramount to the clinical translation of this technology.

WORKS CITED IN THIS CHAPTER

1. Fitzpatrick, G.M., Cliff, R. & Tandon, N. Thrombosomes: a platelet-derived hemostatic agent for control of noncompressible hemorrhage. *Transfusion* **53 Suppl 1**, 100S-106S (2013).
2. Okamura, Y., *et al.* Hemostatic effects of phospholipid vesicles carrying fibrinogen gamma chain dodecapeptide in vitro and in vivo. *Bioconjug Chem* **16**, 1589-1596 (2005).
3. Levi, M., *et al.* Fibrinogen-coated albumin microcapsules reduce bleeding in severely thrombocytopenic rabbits. *Nat Med* **5**, 107-111 (1999).
4. Collier, B.S., *et al.* Thromboerythrocytes. In vitro studies of a potential autologous, semi-artificial alternative to platelet transfusions. *J Clin Invest* **89**, 546-555 (1992).
5. Modery-Pawłowski, C.L., *et al.* Approaches to synthetic platelet analogs. *Biomaterials* **34**, 526-541 (2013).
6. Blajchman, M.A. Substitutes and alternatives to platelet transfusions in thrombocytopenic patients. *Journal of thrombosis and haemostasis : JTH* **1**, 1637-1641 (2003).
7. Siller-Matula, J.M., Plasenzotti, R., Spiel, A., Quehenberger, P. & Jilma, B. Interspecies differences in coagulation profile. *Thrombosis and haemostasis* **100**, 397-404 (2008).
8. Frink, M., Andruszkow, H., Zeckey, C., Krettek, C. & Hildebrand, F. Experimental trauma models: an update. *Journal of biomedicine & biotechnology* **2011**, 797383 (2011).
9. Langleben, D. & Moroz, L.A. Interspecies variation in the cellular phase of blood fibrinolytic activity. *Proc Soc Exp Biol Med* **196**, 270-272 (1991).
10. Fairbairn, L., Kapetanovic, R., Sester, D.P. & Hume, D.A. The mononuclear phagocyte system of the pig as a model for understanding human innate immunity and disease. *Journal of leukocyte biology* **89**, 855-871 (2011).
11. Johnson, D., *et al.* The effects of QuikClot Combat Gauze on hemorrhage control in the presence of hemodilution. *U.S. Army Medical Department journal*, 36-39 (2012).
12. Gegel, B., Burgert, J., Loughren, M. & Johnson, D. The effects of BleedArrest on hemorrhage control in a porcine model. *U.S. Army Medical Department journal*, 31-35 (2012).
13. Velmahos, G.C., *et al.* Abdominal insufflation decreases blood loss without worsening the inflammatory response: implications for prehospital control of internal bleeding. *Am Surg* **74**, 297-301 (2008).
14. Velmahos, G.C., *et al.* Abdominal insufflation for control of bleeding after severe splenic injury. *J Trauma* **63**, 285-288; discussion 288-290 (2007).

15. Jaskille, A., *et al.* Abdominal insufflation decreases blood loss and mortality after porcine liver injury. *J Trauma* **59**, 1305-1308; discussion 1308 (2005).
16. Gurney, J., *et al.* A hemoglobin based oxygen carrier, bovine polymerized hemoglobin (HBOC-201) versus Hetastarch (HEX) in an uncontrolled liver injury hemorrhagic shock swine model with delayed evacuation. *J Trauma* **57**, 726-738 (2004).
17. Baker, T.A., *et al.* Effects of exogenous ubiquitin in a polytrauma model with blunt chest trauma. *Critical care medicine* **40**, 2376-2384 (2012).
18. Alam, H.B., *et al.* Hemostatic and pharmacologic resuscitation: results of a long-term survival study in a swine polytrauma model. *J Trauma* **70**, 636-645 (2011).
19. Alam, H.B., *et al.* Testing of blood products in a polytrauma model: results of a multi-institutional randomized preclinical trial. *J Trauma* **67**, 856-864 (2009).
20. Baker, T.A., *et al.* Systemic release of cytokines and heat shock proteins in porcine models of polytrauma and hemorrhage*. *Critical care medicine* **40**, 876-885 (2012).
21. Dong, F., *et al.* Immune effects of resuscitation with HBOC-201, a hemoglobin-based oxygen carrier, in swine with moderately severe hemorrhagic shock from controlled hemorrhage. *Shock* **25**, 50-55 (2006).
22. Philbin, N., *et al.* A hemoglobin-based oxygen carrier, bovine polymerized hemoglobin (HBOC-201) versus hetastarch (HEX) in a moderate severity hemorrhagic shock swine model with delayed evacuation. *Resuscitation* **66**, 367-378 (2005).
23. Sava, J., *et al.* Abdominal insufflation for prevention of exsanguination. *J Trauma* **54**, 590-594 (2003).
24. Bertram, J.P., *et al.* Intravenous hemostat: nanotechnology to halt bleeding. *Science translational medicine* **1**, 11ra22 (2009).
25. Shoffstall, A.J., *et al.* Intravenous hemostatic nanoparticles increase survival following blunt trauma injury. *Biomacromolecules* **13**, 3850-3857 (2012).
26. Szebeni, J., *et al.* Prevention of infusion reactions to PEGylated liposomal doxorubicin via tachyphylaxis induction by placebo vesicles: a porcine model. *Journal of controlled release : official journal of the Controlled Release Society* **160**, 382-387 (2012).
27. Szebeni, J., *et al.* A porcine model of complement-mediated infusion reactions to drug carrier nanosystems and other medicines. *Advanced drug delivery reviews* **64**, 1706-1716 (2012).
28. Johnson, R.A., *et al.* Histamine release associated with intravenous delivery of a fluorocarbon-based sevoflurane emulsion in canines. *Journal of pharmaceutical sciences* **100**, 2685-2692 (2011).
29. Dennis, M.S., *et al.* Platelet glycoprotein IIb-IIIa protein antagonists from snake venoms: evidence for a family of platelet-aggregation inhibitors. *Proceedings of the National Academy of Sciences of the United States of America* **87**, 2471-2475 (1990).
30. Deng, Z.J., Liang, M., Monteiro, M., Toth, I. & Minchin, R.F. Nanoparticle-induced unfolding of fibrinogen promotes Mac-1 receptor activation and inflammation. *Nature nanotechnology* **6**, 39-44 (2011).

31. Gorbet, M.B. & Sefton, M.V. Biomaterial-associated thrombosis: roles of coagulation factors, complement, platelets and leukocytes. *Biomaterials* **25**, 5681-5703 (2004).
32. Castegren, M., Skorup, P., Lipcsey, M., Larsson, A. & Sjolín, J. Endotoxin Tolerance Variation over 24 h during Porcine Endotoxemia: Association with Changes in Circulation and Organ Dysfunction. *PloS one* **8**, e53221 (2013).
33. Szebeni, J., *et al.* Liposome-induced complement activation and related cardiopulmonary distress in pigs: factors promoting reactogenicity of Doxil and AmBisome. *Nanomedicine* **8**, 176-184 (2012).
34. Ziats, N.P., Pankowsky, D.A., Tierney, B.P., Ratnoff, O.D. & Anderson, J.M. Adsorption of Hageman factor (factor XII) and other human plasma proteins to biomedical polymers. *The Journal of laboratory and clinical medicine* **116**, 687-696 (1990).
35. van der Kamp, K.W. & van Oeveren, W. Factor XII fragment and kallikrein generation in plasma during incubation with biomaterials. *J Biomed Mater Res* **28**, 349-352 (1994).
36. Kaplan, A.P. & Ghebrehiwet, B. The plasma bradykinin-forming pathways and its interrelationships with complement. *Molecular immunology* **47**, 2161-2169 (2010).
37. Monien, B.H. & Desai, U.R. Antithrombin activation by nonsulfated, non-polysaccharide organic polymer. *Journal of medicinal chemistry* **48**, 1269-1273 (2005).
38. Karahan, M., Mustafaeva, Z. & Ozeroglu, C. Investigation of ternary complex formations of polyacrylic acid with bovine serum albumin in the presence of metal ions by fluorescence and dynamic light scattering measurements. *The protein journal* **29**, 336-342 (2010).
39. Monien, B.H., Cheang, K.I. & Desai, U.R. Mechanism of poly(acrylic acid) acceleration of antithrombin inhibition of thrombin: implications for the design of novel heparin mimics. *Journal of medicinal chemistry* **48**, 5360-5368 (2005).
40. Thibault, G., Tardif, P. & Lapalme, G. Comparative specificity of platelet alpha(IIb)beta(3) integrin antagonists. *The Journal of pharmacology and experimental therapeutics* **296**, 690-696 (2001).
41. Chanan-Khan, A., *et al.* Complement activation following first exposure to pegylated liposomal doxorubicin (Doxil): possible role in hypersensitivity reactions. *Annals of oncology : official journal of the European Society for Medical Oncology / ESMO* **14**, 1430-1437 (2003).

Chapter 6: Conclusions

Trauma is the leading cause of death for people ages 1-44, with blood loss comprising 60-70% of mortality in the absence of lethal CNS or cardiac injury. Immediate intervention is critical to improving chances of survival. While there are several products to control bleeding for external and compressible wounds including pressure dressings, tourniquets or topical materials (e.g. QuikClot, HemCon), there are no products that can be administered in the field for internal bleeding.

We have developed hemostatic nanoparticles (GRGDS-NPs) that reduce bleeding times by ~50% in a rat femoral artery injury model. Here, we investigated their impact on survival following administration in a lethal liver resection injury in rats. Administration of these hemostatic nanoparticles reduced blood loss following the liver injury and dramatically and significantly increased 1-hour survival from 40-47% in controls to 80%. Furthermore, we saw no complications following administration of these nanoparticles in rats. We further characterized the nanoparticles' effect on clotting time (CT) and maximum clot firmness (MCF) using rotational thromboelastometry (ROTEM), a clinical measurement of whole-blood coagulation. Clotting time is significantly reduced, with no change in MCF. Administration of these hemostatic nanoparticles after massive trauma may help staunch bleeding and improve survival in the critical window following injury, and this could fundamentally change trauma care.

We showed that intravenously administered hemostatic nanoparticles (GRGDS-NP1) reduce bleeding and increase survival after lethal liver trauma in the rat. We further investigated the effect of peptide density on hemostasis and biodistribution. We increased the peptide concentration 100-fold (GRGDS-NP100) and undertook a dose-response study in the rat lethal liver trauma model. We found that the GRGDS-NP100 hemostatic nanoparticles were efficacious at doses 8 times lower than the GRGDS-NP1, increasing 1-hour survival to 92%, compared to a scrambled peptide control, 45% (OR=14.4, 95% CI=[1.36, 143]), a saline control, 47% (OR=13.5, 95% CI=[1.42, 125]), and GRGDS-NP1, 80% (OR=1.30, n.s.). *In vitro* analysis using rotational thromboelastometry (ROTEM) recapitulated the increased dose-sensitivity of GRGDS-NP100 and was then used to titrate an optimal peptide density. This work demonstrates the impact of changing synthetic platelet ligand density on hemostasis, and lays the foundation for methods to determine optimal ligand concentration parameters, providing a critical step toward translation of this technology.

We then investigated the particles in a porcine liver injury model. We found that the administration of our nanoparticles after injury induced a massive hemorrhagic response, leading to the full exsanguination of the pig in several minutes. We found that this response occurred at nanoparticle doses down to >2 mg/kg, and that 0.2 mg/kg caused prolonged bleeding.

The administration of particles in a naïve pig (uninjured) then revealed that the response is likely related to complement activation related pseudoallergy (CARPA), and that the response was independent of peptide choice (GRGDS, GRADSP, or no peptide).

However, we discovered that the induction of CARPA may be mediated by tuning the nanoparticle charge, as measured by electrophoretic mobility (zeta potential). Neutral particles appear to not activate the CARPA response.

The mechanisms of CARPA are currently poorly understood, and are exaggerated in the pig model compared to humans, as evidenced by the clinical administration of Doxil (a liposome-based chemotherapeutic nanoparticle, zeta potential = -13.3 mV^1), with relatively few severe adverse reactions, but commonly observed mild-moderate hypersensitivity reactions. However, consequences of CARPA during administration of this intravenous hemostat could be catastrophic, and the mitigation by tachyphylaxis or pharmaceutical prophylaxis is likely contraindicated with concomitant trauma. Therefore, the use of a porcine model to ensure a minimized risk for CARPA, and elucidating its mechanisms so that patient-exclusion criteria, based on heightened risk factors, will be paramount to the clinical translation of this technology.

In summation, this work has advanced the understanding of intravenous hemostatic agent administration during acute hemorrhagic trauma, and elucidated several key factors that may be tuned to improve their hemostatic efficacy and reduce the risk for complications, namely targeting ligand density and zeta potential. This work has laid the foundation for the optimization of these parameters in both *in vitro* and *in vivo* models, and demonstrated methods for their tuning. Hemostatic nanoparticles for the treatment of hemorrhage have the potential to improve survival after lethal internal trauma, for which there are few, if any, alternative treatments available for medics to apply in the field.

WORKS CITED IN THIS CHAPTER

1. Szebeni, J., *et al.* Liposome-induced complement activation and related cardiopulmonary distress in pigs: factors promoting reactogenicity of Doxil and AmBisome. *Nanomedicine* **8**, 176-184 (2012).

Chapter 7: Recommendations for Future Work

RESUSPENSION WITHOUT SONICATION

Currently, sonication is required to fully resuspend these nanoparticles to their pre-lyophilization size distribution. However, for this technology to be useful, it must be able to be stored long-term and be able to be injected (resuspended) readily, when needed. This may be able to be mitigated by adding lyoprotectants such as trehalose and surfactants, such as Tween 80 (polysorbate 80). The use of trehalose appears to be relatively safe and is being pursued in preclinical studies to aid in resuspension of freeze-dried platelet product.¹ Tween 80 is a commonly used surfactant in the pharmaceutical industry, despite some concern about toxicity.²

PULMONARY SAFETY

The evidence presented in this thesis has suggested that the injected nanoparticles have the tendency to accumulate in the lungs, despite their small, sub-capillary size. It has also been shown that the particles do not negatively impact breathing in the rat trauma model, and are not found histologically in great quantities in the deep lung. However, this will need to be further characterized as the studies continue. This should specifically be addressed by analyzing the pulmonary artery pressures and the blood gas levels after particle administration, with and without the presence of injury.

One potential hypothesis to explain the large presence of particle entrapment in the lungs could involve pulmonary intravascular macrophages (PIM).³⁻⁵ Pulmonary intravascular macrophages are constitutively expressed in cattle, horse, pig, sheep, goat, cats, and can be induced in rats during endotoxemia and bacterial infection.^{6,7}

PEPTIDE CONJUGATION DENSITY

We have shown that peptide conjugation density plays a role in the hemostatic efficacy of the nanoparticles. While a rough assay was performed with blends of 1%, 10%, and 100% of quadblock polymer with pegylated PLGA, additional research is required to titrate, and quantify the optimal ligand concentration. The blend-approach appears to be the most efficient synthesis paradigm where a PLGA-PLL-PEG-GRGDS quadblock is formed, characterized for peptide content, and blended with PLGA-PLL-PEG to quantitatively control peptide conjugation. A confounding factor that future studies must take into account is the impact of peptide conjugation density on zeta potential, and therefore the impact on the risk for complement activation.

ELUCIDATING CARPA MECHANISMS AND ITS MITIGATION

The mechanism of CARPA and its relation to the coagulation cascade have not yet been fully elucidated. However, there are prior indications that biomaterials in contact with blood have the potential to elicit complement activation, which are mediated by FXII activation, and its fragments (factor XII_f).^{8,9} These papers have shown that charged, or hydrophilic materials, tend to adsorb proteins and produce FXII fragments as well as kallikrein (which in turn cause bradykinin formation – a strong vasodilator). While these previous studies have looked at macroscopic devices which

contact blood for long periods of time, there have been no similar studies of biomaterial interactions with nanoparticles in vivo, which may produce more transient responses as they are cleared or endocytosed. To that end, most blood-contacting materials used in devices, have relatively small surface areas exposed to the blood (<1.5 cm², for a standard 22G intravenous catheter). In contrast, our nanoparticle surface area is approximately 104 cm²/mg (based on an assumed PLGA density 1.34 g/cm³, and a nanoparticle diameter of 430 nm). This equates to a surprisingly large blood contact area of 6,248 cm² for a 60 mg dose of nanoparticles.

If CARPA is indeed mediated by factor XII activation by adsorption to the charged nanoparticle surface, then its fragments may well induce coagulopathy by activating plasminogen, and further cause additional hemorrhage due to bradykinin (or histamine) vasodilation.¹⁰ While long-term coagulopathy was not observed clotting time and APTT assays, it is possible that this coagulopathy is transient, and only catastrophic when occurring simultaneously with an injury.

The link from coagulation cascade activation to complement activation (FXII^f → complement C1 activation) is well documented.¹⁰ However, the link between nanoparticle-induced CARPA and factor XII does not appear to have been studied. However, the charge dependence of both biomaterial interactions (which produce XII^f) and CARPA may suggest that the mechanisms are linked. Future studies may be aimed at testing this hypothesis.

This study has shown that CARPA induced by nanoparticle administration produces massive hemorrhage when administered during a large hemorrhagic injury. However, we have also shown that this response is transient and can be modulated by tuning the parameters of intravenous hemostatic nanoparticles, specifically by neutralizing their charge (zeta potential). The GRGDS targeting ligand is inherently negatively charged due to the presence of Arg (+), Asp (-) and the carboxylic acid terminus (-). One potential mitigation for this study would be to substitute the GRGDS targeting peptide for one with a neutral charge, such as a cyclic RGD (cRGD), which has both a higher specificity for activated platelet GPIIb/IIIa and a net neutral charge.¹¹ A reaction scheme where a cRGD moiety is conjugated to a reactive PEG would be ideal, such that it could be incorporated directly into the current nanoparticle synthesis paradigm.

OTHER POTENTIAL APPLICATIONS OF THIS TECHNOLOGY

While this thesis has focused on general trauma, associated with blunt solid organ injury, there are many other potential medicinal uses for this technology.

Gastrointestinal bleeding

Hemorrhage in the gastrointestinal system, for example from a peptic ulcer or varix, can be a life-threatening complication, and is currently addressed endoscopically through submucosal injection, thermal coagulation or mechanical hemostasis.^{12,13} However these techniques all require endoscopic intervention and visualization of the bleeding in order to apply therapy. Intravenous hemostatic nanoparticles could be administered if bleeding were suspected, used to induce hemostasis at the bleeding site,

and if loaded with a contrast agent, could potentially be combined with an MRI/CT imaging modality to locate the site of hemorrhage direct additional intervention (endoscopy), if required, to staunch bleeding.

Spinal cord injury

One of the first events to occur after spinal cord injury (SCI) is pronounced hemorrhage.¹⁴⁻¹⁶ This is immediately followed by a complex secondary injury cascade, comprised of ischemia, anoxia, free-radical formation, and excitotoxicity that occur over hours and days following injury.^{14,17,18} The extent of hemorrhage as viewed using clinical MRI strongly correlates with functional outcomes, suggesting a potential approach for intervention: faster induction of hemostasis to preserve more tissue.¹⁹ Additionally, Tator et al has shown that the initial extent of hemorrhage correlates well with formation of the cystic cavity several weeks later — the size and morphology of the fusiform cavity being approximately equal to that of the initial extent of hemorrhage.^{15,20-22} For example, immediately after injury, at the epicenter of the injury, there is extensive hemorrhage in the gray matter, dorsal column, and some that radiates into the white matter. This protrudes longitudinally both rostral and caudal to the injury, affecting mainly the dorsal column at either end at its furthest extents. These dimensions correlate well with those of the cystic cavity.¹⁵ This correlative evidence is further supported by a rodent study that directly observed neural cytotoxicity when blood was injected into the subdural space.^{23,24} Furthermore, several groups have directly studied the impact of reducing hemorrhage after CNS trauma, by either using

novel hemostatic agents, or by pharmaceutically stabilizing the endothelium of the blood spinal cord barrier to reduce the effects of progressive hemorrhagic necrosis.²⁵⁻²⁸

In each case, in rodent injury models, significant functional and histological improvements were seen. From this body of evidence linking hemorrhage to the extent of injury, we hypothesize that the administration of hemostatic nanoparticles immediately after contusion spinal cord injury will decrease bleeding and subsequently lead to improved histological and functional outcomes.

While we are unable to prevent the primary injury, it may be possible to intervene in the secondary injury cascade, which comprises approximately one-third of the observed functional deficit.^{23,29} Preservation of tissue by reduction of extravascular blood could have tremendous implications for the patient's outcome, reducing paralysis, increasing sensation and overall leading to a better quality of life.

Other traumas

Other traumas that are currently under investigation, and could potentially be ameliorated by treatment with hemostatic nanoparticles include blast trauma and traumatic brain injury, both of which include noncompressible hemorrhage. Other potential applications include the management of intraoperative bleeding in surgery, and a multitude of other applications that arise when considering the drug-delivery capability of these nanoparticles. Since these nanoparticles are injury targeted (assuming activated platelets are at the site), they could be loaded with steroids, growth

factors, or analgesics for wound-healing, or with imaging contrast agents for detection, and used for informing interventional procedures.

WORKS CITED IN THIS CHAPTER

1. Fitzpatrick, G.M., Cliff, R. & Tandon, N. Thrombosomes: a platelet-derived hemostatic agent for control of noncompressible hemorrhage. *Transfusion* 53 Suppl 1, 100S-106S (2013).
2. Varma, R.K., et al. Polysorbate 80: a pharmacological study. *Arzneimittel-Forschung* 35, 804-808 (1985).
3. Winkler, G.C. Review of the significance of pulmonary intravascular macrophages with respect to animal species and age. *Experimental cell biology* 57, 281-286 (1989).
4. Winkler, G.C. Pulmonary intravascular macrophages in domestic animal species: review of structural and functional properties. *The American journal of anatomy* 181, 217-234 (1988).
5. Szebeni, J., et al. A porcine model of complement-mediated infusion reactions to drug carrier nanosystems and other medicines. *Advanced drug delivery reviews* 64, 1706-1716 (2012).
6. Schneberger, D., Aharonson-Raz, K. & Singh, B. Pulmonary intravascular macrophages and lung health: what are we missing? *American journal of physiology. Lung cellular and molecular physiology* 302, L498-503 (2012).
7. Klingensmith, W.C., 3rd, Tsan, M.F. & Wagner, H.N., Jr. Factors affecting the uptake of ^{99m}Tc-sulfur colloid by the lung and kidney. *Journal of nuclear medicine : official publication, Society of Nuclear Medicine* 17, 681-684 (1976).
8. Ziats, N.P., Pankowsky, D.A., Tierney, B.P., Ratnoff, O.D. & Anderson, J.M. Adsorption of Hageman factor (factor XII) and other human plasma proteins to biomedical polymers. *The Journal of laboratory and clinical medicine* 116, 687-696 (1990).
9. van der Kamp, K.W. & van Oeveren, W. Factor XII fragment and kallikrein generation in plasma during incubation with biomaterials. *J Biomed Mater Res* 28, 349-352 (1994).
10. Kaplan, A.P. & Ghebrehiwet, B. The plasma bradykinin-forming pathways and its interrelationships with complement. *Molecular immunology* 47, 2161-2169 (2010).
11. Thibault, G., Tardif, P. & Lapalme, G. Comparative specificity of platelet alpha(IIb)beta(3) integrin antagonists. *The Journal of pharmacology and experimental therapeutics* 296, 690-696 (2001).
12. Enestvedt, B.K., Gralnek, I.M., Mattek, N., Lieberman, D.A. & Eisen, G.M. Endoscopic therapy for peptic ulcer hemorrhage: practice variations in a multi-center U.S. consortium. *Digestive diseases and sciences* 55, 2568-2576 (2010).
13. Gralnek, I.M., Barkun, A.N. & Bardou, M. Management of acute bleeding from a peptic ulcer. *The New England journal of medicine* 359, 928-937 (2008).

14. Beattie, M.S., Farooqui, A.A. & Bresnahan, J.C. Review of current evidence for apoptosis after spinal cord injury. *J Neurotrauma* 17, 915-925 (2000).
15. Mautes, A.E., Weinzierl, M.R., Donovan, F. & Noble, L.J. Vascular events after spinal cord injury: contribution to secondary pathogenesis. *Phys Ther* 80, 673-687 (2000).
16. Osterholm, J.L. The pathophysiological response to spinal cord injury. The current status of related research. *J Neurosurg* 40, 5-33 (1974).
17. Sekhon, L.H. & Fehlings, M.G. Epidemiology, demographics, and pathophysiology of acute spinal cord injury. *Spine (Phila Pa 1976)* 26, S2-12 (2001).
18. Park, E., Velumian, A.A. & Fehlings, M.G. The role of excitotoxicity in secondary mechanisms of spinal cord injury: a review with an emphasis on the implications for white matter degeneration. *J Neurotrauma* 21, 754-774 (2004).
19. Ramon, S., et al. Clinical and magnetic resonance imaging correlation in acute spinal cord injury. *Spinal Cord* 35, 664-673 (1997).
20. Popa, C., et al. Vascular dysfunctions following spinal cord injury. *J Med Life* 3, 275-285.
21. Sinescu, C., et al. Molecular basis of vascular events following spinal cord injury. *J Med Life* 3, 254-261.
22. Tator, C.H. & Koyanagi, I. Vascular mechanisms in the pathophysiology of human spinal cord injury. *J Neurosurg* 86, 483-492 (1997).
23. Bullock, R. & Fujisawa, H. The role of glutamate antagonists for the treatment of CNS injury. *J Neurotrauma* 9 Suppl 2, S443-462 (1992).
24. Duhaime, A.C., Gennarelli, L.M. & Yachnis, A. Acute subdural hematoma: is the blood itself toxic? *J Neurotrauma* 11, 669-678 (1994).
25. Ellis-Behnke, R. At the nanoscale: nanohemostat, a new class of hemostatic agent. *Wiley Interdiscip Rev Nanomed Nanobiotechnol* 3, 70-78.
26. Simard, J.M., et al. Key role of sulfonylurea receptor 1 in progressive secondary hemorrhage after brain contusion. *J Neurotrauma* 26, 2257-2267 (2009).
27. Simard, J.M., et al. Endothelial sulfonylurea receptor 1-regulated NC Ca-ATP channels mediate progressive hemorrhagic necrosis following spinal cord injury. *J Clin Invest* 117, 2105-2113 (2007).
28. Simard, J.M., et al. Brief suppression of Abcc8 prevents autodestruction of spinal cord after trauma. *Sci Transl Med* 2, 28ra29.
29. Fehlings, M.G. & Sekhon, L.H. Acute interventions in spinal cord injury: what do we know, what should we do? *Clin Neurosurg* 48, 226-242 (2001).

NRESLIV

tri-grgds-paa Blood = 5.82814 + 1.0886 Died + 0.124725 NBMI + 0.82433 NRESLIV

Coefficients

Term	Coef	SE Coef	T	P
Constant	5.92785	0.255586	23.1931	0.000
TX				
saline	-0.09871	0.243299	-0.4057	0.687
tri-blank-paa	0.19842	0.237157	0.8367	0.408
Died	1.08860	0.344844	3.1568	0.003
NBMI	0.12473	0.344656	0.3619	0.720
NRESLIV	0.82433	0.337375	2.4434	0.020

Summary of Model

S = 1.05475 R-Sq = 35.09% R-Sq(adj) = 25.81%
 PRESS = 53.7141 R-Sq(pred) = 10.45%

Analysis of Variance

Source	DF	Seq SS	Adj SS	Adj MS	F	P
Regression	5	21.0467	21.0467	4.2093	3.78365	0.007631
TX	2	2.4851	0.7793	0.3896	0.35024	0.706959
Died	1	11.4133	11.0865	11.0865	9.96535	0.003275
NBMI	1	0.5066	0.1457	0.1457	0.13096	0.719615
NRESLIV	1	6.6417	6.6417	6.6417	5.97004	0.019736
Error	35	38.9378	38.9378	1.1125		
Total	40	59.9844				

Fits and Diagnostics for Unusual Observations

Obs	Blood	Fit	SE Fit	Residual	St Resid
36	7.11	5.07285	0.443809	2.03715	2.12904 R

R denotes an observation with a large standardized residual.

General Regression Analysis: Blood versus Died, NRESLIV, TX

Regression Equation

TX
 saline Blood = 5.77269 + 1.06541 Died + 0.839697 NRESLIV
 tri-blank-paa Blood = 6.11211 + 1.06541 Died + 0.839697 NRESLIV
 tri-grgds-paa Blood = 5.79674 + 1.06541 Died + 0.839697 NRESLIV

Coefficients

Term	Coef	SE Coef	T	P
Constant	5.89384	0.234796	25.1019	0.000
TX				
saline	-0.12115	0.232401	-0.5213	0.605

tri-blank-paa	0.21826	0.227928	0.9576	0.345
Died	1.06541	0.334720	3.1830	0.003
NRESLIV	0.83970	0.330627	2.5397	0.016

Summary of Model

S = 1.04195 R-Sq = 34.84% R-Sq(adj) = 27.60%
 PRESS = 51.1743 R-Sq(pred) = 14.69%

Analysis of Variance

Source	DF	Seq SS	Adj SS	Adj MS	F	P
Regression	4	20.9010	20.9010	5.2252	4.8130	0.003257
TX	2	2.4851	1.0121	0.5060	0.4661	0.631165
Died	1	11.4133	10.9991	10.9991	10.1314	0.003002
NRESLIV	1	7.0026	7.0026	7.0026	6.4501	0.015555
Error	36	39.0835	39.0835	1.0857		
Total	40	59.9844				

Fits and Diagnostics for Unusual Observations

Obs	Blood	Fit	SE Fit	Residual	St Resid
36	7.11	5.11294	0.424547	1.99706	2.09879 R

R denotes an observation with a large standardized residual.

General Linear Model: Blood/L versus TX, Died

Factor	Type	Levels	Values
TX	fixed	3	saline, tri-blank-paa, tri-grgds-paa
Died	random	2	0, 1

Analysis of Variance for Blood/L, using Adjusted SS for Tests

Source	DF	Seq SS	Adj SS	Adj MS	F	P
TX	2	0.4580	0.1711	0.0856	0.43	0.657
Died	1	1.6823	1.6823	1.6823	8.37	0.006
Error	37	7.4375	7.4375	0.2010		
Total	40	9.5778				

S = 0.448346 R-Sq = 22.35% R-Sq(adj) = 16.05%

Unusual Observations for Blood/L

Obs	Blood/L	Fit	SE Fit	Residual	St Resid
1	3.25930	2.37981	0.14536	0.87949	2.07 R
36	3.53700	2.34837	0.13804	1.18863	2.79 R

R denotes an observation with a large standardized residual.

General Linear Model: Blood, Blood/B, Blood/L versus TX, Died

Factor	Type	Levels	Values
TX	fixed	3	saline, tri-blank-paa, tri-grgds-paa
Died	random	2	0, 1

Analysis of Variance for Blood, using Adjusted SS for Tests

Source	DF	Seq SS	Adj SS	Adj MS	F	P
TX	2	2.485	1.364	0.682	0.55	0.583
Died	1	11.413	11.413	11.413	9.16	0.004
Error	37	46.086	46.086	1.246		
Total	40	59.984				

S = 1.11605 R-Sq = 23.17% R-Sq(adj) = 16.94%

Unusual Observations for Blood

Obs	Blood	Fit	SE Fit	Residual	St Resid
2	7.89000	5.65643	0.36183	2.23357	2.12 R
37	3.48000	5.81917	0.34362	-2.33917	-2.20 R

R denotes an observation with a large standardized residual.

Analysis of Variance for Blood/B, using Adjusted SS for Tests

Source	DF	Seq SS	Adj SS	Adj MS	F	P
TX	2	25.76	4.57	2.29	0.10	0.903
Died	1	244.16	244.16	244.16	10.98	0.002
Error	37	822.71	822.71	22.24		
Total	40	1092.63				

S = 4.71545 R-Sq = 24.70% R-Sq(adj) = 18.60%

Unusual Observations for Blood/B

Obs	Blood/B	Fit	SE Fit	Residual	St Resid
2	33.5604	23.8709	1.5288	9.6895	2.17 R

R denotes an observation with a large standardized residual.

Analysis of Variance for Blood/L, using Adjusted SS for Tests

Source	DF	Seq SS	Adj SS	Adj MS	F	P
TX	2	0.4580	0.1711	0.0856	0.43	0.657
Died	1	1.6823	1.6823	1.6823	8.37	0.006
Error	37	7.4375	7.4375	0.2010		
Total	40	9.5778				

S = 0.448346 R-Sq = 22.35% R-Sq(adj) = 16.05%

Unusual Observations for Blood/L

Obs	Blood/L	Fit	SE Fit	Residual	St Resid
-----	---------	-----	--------	----------	----------

1	3.25930	2.37981	0.14536	0.87949	2.07 R
36	3.53700	2.34837	0.13804	1.18863	2.79 R

Power analysis of survival (SAS Code)

A power analysis of the liver injury model and preliminary injury model results yielded an initial sample size estimate of 20 animals (power=0.8, alpha=0.05). However, fewer animals than expected were needed for the quadblock nanoparticle study, where survival was above 92%. Below is the actual power calculation for that study, and shows that the actual power obtained was above 0.8, even though fewer animals were used.

```
proc power;
  logistic
    vardist("tx") = ordinal((1 2) : (0.458 0.542))
    testpredictor = "tx"
    responseprob = 0.545
    testoddsratio = 14.4
    alpha = 0.05
    ntotal = 24
    power = .;

    plot x=power min=.65 max=.95
run;
```

Binomial logistic regression analysis for lethality data (SAS Code)

This statistical method is one suggested by our biostatistician as the most appropriate to make multiple comparisons between treatment groups with lethality as the outcome. I wrote this code using SAS 9.2, and can be easily adjusted for inputting binomial data. Confidence of odds ratios (O.R.) between groups is used to determine significance between groups: i.e. O.R. that does not cross 1 is significant.

```
DATA TestSurvival (drop=i tx_n);
```

```

*****EDIT THIS PART OF THE SCRIPT TO INPUT
DATA*****;

*This is the number of tx groups;
tx_n = 7;

*This is the names of the tx groups (must match tx_n above);
array tx_name{7} $ _temporary_ ('LR' 'NOVO' 'G20' 'G40' 'S20'
'S40' 'NONE');

*This is the total n per group (must match tx_n above);
array tx_ntot{7} _temporary_ (10 14 21 10 19 10 10);

*This is the number of animals that died out of each group
(must match tx_n);
array tx_ndied{7} _temporary_ (3 3 1 3 5 1 4);

*****DO NOT CHANGE ANYTHING BELOW
HERE*****;
do i = 1 to tx_n;
  do j = 1 to tx_ntot{i};
    if j > tx_ndied{i} then do;
      TX = tx_name{i};
      DIED = 0;
      output;
    end;
  else do;
    TX = tx_name{i};
    DIED = 1;
    output;
  end;
end;
end;
run;

*This part "proc logistic" runs the logistic regression;

proc logistic data=TestSurvival descending;
title "Test case died = 1";
  *Change ref = 'your group here' to set the reference.
  (ref = ... Must be listed in tx_name);
class tx(ref='NONE' param=ref);
model died = tx;
  oddsratio tx;
output out=predictions1 predicted=pred lower=lcl upper=ucl;
run;

```

Analysis for nanoparticle biodistribution via histology (Matlab Code)

```

% Program loads set of 8-bit grayscale images and performs threshold
% according to below set value. Counts and sums area above thresh.
% Andrew Shoffstall 12-10-12.

% SET THRESHOLD VALUE
mythreshlevel = 100/255;

% GET FILES
[FileName,PathName,FilterIndex] = uigetfile(['*.jpg','*.tif'],
'MultiSelect', 'on');
filelen = size(FileName,2);

if(filelen > 0)
    %% Load Files
    m = cell(ceil(sqrt(size(filelen,1))^2,1);
    nrows = ceil(sqrt(filelen));
    for(ii=1:filelen)
        m{ii} = imread(strcat(PathName,FileName{ii}));
    end

    %% Perform Threshold Analy
    m_thresh = cell(ceil(sqrt(size(filelen,1))^2,1);
    pix_cnt = zeros(filelen,2);
    for(ii=1:filelen)
        m_thresh{ii} = im2bw(m{ii},mythreshlevel);
        cc = bwconncomp(m_thresh{ii}, 4);
        pix_cnt(ii,1) = sum(sum(m_thresh{ii}));
        pix_cnt(ii,2) = cc.NumObjects;
    end

    %% Display Images
    blk_m = zeros(size(m{1}));
    blk_mthresh = zeros(size(m_thresh{1}));
    nrows = ceil(sqrt(filelen));
    for(ii=1:(nrows^2-filelen))
        m{filelen+ii} = blk_m;
        m_thresh{filelen+ii} = blk_mthresh;
    end
    M = horzcat(m{1:nrows});
    M_thresh = horzcat(m_thresh{1:nrows});
    for(ii=1:nrows-1)
        M = vertcat(M,horzcat(m{(ii*nrows+1):((ii+1)*nrows)}));
        M_thresh =
vertcat(M_thresh,horzcat(m_thresh{(ii*nrows+1):((ii+1)*nrows)}));
    end

    figure();
    imshow(M);
    hold on;
    for(ii=1:nrows-1)
        % Draw Horizontal Lines
        line([1,nrows*size(m{1},2)], [ii*size(m{1},1),ii*size(m{1},1)]);
        % Draw Vertical Lines
        line([ii*size(m{1},2),ii*size(m{1},2)], [1,nrows*size(m{1},1)]);
    end
    hold off;

```

```

figure();
imshow(M_thresh);
hold on;
for(ii=1:nrows-1)
    % Draw Horizontal Lines
    line([1,nrows*size(m{1},2)],[ii*size(m{1},1),ii*size(m{1},1)]);
    % Draw Vertical Lines
    line([ii*size(m{1},2),ii*size(m{1},2)],[1,nrows*size(m{1},1)]);
end
hold off;

%% Print data
for(ii=1:filelen)
    disp(sprintf('%s\t%i\t%i',
FileName{ii},pix_cnt(ii,1),pix_cnt(ii,2)));
end
end

```

Bibliography

- Abdelwahed, W., et al. "Freeze-Drying of Nanoparticles: Formulation, Process and Storage Considerations." *Adv Drug Deliv Rev* 58.15 (2006): 1688-713. Print.
- Achneck, H. E., et al. "A Comprehensive Review of Topical Hemostatic Agents: Efficacy and Recommendations for Use." *Ann Surg* 251.2 (2010): 217-28. Print.
- Acosta, J. A., et al. "Lethal Injuries and Time to Death in a Level I Trauma Center." *J Am Coll Surg* 186.5 (1998): 528-33. Print.
- Agam, G., and A. A. Livne. "Erythrocytes with Covalently Bound Fibrinogen as a Cellular Replacement for the Treatment of Thrombocytopenia." *Eur J Clin Invest* 22.2 (1992): 105-12. Print.
- Agbanyo, F. R., et al. "Thrombospondin-Platelet Interactions. Role of Divalent Cations, Wall Shear Rate, and Platelet Membrane Glycoproteins." *J Clin Invest* 92.1 (1993): 288-96. Print.
- Akin, M. "Response to Low-Dose Desmopressin by a Subcutaneous Route in Children with Type 1 Von Willebrand Disease." *Hematology* (2013). Print.
- Alam, H. B., et al. "Testing of Blood Products in a Polytrauma Model: Results of a Multi-Institutional Randomized Preclinical Trial." *J Trauma* 67.4 (2009): 856-64. Print.
- Alam, H. B., et al. "Hemostatic and Pharmacologic Resuscitation: Results of a Long-Term Survival Study in a Swine Polytrauma Model." *J Trauma* 70.3 (2011): 636-45. Print.
- Alevriadou, B. R., et al. "Real-Time Analysis of Shear-Dependent Thrombus Formation and Its Blockade by Inhibitors of Von Willebrand Factor Binding to Platelets." *Blood* 81.5 (1993): 1263-76. Print.
- Ali, Mir Mukkaram., and Stephen E. Zale. Cancer Cell Targeting Using Nanoparticles. Bind Biosciences, Inc assignee. Mar 30, 2007.
- Alving, B. M., et al. "Frozen Platelets and Platelet Substitutes in Transfusion Medicine." *Transfusion* 37.8 (1997): 866-76. Print.
- Andrieux, A., et al. "Amino Acid Sequences in Fibrinogen Mediating Its Interaction with Its Platelet Receptor, Gpiibiiia." *J Biol Chem* 264.16 (1989): 9258-65. Print.
- Arnold, D. M. "Positioning New Treatments in the Management of Immune Thrombocytopenia." *Pediatr Blood Cancer* 60 Suppl 1 (2013): S19-22. Print.
- Bahl, Y., and H. Sah. "Dynamic Changes in Size Distribution of Emulsion Droplets During Ethyl Acetate-Based Microencapsulation Process." *AAPS PharmSciTech* 1.1 (2000): E5. Print.
- Baker, T. A., et al. "Effects of Exogenous Ubiquitin in a Polytrauma Model with Blunt Chest Trauma." *Crit Care Med* 40.8 (2012): 2376-84. Print.
- . "Systemic Release of Cytokines and Heat Shock Proteins in Porcine Models of Polytrauma and Hemorrhage*." *Crit Care Med* 40.3 (2012): 876-85. Print.
- Beattie, M. S., A. A. Farooqui, and J. C. Bresnahan. "Review of Current Evidence for Apoptosis after Spinal Cord Injury." *J Neurotrauma* 17.10 (2000): 915-25. Print.

- Beer, J. H., K. T. Springer, and B. S. Coller. "Immobilized Arg-Gly-Asp (Rgd) Peptides of Varying Lengths as Structural Probes of the Platelet Glycoprotein Iib/Iiia Receptor." *Blood* 79.1 (1992): 117-28. Print.
- Benharash, P., F. Bongard, and B. Putnam. "Use of Recombinant Factor Viia for Adjunctive Hemorrhage Control in Trauma and Surgical Patients." *Am Surg* 71.9 (2005): 776-80. Print.
- Bertram, J. P., et al. "Functionalized Poly(Lactic-Co-Glycolic Acid) Enhances Drug Delivery and Provides Chemical Moieties for Surface Engineering While Preserving Biocompatibility." *Acta Biomater* 5.8 (2009): 2860-71. Print.
- Bertram, J. P., et al. "Intravenous Hemostat: Nanotechnology to Halt Bleeding." *Sci Transl Med* 1.11 (2009): 11ra22. Print.
- Bhattacharyya, S., et al. "Inorganic Nanoparticles in Cancer Therapy." *Pharm Res* 28.2 (2011): 237-59. Print.
- Blajchman, M. A. "Novel Platelet Products, Substitutes and Alternatives." *Transfus Clin Biol* 8.3 (2001): 267-71. Print.
- . "Platelet Substitutes." *Vox Sang* 78 Suppl 2 (2000): 183-6. Print.
- . "Substitutes and Alternatives to Platelet Transfusions in Thrombocytopenic Patients." *J Thromb Haemost* 1.7 (2003): 1637-41. Print.
- Blajchman, M. A., et al. "The Contribution of the Haematocrit to Thrombocytopenic Bleeding in Experimental Animals." *Br J Haematol* 86.2 (1994): 347-50. Print.
- Blajchman, M. A., and D. H. Lee. "The Thrombocytopenic Rabbit Bleeding Time Model to Evaluate the in Vivo Hemostatic Efficacy of Platelets and Platelet Substitutes." *Transfus Med Rev* 11.2 (1997): 95-105. Print.
- Blajchman, M. A., et al. "Hemostatic Function, Survival, and Membrane Glycoprotein Changes in Young Versus Old Rabbit Platelets." *J Clin Invest* 68.5 (1981): 1289-94. Print.
- Blajchman, M. A., et al. "Shortening of the Bleeding Time in Rabbits by Hydrocortisone Caused by Inhibition of Prostacyclin Generation by the Vessel Wall." *J Clin Invest* 63.5 (1979): 1026-35. Print.
- Bodmeier, R., and J. W. McGinity. "The Preparation and Evaluation of Drug-Containing Poly(DL-Lactide) Microspheres Formed by the Solvent Evaporation Method." *Pharm Res* 4.6 (1987): 465-71. Print.
- Boffard, K. D., et al. "Recombinant Factor Viia as Adjunctive Therapy for Bleeding Control in Severely Injured Trauma Patients: Two Parallel Randomized, Placebo-Controlled, Double-Blind Clinical Trials." *J Trauma* 59.1 (2005): 8-15; discussion 15-8. Print.
- Boxenbaum, H. "Interspecies Variation in Liver Weight, Hepatic Blood Flow, and Antipyrine Intrinsic Clearance: Extrapolation of Data to Benzodiazepines and Phenytoin." *J Pharmacokinet Biopharm* 8.2 (1980): 165-76. Print.
- Broze, G. J., Jr., Z. F. Yin, and N. Lasky. "A Tail Vein Bleeding Time Model and Delayed Bleeding in Hemophilic Mice." *Thromb Haemost* 85.4 (2001): 747-8. Print.
- Buchanan, M. R., et al. "Shortening of the Bleeding Time in Thrombocytopenic Rabbits after Exposure of Jugular Vein to High Aspirin Concentration." *Prostaglandins Med* 3.6 (1979): 333-42. Print.

- Buczko, W., M. C. Gambino, and G. De Gaetano. "Prolongation of Rat Tail Bleeding Time by Ketanserin: Mechanisms of Action." *Eur J Pharmacol* 103.3-4 (1984): 261-8. Print.
- Bullock, R., and H. Fujisawa. "The Role of Glutamate Antagonists for the Treatment of Cns Injury." *J Neurotrauma* 9 Suppl 2 (1992): S443-62. Print.
- Butler, K. D., et al. "Prolongation of Rat Tail Bleeding Time Caused by Oral Doses of a Thromboxane Synthetase Inhibitor Which Have Little Effect on Platelet Aggregation." *Thromb Haemost* 47.1 (1982): 46-9. Print.
- Castegren, M., et al. "Endotoxin Tolerance Variation over 24 H During Porcine Endotoxemia: Association with Changes in Circulation and Organ Dysfunction." *PLoS One* 8.1 (2013): e53221. Print.
- Champion, H. R., et al. "A Profile of Combat Injury." *J Trauma* 54.5 Suppl (2003): S13-9. Print.
- Chanan-Khan, A., et al. "Complement Activation Following First Exposure to Pegylated Liposomal Doxorubicin (Doxil): Possible Role in Hypersensitivity Reactions." *Ann Oncol* 14.9 (2003): 1430-7. Print.
- Chang, T. M. "From Artificial Red Blood Cells, Oxygen Carriers, and Oxygen Therapeutics to Artificial Cells, Nanomedicine, and Beyond." *Artif Cells Blood Substit Immobil Biotechnol* 40.3 (2012): 197-9. Print.
- Chappell, D., et al. "A Rational Approach to Perioperative Fluid Management." *Anesthesiology* 109.4 (2008): 723-40. Print.
- Chen, T., et al. "Protected Peptide Nanoparticles: Experiments and Brownian Dynamics Simulations of the Energetics of Assembly." *Nano Lett* 9.6 (2009): 2218-22. Print.
- Chen, T., et al. "Coarse-Grained Simulations of Rapid Assembly Kinetics for Polystyrene-B-Poly(Ethylene Oxide) Copolymers in Aqueous Solutions." *J Phys Chem B* 112.51 (2008): 16357-66. Print.
- Cheng, J., et al. "Formulation of Functionalized Plga-Peg Nanoparticles for in Vivo Targeted Drug Delivery." *Biomaterials* 28.5 (2007): 869-76. Print.
- Clifford, C. C. "Treating Traumatic Bleeding in a Combat Setting." *Mil Med* 169.12 Suppl (2004): 8-10, 4. Print.
- Coller, B. S., et al. "Studies of Activated Gpiib/Iiia Receptors on the Luminal Surface of Adherent Platelets. Paradoxical Loss of Luminal Receptors When Platelets Adhere to High Density Fibrinogen." *J Clin Invest* 92.6 (1993): 2796-806. Print.
- Coller, B. S., et al. "Thromboerythrocytes. In Vitro Studies of a Potential Autologous, Semi-Artificial Alternative to Platelet Transfusions." *J Clin Invest* 89.2 (1992): 546-55. Print.
- D'Addio, S. M., et al. "Novel Method for Concentrating and Drying Polymeric Nanoparticles: Hydrogen Bonding Coacervate Precipitation." *Mol Pharm* 7.2: 557-64. Print.
- . "Novel Method for Concentrating and Drying Polymeric Nanoparticles: Hydrogen Bonding Coacervate Precipitation." *Mol Pharm* 7.2 (2010): 557-64. Print.
- Dahlback, B. "Blood Coagulation." *Lancet* 355.9215 (2000): 1627-32. Print.
- Danhier, F., et al. "Plga-Based Nanoparticles: An Overview of Biomedical Applications." *J Control Release* 161.2 (2012): 505-22. Print.

- Davie, E. W., K. Fujikawa, and W. Kisiel. "The Coagulation Cascade: Initiation, Maintenance, and Regulation." *Biochemistry* 30.43 (1991): 10363-70. Print.
- Davie, E. W., and O. D. Ratnoff. "Waterfall Sequence for Intrinsic Blood Clotting." *Science* 145.3638 (1964): 1310-2. Print.
- Davies, A. R., et al. "Interactions of Platelets with Synthocytes, a Novel Platelet Substitute." *Platelets* 13.4 (2002): 197-205. Print.
- De Clerck, F., J. Goossens, and R. Reneman. "Effects of Anti-Inflammatory, Anticoagulant and Vasoactive Compounds on Tail Bleeding Time, Whole Blood Coagulation Time and Platelet Retention by Glass Beads in Rats." *Thromb Res* 8.2 (1976): 179-93. Print.
- Decuzzi, P., et al. "Size and Shape Effects in the Biodistribution of Intravascularly Injected Particles." *J Control Release* 141.3 (2010): 320-7. Print.
- Deitch, E. A., et al. "Lymph from a Primate Baboon Trauma Hemorrhagic Shock Model Activates Human Neutrophils." *Shock* 25.5 (2006): 460-3. Print.
- Deitch, E. A., et al. "The Role of Lymph Factors in Lung Injury, Bone Marrow Suppression, and Endothelial Cell Dysfunction in a Primate Model of Trauma-Hemorrhagic Shock." *Shock* 22.3 (2004): 221-8. Print.
- Dejana, E., et al. "Bleeding Time in Laboratory Animals. Iii - Do Tail Bleeding Times in Rats Only Measure a Platelet Defect? (the Aspirin Puzzle)." *Thromb Res* 15.1-2 (1979): 199-207. Print.
- Deng, Z. J., et al. "Nanoparticle-Induced Unfolding of Fibrinogen Promotes Mac-1 Receptor Activation and Inflammation." *Nat Nanotechnol* 6.1 (2011): 39-44. Print.
- Dennis, M. S., et al. "Platelet Glycoprotein Iib-Iiia Protein Antagonists from Snake Venoms: Evidence for a Family of Platelet-Aggregation Inhibitors." *Proc Natl Acad Sci U S A* 87.7 (1990): 2471-5. Print.
- Dong, F., et al. "Immune Effects of Resuscitation with Hboc-201, a Hemoglobin-Based Oxygen Carrier, in Swine with Moderately Severe Hemorrhagic Shock from Controlled Hemorrhage." *Shock* 25.1 (2006): 50-5. Print.
- Duchesne, J. C., et al. "Current Evidence Based Guidelines for Factor Viia Use in Trauma: The Good, the Bad, and the Ugly." *Am Surg* 74.12 (2008): 1159-65. Print.
- Duhaime, A. C., L. M. Gennarelli, and A. Yachnis. "Acute Subdural Hematoma: Is the Blood Itself Toxic?" *J Neurotrauma* 11.6 (1994): 669-78. Print.
- Ellis-Behnke, R. "At the Nanoscale: Nanohemostat, a New Class of Hemostatic Agent." *Wiley Interdiscip Rev Nanomed Nanobiotechnol* 3.1: 70-8. Print.
- Enestvedt, B. K., et al. "Endoscopic Therapy for Peptic Ulcer Hemorrhage: Practice Variations in a Multi-Center U.S. Consortium." *Dig Dis Sci* 55.9 (2010): 2568-76. Print.
- Fairbairn, L., et al. "The Mononuclear Phagocyte System of the Pig as a Model for Understanding Human Innate Immunity and Disease." *J Leukoc Biol* 89.6 (2011): 855-71. Print.
- Fakhari, A., et al. "Controlling Ligand Surface Density Optimizes Nanoparticle Binding to Icam-1." *J Pharm Sci* 100.3 (2011): 1045-56. Print.
- Falanga, A., and M. Marchetti. "Anticancer Treatment and Thrombosis." *Thromb Res* 129.3 (2012): 353-9. Print.

- Favaloro, E. J. "Clinical Utility of the Pfa-100." *Semin Thromb Hemost* 34.8 (2008): 709-33. Print.
- Fehlings, M. G., and L. H. Sekhon. "Acute Interventions in Spinal Cord Injury: What Do We Know, What Should We Do?" *Clin Neurosurg* 48 (2001): 226-42. Print.
- Figuerola, C. E., et al. "Highly Loaded Nanoparticulate Formulation of Progesterone for Emergency Traumatic Brain Injury Treatment." *Ther Deliv* 3.11 (2012): 1269-79. Print.
- Fitzpatrick, G. M., R. Cliff, and N. Tandon. "Thrombosomes: A Platelet-Derived Hemostatic Agent for Control of Noncompressible Hemorrhage." *Transfusion* 53 Suppl 1 (2013): 100S-6S. Print.
- Freilich, D., et al. "Hboc-201 Vasoactivity in a Phase Iii Clinical Trial in Orthopedic Surgery Subjects--Extrapolation of Potential Risk for Acute Trauma Trials." *J Trauma* 66.2 (2009): 365-76. Print.
- Frink, M., et al. "Experimental Trauma Models: An Update." *J Biomed Biotechnol* 2011 (2011): 797383. Print.
- Fujiwara, M., R. H. Grubbs, and J. D. Baldeschwieler. "Characterization of Ph-Dependent Poly(Acrylic Acid) Complexation with Phospholipid Vesicles." *J Colloid Interface Sci* 185.1 (1997): 210-6. Print.
- Gailani, D., and G. J. Broze, Jr. "Factor Xi Activation in a Revised Model of Blood Coagulation." *Science* 253.5022 (1991): 909-12. Print.
- Galindo-Rodriguez, S., et al. "Physicochemical Parameters Associated with Nanoparticle Formation in the Salting-out, Emulsification-Diffusion, and Nanoprecipitation Methods." *Pharm Res* 21.8 (2004): 1428-39. Print.
- Garg, A., et al. "Targeting Colon Cancer Cells Using Pegylated Liposomes Modified with a Fibronectin-Mimetic Peptide." *Int J Pharm* 366.1-2 (2009): 201-10. Print.
- Gegel, B., et al. "The Effects of Bleedarrest on Hemorrhage Control in a Porcine Model." *US Army Med Dep J* (2012): 31-5. Print.
- Gindy, M. E., et al. "Preparation of Poly(Ethylene Glycol) Protected Nanoparticles with Variable Bioconjugate Ligand Density." *Biomacromolecules* 9.10 (2008): 2705-11. Print.
- Gindy, M. E., A. Z. Panagiotopoulos, and R. K. Prud'homme. "Composite Block Copolymer Stabilized Nanoparticles: Simultaneous Encapsulation of Organic Actives and Inorganic Nanostructures." *Langmuir* 24.1 (2008): 83-90. Print.
- Gorbet, M. B., and M. V. Sefton. "Biomaterial-Associated Thrombosis: Roles of Coagulation Factors, Complement, Platelets and Leukocytes." *Biomaterials* 25.26 (2004): 5681-703. Print.
- Gralnek, I. M., A. N. Barkun, and M. Bardou. "Management of Acute Bleeding from a Peptic Ulcer." *N Engl J Med* 359.9 (2008): 928-37. Print.
- Greene, T. K., et al. "Towards a Standardization of the Murine Tail Bleeding Model." *J Thromb Haemost* 8.12 (2010): 2820-2. Print.
- Grislain, L., et al. "Pharmacokinetics and Distribution of a Biodegradable Drug-Carrier." *Int J Pharm* 15.3 (1983): 335-45. Print.
- Gu, F., et al. "Precise Engineering of Targeted Nanoparticles by Using Self-Assembled Biointegrated Block Copolymers." *Proc Natl Acad Sci U S A* 105.7 (2008): 2586-91. Print.

- Guo, G., et al. "Trauma and Pulmonary Thromboembolism: An Experimental Study on Their Correlation." *Chin J Traumatol* 10.4 (2007): 237-41. Print.
- Gurney, J., et al. "A Hemoglobin Based Oxygen Carrier, Bovine Polymerized Hemoglobin (Hboc-201) Versus Hetastarch (Hex) in an Uncontrolled Liver Injury Hemorrhagic Shock Swine Model with Delayed Evacuation." *J Trauma* 57.4 (2004): 726-38. Print.
- Guyton, Arthur C., and John E. Hall. *Textbook of Medical Physiology*. 11th ed. Philadelphia: Elsevier Saunders, 2006. Print.
- Hartog, C. S., et al. "Systematic Analysis of Hydroxyethyl Starch (Hes) Reviews: Proliferation of Low-Quality Reviews Overwhelms the Results of Well-Performed Meta-Analyses." *Intensive Care Med* 38.8 (2012): 1258-71. Print.
- Hermanson, GT. *Bioconjugate Techniques*. Bioconjugate Techniques. Ed. Hermanson, GT. 2nd ed. Vol. 1. 1 vols. San Diego, CA: Academic Press, 2008. Print.
- Hindriks, G., et al. "Platelet Adhesion to Laminin: Role of Ca²⁺ and Mg²⁺ Ions, Shear Rate, and Platelet Membrane Glycoproteins." *Blood* 79.4 (1992): 928-35. Print.
- Hodgetts, T. J., P. F. Mahoney, and E. Kirkman. "Damage Control Resuscitation." *J R Army Med Corps* 153.4 (2007): 299-300. Print.
- Hodgetts, T. J., et al. "Abc to <C>Abc: Redefining the Military Trauma Paradigm." *Emerg Med J* 23.10 (2006): 745-6. Print.
- Holcomb, J. B., et al. "Fibrin Sealant Foam Sprayed Directly on Liver Injuries Decreases Blood Loss in Resuscitated Rats." *J Trauma* 49.2 (2000): 246-50. Print.
- Holcomb, J. B., et al. "Causes of Death in U.S. Special Operations Forces in the Global War on Terrorism: 2001-2004." *Ann Surg* 245.6 (2007): 986-91. Print.
- Hrkach, J. S., et al. "Nanotechnology for Biomaterials Engineering: Structural Characterization of Amphiphilic Polymeric Nanoparticles by 1h Nmr Spectroscopy." *Biomaterials* 18.1 (1997): 27-30. Print.
- Hui, Y. H., et al. "Pharmacokinetic Comparisons of Tail-Bleeding with Cannula- or Retro-Orbital Bleeding Techniques in Rats Using Six Marketed Drugs." *J Pharmacol Toxicol Methods* 56.2 (2007): 256-64. Print.
- Jabbari, E. "Targeted Delivery with Peptidomimetic Conjugated Self-Assembled Nanoparticles." *Pharm Res* 26.3 (2009): 612-30. Print.
- Jaskille, A., et al. "Abdominal Insufflation Decreases Blood Loss and Mortality after Porcine Liver Injury." *J Trauma* 59.6 (2005): 1305-8; discussion 08. Print.
- Johansen, P. B., et al. "Automated Registration of Tail Bleeding in Rats." *Thromb Haemost* 99.5 (2008): 956-62. Print.
- Johansson, P. I., J. Stensballe, and S. R. Ostrowski. "Current Management of Massive Hemorrhage in Trauma." *Scand J Trauma Resusc Emerg Med* 20 (2012): 47. Print.
- Johnson, D., et al. "The Effects of Quikclot Combat Gauze on Hemorrhage Control in the Presence of Hemodilution." *US Army Med Dep J* (2012): 36-9. Print.
- Johnson, R. A., et al. "Histamine Release Associated with Intravenous Delivery of a Fluorocarbon-Based Sevoflurane Emulsion in Canines." *J Pharm Sci* 100.7 (2011): 2685-92. Print.
- Kaplan, A. P., and B. Ghebrehiwet. "The Plasma Bradykinin-Forming Pathways and Its Interrelationships with Complement." *Mol Immunol* 47.13 (2010): 2161-9. Print.

- Karahan, M., Z. Mustafaeva, and C. Ozeroglu. "Investigation of Ternary Complex Formations of Polyacrylic Acid with Bovine Serum Albumin in the Presence of Metal Ions by Fluorescence and Dynamic Light Scattering Measurements." *Protein J* 29.5 (2010): 336-42. Print.
- Kauvar, D. S., et al. "Fresh Whole Blood Transfusion: A Controversial Military Practice." *J Trauma* 61.1 (2006): 181-4. Print.
- Kauvar, D. S., R. Lefering, and C. E. Wade. "Impact of Hemorrhage on Trauma Outcome: An Overview of Epidemiology, Clinical Presentations, and Therapeutic Considerations." *J Trauma* 60.6 Suppl (2006): S3-11. Print.
- Kauvar, D. S., and C. E. Wade. "The Epidemiology and Modern Management of Traumatic Hemorrhage: Us and International Perspectives." *Crit Care* 9 Suppl 5 (2005): S1-9. Print.
- Kelly, J. F., et al. "Injury Severity and Causes of Death from Operation Iraqi Freedom and Operation Enduring Freedom: 2003-2004 Versus 2006." *J Trauma* 64.2 Suppl (2008): S21-6; discussion S26-7. Print.
- Klingensmith, W. C., 3rd, M. F. Tsan, and H. N. Wagner, Jr. "Factors Affecting the Uptake of 99mTc-Sulfur Colloid by the Lung and Kidney." *J Nucl Med* 17.8 (1976): 681-4. Print.
- Knudson, M. M., et al. "Thromboembolism after Trauma: An Analysis of 1602 Episodes from the American College of Surgeons National Trauma Data Bank." *Ann Surg* 240.3 (2004): 490-6; discussion 96-8. Print.
- Kohn, Dennis F. *Anesthesia and Analgesia in Laboratory Animals*. American College of Laboratory Animal Medicine Series. San Diego: Academic Press, 1997. Print.
- Krug, E. G., G. K. Sharma, and R. Lozano. "The Global Burden of Injuries." *Am J Public Health* 90.4 (2000): 523-6. Print.
- Lam, S. C., et al. "Evidence That Arginyl-Glycyl-Aspartate Peptides and Fibrinogen Gamma Chain Peptides Share a Common Binding Site on Platelets." *J Biol Chem* 262.3 (1987): 947-50. Print.
- Langleben, D., and L. A. Moroz. "Interspecies Variation in the Cellular Phase of Blood Fibrinolytic Activity." *Proc Soc Exp Biol Med* 196.3 (1991): 270-2. Print.
- Lavik, E. B., et al. "A Simple Synthetic Route to the Formation of a Block Copolymer of Poly(Lactic-Co-Glycolic Acid) and Polylysine for the Fabrication of Functionalized, Degradable Structures for Biomedical Applications." *J Biomed Mater Res* 58.3 (2001): 291-4. Print.
- Lee, Christine A., Erik Berntorp, and Keith Hoots. *Textbook of Hemophilia*. 2nd ed. Chichester, West Sussex, UK ; Hoboken, NJ: Wiley-Blackwell, 2010. Print.
- Lee, D. H., and M. A. Blajchman. "Novel Treatment Modalities: New Platelet Preparations and Substitutes." *Br J Haematol* 114.3 (2001): 496-505. Print.
- Letchford, K., and H. Burt. "A Review of the Formation and Classification of Amphiphilic Block Copolymer Nanoparticulate Structures: Micelles, Nanospheres, Nanocapsules and Polymersomes." *Eur J Pharm Biopharm* 65.3 (2007): 259-69. Print.
- Levi, M., et al. "Fibrinogen-Coated Albumin Microcapsules Reduce Bleeding in Severely Thrombocytopenic Rabbits." *Nat Med* 5.1 (1999): 107-11. Print.

- Limayem, I., C. Charcosset, and H. Fessi. "Purification of Nanoparticle Suspensions by a Concentration/Diafiltration Process." *Separation and Purification Technology* 38.1 (2004): 1-9. Print.
- Liu, Y., et al. "Ostwald Ripening of Beta-Carotene Nanoparticles." *Phys Rev Lett* 98.3 (2007): 036102. Print.
- Ljung, R. "Hemophilia and Prophylaxis." *Pediatr Blood Cancer* 60 Suppl 1 (2013): S23-6. Print.
- Lucas, O. N. "Limitations of Clotting and Bleeding Time Tests for Screening Haemorrhagic Disorders." *J Can Dent Assoc (Tor)* 32.10 (1966): 599-602. Print.
- Macfarlane, R. G. "An Enzyme Cascade in the Blood Clotting Mechanism, and Its Function as a Biochemical Amplifier." *Nature* 202 (1964): 498-9. Print.
- Markwardt, F., et al. "The Influence of Drugs on Disseminated Intravascular Coagulation (Dic). Iii. Effects of Busulfan-Induced Thrombocytopenia and Inhibition of Platelet Function by Acetylsalicylic Acid." *Thromb Res* 15.1-2 (1979): 79-88. Print.
- Martin, F. J., et al. "Acute Toxicity of Intravenously Administered Microfabricated Silicon Dioxide Drug Delivery Particles in Mice: Preliminary Findings." *Drugs R D* 6.2 (2005): 71-81. Print.
- Martinowitz, U., et al. "Treating Traumatic Bleeding in a Combat Setting: Possible Role of Recombinant Activated Factor Vii." *Mil Med* 169.12 Suppl (2004): 16-8, 4. Print.
- Matsuoka, T., J. Hildreth, and D. H. Wisner. "Liver Injury as a Model of Uncontrolled Hemorrhagic Shock: Resuscitation with Different Hypertonic Regimens." *J Trauma* 39.4 (1995): 674-80. Print.
- Matsuoka, T., and D. H. Wisner. "Resuscitation of Uncontrolled Liver Hemorrhage: Effects on Bleeding, Oxygen Delivery, and Oxygen Consumption." *J Trauma* 41.3 (1996): 439-45. Print.
- Matteucci, M. E., et al. "Flocculated Amorphous Nanoparticles for Highly Supersaturated Solutions." *Pharm Res* 25.11 (2008): 2477-87. Print.
- Mautes, A. E., et al. "Vascular Events after Spinal Cord Injury: Contribution to Secondary Pathogenesis." *Phys Ther* 80.7 (2000): 673-87. Print.
- Merkel, T. J., et al. "The Effect of Particle Size on the Biodistribution of Low-Modulus Hydrogel Print Particles." *J Control Release* 162.1 (2012): 37-44. Print.
- Michelson, A. D. "Methods for the Measurement of Platelet Function." *Am J Cardiol* 103.3 Suppl (2009): 20A-26A. Print.
- Michelson, Alan D. *Platelets*. 2nd ed. Amsterdam ; Boston: Academic Press/Elsevier, 2007. Print.
- Miller, C. A. "Spontaneous Emulsification Produced by Diffusion - a Review." *Colloids and Surfaces* 29.1 (1988): 89-102. Print.
- Miller, D. L., et al. "Ct Evaluation of Hepatic and Splenic Trauma with Eoe-13. An Experimental Study in Monkeys." *Invest Radiol* 20.1 (1985): 68-72. Print.
- Modery, C. L., et al. "Heteromultivalent Liposomal Nanoconstructs for Enhanced Targeting and Shear-Stable Binding to Active Platelets for Site-Selective Vascular Drug Delivery." *Biomaterials* 32.35 (2011): 9504-14. Print.

- Modery-Pawlowski, C. L., et al. "Approaches to Synthetic Platelet Analogs." *Biomaterials* 34.2 (2013): 526-41. Print.
- Modery-Pawlowski, C. L., et al. "In Vitro and in Vivo Hemostatic Capabilities of a Functionally Integrated Platelet-Mimetic Liposomal Nanoconstruct." *Biomaterials* (2013). Print.
- Monien, B. H., K. I. Cheang, and U. R. Desai. "Mechanism of Poly(Acrylic Acid) Acceleration of Antithrombin Inhibition of Thrombin: Implications for the Design of Novel Heparin Mimics." *J Med Chem* 48.16 (2005): 5360-8. Print.
- Monien, B. H., and U. R. Desai. "Antithrombin Activation by Nonsulfated, Non-Polysaccharide Organic Polymer." *J Med Chem* 48.4 (2005): 1269-73. Print.
- Morrison, J. J., and T. E. Rasmussen. "Noncompressible Torso Hemorrhage: A Review with Contemporary Definitions and Management Strategies." *Surg Clin North Am* 92.4 (2012): 843-58. Print.
- Morse, B. C., et al. "The Effects of Protocolized Use of Recombinant Factor Viia within a Massive Transfusion Protocol in a Civilian Level I Trauma Center." *Am Surg* 77.8 (2011): 1043-9. Print.
- Naito, K., and K. Fujikawa. "Activation of Human Blood Coagulation Factor Xi Independent of Factor Xii. Factor Xi Is Activated by Thrombin and Factor Xia in the Presence of Negatively Charged Surfaces." *J Biol Chem* 266.12 (1991): 7353-8. Print.
- Ng, Q. K., et al. "Engineering Clustered Ligand Binding into Nonviral Vectors: Alphavbeta3 Targeting as an Example." *Mol Ther* 17.5 (2009): 828-36. Print.
- Nivelstein, P. F., P. A. D'Alessio, and J. J. Sixma. "Fibronectin in Platelet Adhesion to Human Collagen Types I and Iii. Use of Nonfibrillar and Fibrillar Collagen in Flowing Blood Studies." *Arteriosclerosis* 8.2 (1988): 200-6. Print.
- Nivelstein, P. F., and P. G. de Groot. "Interaction of Blood Platelets with the Vessel Wall." *Haemostasis* 18.4-6 (1988): 342-59. Print.
- Nivelstein, P. F., and J. J. Sixma. "Glycoprotein Iib-Iiia and Rgd(S) Are Not Important for Fibronectin-Dependent Platelet Adhesion under Flow Conditions." *Blood* 72.1 (1988): 82-8. Print.
- Nishikawa, K., et al. "Fibrinogen Gamma-Chain Peptide-Coated, Adp-Encapsulated Liposomes Rescue Thrombocytopenic Rabbits from Non-Compressible Liver Hemorrhage." *J Thromb Haemost* 10.10 (2012): 2137-48. Print.
- Nunez, T. C., and B. A. Cotton. "Transfusion Therapy in Hemorrhagic Shock." *Curr Opin Crit Care* 15.6 (2009): 536-41. Print.
- Ojito, J. W., et al. "Comparison of Point-of-Care Activated Clotting Time Systems Utilized in a Single Pediatric Institution." *J Extra Corpor Technol* 44.1 (2012): 15-20. Print.
- Okamura, Y., et al. "Visualization of Liposomes Carrying Fibrinogen Gamma-Chain Dodecapeptide Accumulated to Sites of Vascular Injury Using Computed Tomography." *Nanomedicine* 6.2 (2010): 391-6. Print.
- Okamura, Y., et al. "Hemostatic Effects of Phospholipid Vesicles Carrying Fibrinogen Gamma Chain Dodecapeptide in Vitro and in Vivo." *Bioconjug Chem* 16.6 (2005): 1589-96. Print.

- Olivier, V., et al. "Influence of Targeting Ligand Flexibility on Receptor Binding of Particulate Drug Delivery Systems." *Bioconjug Chem* 14.6 (2003): 1203-8. Print.
- Osterholm, J. L. "The Pathophysiological Response to Spinal Cord Injury. The Current Status of Related Research." *J Neurosurg* 40.1 (1974): 5-33. Print.
- Osterud, B., and S. I. Rapaport. "Activation of Factor Ix by the Reaction Product of Tissue Factor and Factor Vii: Additional Pathway for Initiating Blood Coagulation." *Proc Natl Acad Sci U S A* 74.12 (1977): 5260-4. Print.
- Pakala, R., and R. Waksman. "Currently Available Methods for Platelet Function Analysis: Advantages and Disadvantages." *Cardiovasc Revasc Med* 12.5 (2011): 312-22. Print.
- Park, E., A. A. Velumian, and M. G. Fehlings. "The Role of Excitotoxicity in Secondary Mechanisms of Spinal Cord Injury: A Review with an Emphasis on the Implications for White Matter Degeneration." *J Neurotrauma* 21.6 (2004): 754-74. Print.
- Patanwala, A. E. "Factor Viia (Recombinant) for Acute Traumatic Hemorrhage." *Am J Health Syst Pharm* 65.17 (2008): 1616-23. Print.
- Peyvandi, F., et al. "Genetic Diagnosis of Haemophilia and Other Inherited Bleeding Disorders." *Haemophilia* 12 Suppl 3 (2006): 82-9. Print.
- Philbin, N., et al. "A Hemoglobin-Based Oxygen Carrier, Bovine Polymerized Hemoglobin (Hboc-201) Versus Hetastarch (Hex) in a Moderate Severity Hemorrhagic Shock Swine Model with Delayed Evacuation." *Resuscitation* 66.3 (2005): 367-78. Print.
- Poindexter, B., and J.G. Vostal. "Guidance for Industry: For Platelet Testing and Evaluation of Platelet Substitute Products." Ed. FDA. Bethesda, MD: U.S. Department of Health and Human Services, 1999. Print.
- Popa, C., et al. "Vascular Dysfunctions Following Spinal Cord Injury." *J Med Life* 3.3: 275-85. Print.
- Prabhu, P., and V. Patravale. "The Upcoming Field of Theranostic Nanomedicine: An Overview." *J Biomed Nanotechnol* 8.6 (2012): 859-82. Print.
- Probst, R. J., et al. "Gender Differences in the Blood Volume of Conscious Sprague-Dawley Rats." *J Am Assoc Lab Anim Sci* 45.2 (2006): 49-52. Print.
- Pusateri, A. E., et al. "Tranexamic Acid and Trauma: Current Status and Knowledge Gaps with Recommended Research Priorities." *Shock* 39.2 (2013): 121-26. Print.
- Ramon, S., et al. "Clinical and Magnetic Resonance Imaging Correlation in Acute Spinal Cord Injury." *Spinal Cord* 35.10 (1997): 664-73. Print.
- Rao, Gundu H. R. *Handbook of Platelet Physiology and Pharmacology*. Boston: Kluwer Academic, 1999. Print.
- Rappold, J. F., and A. E. Pusateri. "Tranexamic Acid in Remote Damage Control Resuscitation." *Transfusion* 53 Suppl 1 (2013): 96S-9S. Print.
- Ravikumar, M., et al. "Mimicking Adhesive Functionalities of Blood Platelets Using Ligand-Decorated Liposomes." *Bioconjug Chem* (2012). Print.
- Ravikumar, M., et al. "Peptide-Decorated Liposomes Promote Arrest and Aggregation of Activated Platelets under Flow on Vascular Injury Relevant Protein Surfaces in Vitro." *Biomacromolecules* 13.5 (2012): 1495-502. Print.
- Regel, G., et al. "Prehospital Care, Importance of Early Intervention on Outcome." *Acta Anaesthesiol Scand Suppl* 110 (1997): 71-6. Print.

- Rendu, F., and B. Brohard-Bohn. "The Platelet Release Reaction: Granules' Constituents, Secretion and Functions." *Platelets* 12.5 (2001): 261-73. Print.
- Richards, A. B., et al. "Trehalose: A Review of Properties, History of Use and Human Tolerance, and Results of Multiple Safety Studies." *Food Chem Toxicol* 40.7 (2002): 871-98. Print.
- Riddel, J. P., Jr., et al. "Theories of Blood Coagulation." *J Pediatr Oncol Nurs* 24.3 (2007): 123-31. Print.
- Rosca, I. D., F. Watari, and M. Uo. "Microparticle Formation and Its Mechanism in Single and Double Emulsion Solvent Evaporation." *J Control Release* 99.2 (2004): 271-80. Print.
- Rossaint, R., et al. "Key Issues in Advanced Bleeding Care in Trauma." *Shock* 26.4 (2006): 322-31. Print.
- Ryan, K. L., et al. "Efficacy of Fda-Approved Hemostatic Drugs to Improve Survival and Reduce Bleeding in Rat Models of Uncontrolled Hemorrhage." *Resuscitation* 70.1 (2006): 133-44. Print.
- Sancey, L., et al. "Clustering and Internalization of Integrin Alphavbeta3 with a Tetrameric Rgd-Synthetic Peptide." *Mol Ther* 17.5 (2009): 837-43. Print.
- Santry, H. P., and H. B. Alam. "Fluid Resuscitation: Past, Present, and the Future." *Shock* 33.3 (2010): 229-41. Print.
- Sauaia, A., et al. "Epidemiology of Trauma Deaths: A Reassessment." *J Trauma* 38.2 (1995): 185-93. Print.
- Sava, J., et al. "Abdominal Insufflation for Prevention of Exsanguination." *J Trauma* 54.3 (2003): 590-4. Print.
- Schmugge, M., M. L. Rand, and J. Freedman. "Platelets and Von Willebrand Factor." *Transfus Apher Sci* 28.3 (2003): 269-77. Print.
- Schneberger, D., K. Aharonson-Raz, and B. Singh. "Pulmonary Intravascular Macrophages and Lung Health: What Are We Missing?" *Am J Physiol Lung Cell Mol Physiol* 302.6 (2012): L498-503. Print.
- Schochl, H., et al. "Thromboelastometric (Rotem) Findings in Patients Suffering from Isolated Severe Traumatic Brain Injury." *J Neurotrauma* 28.10 (2011): 2033-41. Print.
- Schrager, J. J., R. D. Branson, and J. A. Johannigman. "Lessons from the Tip of the Spear: Medical Advancements from Iraq and Afghanistan." *Respir Care* 57.8 (2012): 1305-13. Print.
- Segers, K., B. Dahlback, and G. A. Nicolaes. "Coagulation Factor V and Thrombophilia: Background and Mechanisms." *Thromb Haemost* 98.3 (2007): 530-42. Print.
- Sekhon, L. H., and M. G. Fehlings. "Epidemiology, Demographics, and Pathophysiology of Acute Spinal Cord Injury." *Spine (Phila Pa 1976)* 26.24 Suppl (2001): S2-12. Print.
- Seligsohn, U. "Factor Xi in Haemostasis and Thrombosis: Past, Present and Future." *Thromb Haemost* 98.1 (2007): 84-9. Print.
- Seyednejad, H., et al. "Topical Haemostatic Agents." *Br J Surg* 95.10 (2008): 1197-225. Print.
- Shek, P. N., and S. A. Howe. "A Novel Method for the Rapid Bleeding of Rats from the Tail Vein." *J Immunol Methods* 53.2 (1982): 255-60. Print.

- Shoffstall, A. J., et al. "Intravenous Hemostatic Nanoparticles Increase Survival Following Blunt Trauma Injury." *Biomacromolecules* 13.11 (2012): 3850-7. Print.
- Siller-Matula, J. M., et al. "Interspecies Differences in Coagulation Profile." *Thromb Haemost* 100.3 (2008): 397-404. Print.
- Simard, J. M., et al. "Key Role of Sulfonylurea Receptor 1 in Progressive Secondary Hemorrhage after Brain Contusion." *J Neurotrauma* 26.12 (2009): 2257-67. Print.
- Simard, J. M., et al. "Endothelial Sulfonylurea Receptor 1-Regulated Nc Ca-Atp Channels Mediate Progressive Hemorrhagic Necrosis Following Spinal Cord Injury." *J Clin Invest* 117.8 (2007): 2105-13. Print.
- Simard, J. M., et al. "Brief Suppression of Abcc8 Prevents Autodestruction of Spinal Cord after Trauma." *Sci Transl Med* 2.28: 28ra29. Print.
- Sinescu, C., et al. "Molecular Basis of Vascular Events Following Spinal Cord Injury." *J Med Life* 3.3: 254-61. Print.
- Stein, D. M., and R. P. Dutton. "Uses of Recombinant Factor Viia in Trauma." *Curr Opin Crit Care* 10.6 (2004): 520-8. Print.
- Stern, S., et al. "Resuscitation with the Hemoglobin-Based Oxygen Carrier, Hboc-201, in a Swine Model of Severe Uncontrolled Hemorrhage and Traumatic Brain Injury." *Shock* 31.1 (2009): 64-79. Print.
- Szczepanska-Sadowska, E., et al. "Central Avp and Blood Pressure Regulation: Relevance to Interspecies Differences and Hypertension." *Ann N Y Acad Sci* 689 (1993): 677-9. Print.
- Szebeni, J., et al. "A Porcine Model of Complement-Mediated Infusion Reactions to Drug Carrier Nanosystems and Other Medicines." *Adv Drug Deliv Rev* 64.15 (2012): 1706-16. Print.
- Szebeni, J., et al. "Liposome-Induced Complement Activation and Related Cardiopulmonary Distress in Pigs: Factors Promoting Reactogenicity of Doxil and Ambisome." *Nanomedicine* 8.2 (2012): 176-84. Print.
- Szebeni, J., et al. "Prevention of Infusion Reactions to Pegylated Liposomal Doxorubicin Via Tachyphylaxis Induction by Placebo Vesicles: A Porcine Model." *J Control Release* 160.2 (2012): 382-7. Print.
- Tator, C. H., and I. Koyanagi. "Vascular Mechanisms in the Pathophysiology of Human Spinal Cord Injury." *J Neurosurg* 86.3 (1997): 483-92. Print.
- Thibault, G., P. Tardif, and G. Lapalme. "Comparative Specificity of Platelet Alpha(Iib)Beta(3) Integrin Antagonists." *J Pharmacol Exp Ther* 296.3 (2001): 690-6. Print.
- Toy, R., et al. "The Effects of Particle Size, Density and Shape on Margination of Nanoparticles in Microcirculation." *Nanotechnology* 22.11 (2011): 115101. Print.
- Vamvakas, E. C., and M. A. Blajchman. "Transfusion-Related Mortality: The Ongoing Risks of Allogeneic Blood Transfusion and the Available Strategies for Their Prevention." *Blood* 113.15 (2009): 3406-17. Print.
- van der Kamp, K. W., and W. van Oeveren. "Factor Xii Fragment and Kallikrein Generation in Plasma During Incubation with Biomaterials." *J Biomed Mater Res* 28.3 (1994): 349-52. Print.

- Varma, R. K., et al. "Polysorbate 80: A Pharmacological Study." *Arzneimittelforschung* 35.5 (1985): 804-8. Print.
- Velasco, I. T., et al. "Hyperosmotic Nacl and Severe Hemorrhagic Shock." *Am J Physiol* 239.5 (1980): H664-73. Print.
- Velmahos, G. C., et al. "Abdominal Insufflation for Control of Bleeding after Severe Splenic Injury." *J Trauma* 63.2 (2007): 285-8; discussion 88-90. Print.
- Velmahos, G. C., et al. "Abdominal Insufflation Decreases Blood Loss without Worsening the Inflammatory Response: Implications for Prehospital Control of Internal Bleeding." *Am Surg* 74.4 (2008): 297-301. Print.
- Vine, A. K. "Recent Advances in Haemostasis and Thrombosis." *Retina* 29.1 (2009): 1-7. Print.
- Weisel, J. W., et al. "Examination of the Platelet Membrane Glycoprotein Iib-Iiia Complex and Its Interaction with Fibrinogen and Other Ligands by Electron Microscopy." *J Biol Chem* 267.23 (1992): 16637-43. Print.
- Whitby, C. P., et al. "Poly(Lactic-Co-Glycolic Acid) as a Particulate Emulsifier." *J Colloid Interface Sci* 375.1 (2012): 142-7. Print.
- Winkler, G. C. "Pulmonary Intravascular Macrophages in Domestic Animal Species: Review of Structural and Functional Properties." *Am J Anat* 181.3 (1988): 217-34. Print.
- . "Review of the Significance of Pulmonary Intravascular Macrophages with Respect to Animal Species and Age." *Exp Cell Biol* 57.6 (1989): 281-6. Print.
- Wise, R. J., et al. "The Role of Von Willebrand Factor Multimers and Propeptide Cleavage in Binding and Stabilization of Factor VIII." *J Biol Chem* 266.32 (1991): 21948-55. Print.
- Wong, K. H., et al. "Microfluidic Models of Vascular Functions." *Annu Rev Biomed Eng* 14 (2012): 205-30. Print.
- Z-Medica. "The Groundbreaking Technology Behind Quikclot® Hemostasis Products". WebPage, 2013. Z-Medica. 2013. <<http://www.z-medica.com/healthcare/How-QuikClot-Works/FAQs.aspx%3E>.
- Ziats, N. P., et al. "Adsorption of Hageman Factor (Factor XII) and Other Human Plasma Proteins to Biomedical Polymers." *J Lab Clin Med* 116.5 (1990): 687-96. Print.